RMZ – MATERIALS AND GEOENVIRONMENT

PERIODICAL FOR MINING, METALLURGY AND GEOLOGY

RMZ – MATERIALI IN GEOOKOLJE

REVIJA ZA RUDARSTVO, METALURGIJO IN GEOLOGIJO

Historical Rewiev

More than 80 years have passed since in 1919 the University Ljubljana in Slovenia was founded. Technical fields were joint in the School of Engineering that included the Geologic and Mining Division while the Metallurgy Division was established in 1939 only. Today the Departments of Geology, Mining and Geotechnology, Materials and Metallurgy are part of the Faculty of Natural Sciences and Engineering, University of Ljubljana.

Before War II the members of the Mining Section together with the Association of Yugoslav Mining and Metallurgy Engineers began to publish the summaries of their research and studies in their technical periodical Rudarski zbornik (Mining Proceedings). Three volumes of Rudarski zbornik (1937, 1938 and 1939) were published. The War interrupted the publication and not untill 1952 the first number of the new journal Rudarsko-metalurški zbornik - RMZ (Mining and Metallurgy Quarterly) has been published by the Division of Mining and Metallurgy, University of Ljubljana. Later the journal has been regularly published quarterly by the Departments of Geology, Mining and Geotechnology, Materials and Metallurgy, and the Institute for Mining, Geotechnology and Environment.

On the meeting of the Advisory and the Editorial Board on May 22nd 1998 Rudarsko-metalurški zbornik has been renamed into "RMZ - Materials and Geoenvironment (RMZ -Materiali in Geookolje)" or shortly RMZ - M&G.

RMZ - M&G is managed by an international advisory and editorial board and is exchanged with other world-known periodicals. All the papers are reviewed by the corresponding professionals and experts.

RMZ - M&G is the only scientific and professional periodical in Slovenia, which is published in the same form nearly 50 years. It incorporates the scientific and professional topics in geology, mining, and geotechnology, in materials and in metallurgy.

The wide range of topics inside the geosciences are wellcome to be published in the RMZ -Materials and Geoenvironment. Research results in geology, hydrogeology, mining, geotechnology, materials, metallurgy, natural and antropogenic pollution of environment, biogeochemistry are proposed fields of work which the journal will handle. RMZ - M&G is co-issued and co-financed by the Faculty of Natural Sciences and Engineering Ljubljana, and the Institute for Mining, Geotechnology and Environment Ljubljana. In addition it is financially supported also by the Ministry of Higher Education, Science and Technology of Republic of Slovenia.

<div align="right">Editor in chief</div>

Table of Contents – Kazalo

Original Scientific Papers – Izvirni znanstveni članki

Effect of cooling rate on the constitution of Al-Mn-Be-Cu

Vpliv ohlajevalne hitrosti na konstitucijo Al-Mn-Be-Cu

Neva Štrekelj[1,*], Iztok Naglič[1], Blaž Karpe[1], Boštjan Markoli[1]

[1]University of Ljubljana, Faculty of Natural Sciences and Engineering, Aškerčeva 12, SI-1000 Ljubljana, Slovenia

*Corresponding author. E-mail: neva.strekelj@omm.ntf.uni-lj.si

Abstract: In this article the constitution of the Al-Mn-Be-Cu alloys and the influence of the cooling rate on the constitution was studied. Cooling rates were determined through the measurements of the dendrite arm spacing and the heat calculations. By the use of computer program which is part of the light microscopy technique, individual fractions of i-phase were determined. It was found that at cooling rates between 500 K s^{-1} and 1 350 K s^{-1} the preferred phase formed was a quasicrystalline phase – especially in the form of the quasicrystalline eutectic (α_{Al} + i-phase). In addition to the quasicrystalline i-phase within eutectic, it is also formed as the primary phase. The fraction of the i-phase varied depending on the diameter of the castings (2 mm and 4 mm) and in most cases it increased with the decreasing diameter. Fractions of the i-phase in the individual castings were higher in the alloy with a higher content of manganese. Morphology of the i-phase depended on the content of the alloying elements and the cooling rate. Thus in the alloy with a higher mole content of the manganese (4.5 at. % Mn) i-phase possessed the dendritic form, while in the alloy with lower manganese content (1.8 at. % Mn) it was in form of needles, which were thicker at the tips. With the distance from the edge of the sample (with decreasing cooling rate) the dendrites grew, the primary branches were thicker and the secondary branches started to grow also. In the case of the needle morphology, the length and the thickness of needles grew with increasing distance from the sample edge.

Izvleček: V članku je obravnavana konstitucija dveh zlitin Al-Mn-Be-Cu in vpliv ohlajevalne hitrosti nanjo. Opravljene so bile ocene

---

Original scientific paper

ohlajevalnih hitrosti z merjenjem sekundarnih dendritnih razdalj in izračunov toplotne bilance strjevanja. Z računalniškim programom, ki je del svetlobnomikroskopske opreme, so bili določeni površinski deleži faze i v ulitkih. Ugotovljeno je bilo, da je pri ohlajevalnih hitrostih med 500 K s^{-1} in 1350 K s^{-1} prednostna tvorba kvazikristalne faze (zlasti v obliki kvazikristalnega evtektika (α_{Al} + faza i)). Poleg kvazikristalne faze i v okviru heterogenega zloga se le-ta pojavlja tudi kot primarna faza. Delež faze i se spreminja glede na premer ulitih valjčkov (2 mm in 4 mm) in v povprečju raste s padajočim premerom. Deleži faze i v posameznih ulitkih so višji pri zlitini z višjim deležem mangana. Morfologija faze i se spreminja v odvisnosti od vsebnosti zlitinskih elementov in hitrosti ohlajanja. Tako je v zlitini z višjim deležem mangana (4,5 at. % Mn) faza i prisotna večinoma v dendritni obliki, medtem ko je v zlitini z nižjo vsebnostjo mangana (1,8 at. % Mn) v obliki iglic, ki so na koncu odebeljene. Z oddaljenostjo od roba vzorca, torej v odvisnosti od ohlajevalne hitrosti, pa dendriti rastejo, primarne veje se debelijo, sekundarne začno rasti. Pri igličasti morfologiji pa dolžina in debelina iglic z oddaljenostjo od roba vzorca rasteta.

Key words: quasicrystals, microstructure, aluminum alloys
Ključne besede: kvazikristali, mikrostruktura, aluminijeve zlitine

Introduction

Quasicrystals were first discovered by D. Shechtman in the year 1984 in an Al$_{86}$Mn$_{14}$ alloy.[1] They are considered to be the third state of matter in addition to the crystal and amorphous state. The atoms are ordered but with non-crystallographic rotational symmetry and without three-dimensional periodicity.[2] Quasicrystals have until now been found in more than a hundred binary and ternary metallic systems. About half of them are metastable and can only be obtained by rapid solidification techniques, such as melt spinning.[3]

In binary Al-Mn alloys the metastable quasicrystalline phases form only at higher cooling rates. In some cases the addition of the third element (e.g. Be) causes the formation of quasicrystalline phases in Al-Mn alloys already at lower cooling rates,[4] that is why it was added in our case. Copper was selected since it has a good solubility in aluminum.

In this paper the constitution of two Al-Mn-Be-Cu alloys was investigated (in as-cast state) mostly to establish the influence of the addition of beryllium and copper during casting with

lower cooling rates. The emphasis was on the effect of cooling rate on the constitution of the Al-Mn-Be-Cu alloys.

MATERIALS AND METHODS

Materials

Two different alloys were prepared (Table 1) using master alloys AlBe5.5, AlCu50 and AlMn20 and pure aluminum (Al 99.9). Major difference between the two Al-Mn-Be-Cu alloys was the content of manganese (4.5 at. % Mn and 1.8 at. % Mn). Synthesis and casting were performed in vacuum. Casting was done in water chilled copper mould at around 750 °C. Castings were cylindrical in shape with different diameters ((2, 4, 6 and 10) mm). By that it was possible to estimate the influence of the cooling rate and chemical composition on the formation, fraction and morphology of the quasicrystalline phase, which in our case was i-phase. In this article only the smaller diameters (2 mm and 4 mm) of the two alloys are discussed, since the cooling rates were sufficient for the formation of more significant amounts of the i-phase.

Methods for estimating the cooling rates

Cooling rate was not monitored during the casting procedure. Instead we performed measuring of DAS (dendrite arm spacing) using LOM and SEM images. Measurements were performed with the Axio Vision software from the edge to the middle of the sample. According to reference[5] the cooling rates were evaluated through DAS measurements. Measurements were performed for the 62MCuKO alloy, while that was not possible for the 22MCuKO alloy because the morphology of the microconstituents was not dendritic. Additionaly to DAS measurements heat calculations were carried out, where the unsteady transport of the heat was taken into account. For the calculations the approximate method – Lumped-System analysis – was used.

Microstructural characterization

Microstructural characterization of the two alloys was performed by light optical microscopy (LOM – ZEISS Axio Imager.A1m) and scanning electron microscopy (SEM - JEOL JSM-5610, JEOL JSM-5800 and JEOL JSM-7600F) in combination with the energy dispersive X-ray spectroscopy (SIRI-

Table 1. Chemical composition of alloys in atomic fractions, x/%

Alloy	x(Al)	x(Mn)	x(Be)	x(Cu)
62MCuKO	92.4	4.5	1.6	1.6
22MCuKO	95.4	1.8	1.2	1.5

US 10/SUTW (Gresham Scientific Instruments) and Oxford Isis 300). The specimens were prepared and etched using a solution of the distilled water and NaOH for both analytical methods, LOM and SEM. By the EDS analysis we determined only the amounts of the aluminum, manganese and copper within the individual phases, while for the beryllium that was not possible. Beryllium cannot be analyzed using EDS because it is a lightweight chemical element.

Estimating the fraction of the i-phase in individual castings

Determination of the fraction of the i-phase was carried out by a computer software Axio Vision and imported SEM images, which were captured from the sample edge towards the center of the sample. Selection of the SEM images was due to the good contrast between the different phases when using backscattered electrons. Principle of determining fraction of the i-phase with Axio Vision software is the separation of the phases by different colors.

Results and discussion

Alloy 62MCuKO

Casting of diameter 2 mm (alloy 62MCuKO)

In addition to the α_{Al} matrix, phases present in the microstructure were: dendritic i-phase within the quasicrystalline eutectic and the θ-Al_2Cu phase as part of the (α_{Al} + θ-Al_2Cu) eutectic (Figure 1). From the edge to the center of the sample the dendrites of the i-phase grew and were more branched. In some places i-phase occured as a primary phase. In some cases the i-phase within the quasicrystalline eutectic was very fine (Figure 2). Phase α_{Al} in average contained atomic fractions 98.0 % Al, 1.0 % Mn and 0.9 % Cu (Table 2), where the copper meant a high probability of θ-Al_2Cu precipitates. Average composition of i-phase was (Table 2): 82.7 % Al, 15.6 % Mn and 1.7 % Cu, which is quite similar to the results in reference.[6]

It was found that the i-phase was also present in the center of the sample which indicated that the cooling rate was sufficient for its formation (reference[7] states, that the critical cooling rate for the formation of the i-phase is 500–520 K s^{-1}). Therefore an assessment of the cooling rate on the edge and the centre of the sample was carried out through DAS measurements and the heat calculations (Table 3). Assessed cooling rate via DAS measurements was: on the edge of the sample 1 350 K s^{-1} and in the middle of the sample 1 000 K s^{-1}. Heat calculations of the edge of the sample (1 296 K s^{-1}) well confirm value of 1 350 K s^{-1}, while the heat calculations for the middle of the sample (1 036 K s^{-1}) are decisive only when the average dT/dt is taken

into account. Both methods for determining the cooling rate are suitable in the case of the sample of 2 mm in diameter because all SEM and LOM images confirm the existence of the i-phase in the middle of the sample (in addition to the presence on the edge of the sample).

The cooling rate was the highest on the edge of the sample, therefore it was expected that there will be the highest fraction of the i-phase. Measurements of the fraction showed that the average fraction on the edge of the sample was 26.7 % and in the middle of the
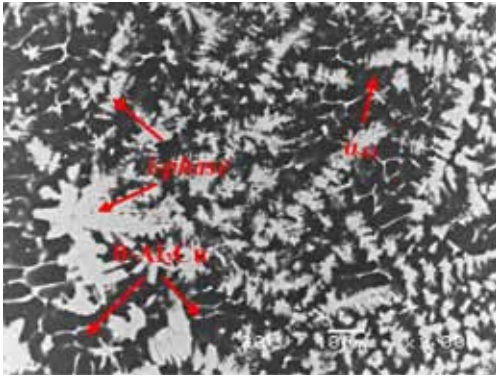

Figure 1. Microstructure of casting with 2 mm diameter (62MCuKO alloy) – SEM (BSE)
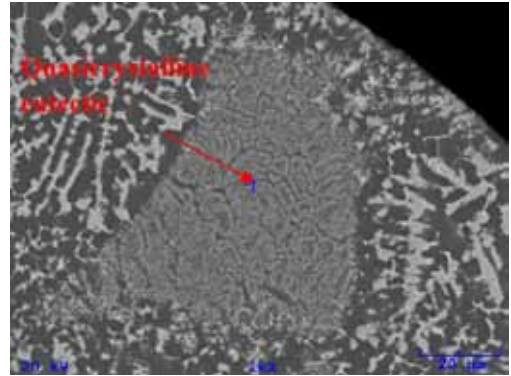
Figure 2. Very fine i-phase within the quasicrystalline eutectic – SEM (BSE)

Table 2. EDS analysis of the phases in the casting with 2 mm diameter (62MCuKO alloy); mass fractions w/% and atomic fractions x/%

	w(Al)	w(Mn)	w(Cu)	x(Al)	x(Mn)	x(Cu)	Phase
1	96.23	1.69	2.08	98.25	0.85	0.90	α_{Al}
2	96.51	2.15	1.34	98.34	1.08	0.85	α_{Al}
3	69.19	27.63	3.17	82.26	16.13	1.60	i-phase
4	71.74	24.92	3.61	83.85	14.36	1.80	i-phase
5	68.83	27.71	3.47	82.03	16.22	1.76	i-phase

Table 3. Results of the heat calculations for the casting with 2 mm diameter (62MCuKO alloy)

	Solidification start t/s	Solidification finish t/s	Solidification time t/s	Max. dT/dt K s^{-1}	Average dT/dt K s^{-1}
D = 2 mm (α_{max} = 2 500–1 700 W m^{-2} K^{-1})	0.16	0.76	0.6	1 296	1 036

sample it was 26 %. The difference is small probably due to the short size of the casting and due to the very small difference in time when the edge and the middle of the sample solidified.

Casting of diameter 4 mm (alloy 62MCuKO)

The microstructure consisted of the α_{Al} matrix, small amount of θ-Al_2Cu phase and dendritic i-phase (Figure 3). Dendrites had thick primary branches but they already grew the secondary ones. In the middle of the sample all dendrite branches were thicker, larger and longer and it was difficult to distinguish primary branches from the secondary. The i-phase in average contained atomic fractions 83.9 % Al, 13.2 % Mn and 1.2 % Cu (Table 4). Average composition of α_{Al} phase was (Table 4): 97.8 % Al, 1.0 % Mn and 1.2 % Cu. Again the content of copper in the matrix indicated presence of the θ-Al_2Cu precipitates.

In addition to the microstructural characterization the estimations of the cooling rate on the edge and in the middle of the sample were made. The cooling rate on the edge of the sample was approximately 800 K s^{-1} according to DAS measurements and about 650 K s^{-1} according to the heat calculations (Table 5). In the middle of the sample this estimations were 600 K s^{-1} and 520 K s^{-1}, respectively. It should be noted that the estimated values of cooling rates through DAS measurements are approximate, since dendritic morphology in some places was not representative. But from the SEM images it was obvious that the i-phase was present in the middle of the sample so the cooling rate should be at least 500 K s^{-1} in the middle of the sample (according to reference [7]). The calculated values were slightly lower that the cooling rates obtained from measurements of the DAS but in the same order of magnitude. The problem was that it is virtually impossible to determinate the accurate heat transfer coefficient which strongly depends on the given conditions of the casting. Furthermore, the model predicts the cooling of the sample without a temperature gradient in its cross-section.

Influence of the cooling rate on the formation of the i-phase is crucial. Fraction of the i-phase is also dependent on the cooling rate, so the measurements

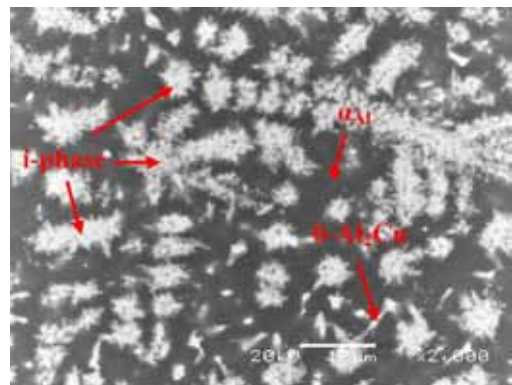**Figure 3.** Microstructure of casting with 4 mm diameter (62MCuKO alloy) – SEM (BSE)

Table 4. EDS analysis of the phases in the casting with 4 mm diameter (62MCuKO alloy)

	$w(Al)$	$w(Mn)$	$w(Cu)$	$x(Al)$	$x(Mn)$	$x(Cu)$	Phase
1	95.68	1.99	2.33	97.98	1.00	1.01	α_{Al}
2	94.71	2.10	3.19	97.54	1.06	1.40	α_{Al}
3	72.98	19.75	7.27	85.09	11.31	3.60	i-phase
4	72.44	22.33	5.24	84.60	12.81	2.60	i-phase
5	68.87	26.91	4.94	82.15	15.34	2.50	i-phase

Table 5. Results of the heat calculation for the casting with 4 mm diameter (62MCuKO alloy)

	Solidification start t/s	Solidification finish t/s	Solidification time t/s	Max. dT/dt K s^{-1}	Average dT/dt K s^{-1}
D = 4 mm (α_{max} = 2500–1700 W m^{-2} K^{-1})	0.202	1.349	1.147	648	516

of the fraction of the i-phase on the edge and in the middle of the sample were carried out. From the edge of the sample towards the center values decreased from 28.6 % to 26.5 %, which is consistant with the decreasing cooling rate.

Alloy 22MCuKO

Casting of diameter 2 mm (alloy 22MCuKO)

In addition to the α_{Al} matrix. the primary i-phase was present (Figure 4) along with the i-phase within the quasicrystalline eutectic. There were traces of the θ-Al$_2$Cu phase as well. The primary i-phase formed a 0.5 mm thick rim which extended from the surface into the specimen. The references[6, 7] also report the existence of only those phases. Quasicrystalline eutectic (α_{Al} + i-phase) had a typical skeletal form, made of thin needles which were thicker at the end. From the edge of the sample to the center the skeletons of i-phase and θ-Al$_2$Cu grew and interspaces were getting smaller. The matrix α_{Al} in average contained atomic fractions 96.5 % Al, 2.3 % Mn and 1.3 % Cu. The EDS measurements were not performed for the i-phase, while the particles were too fine and small.

Since the morphology of the i-phase was not dendritic, the DAS measurements were not possible. Cooling rates were estimated on the basis of the previous measurements and estimations (62MCuKO alloy), since the diameter was the same. It was assessed that the cooling rate on the edge of the sample was about 1 300 K s^{-1} and in the middle of the sample around 1 000 K s^{-1}. That

is quite possible considering the presence of the i-phase in the whole cross-section of the sample.

The 22MCuKO alloy contained considerably less manganese, therefore it was expected that the fraction of the i-phase in these castings will be lower than in the previously discussed castings (62MCu-KO alloy). Fraction of the i-phase was on the edge of the sample 8.7 % and in the middle 8.4 %. Once again the difference in the fractions between the edge and the middle of the sample was small, but it was large in comparison with the casting of the same diameter but different chemical composition.

Casting of diameter 4 mm (alloy 22MCuKO)

Casting of 4 mm diameter had microstructure composed of matrix α_{Al} and two binary eutectics $(\alpha_{Al} + \text{i-phase})$ and $(\alpha_{Al} + \theta\text{-Al}_2\text{Cu})$ (Figure 5). Primary i-phase was not detected like in the previous sample. Towards the center of the sample dendrite networks grew. Considering the typical morphology of the quasicrystalline eutectic and due to the smallness of i-phase only EDS measurements of the matrix α_{Al} were carried out. In average the α_{Al} phase contained atomic fractions 96.4 % Al, 1.5 % Mn and 2.1 % Cu.

Because of the absence of the dendrite morphology of the i-phase it was impossible to estimate cooling rate via DAS measurements. The estimates of the casting of the same diameter (4 mm) were taken; on the edge of the sample around 800 K s^{-1} and in the center 600 K s^{-1}. In addition to the value of 800 K s^{-1}, value of 600 K s^{-1} in the middle of the sample is reasonable, since the i-phase was present also in the entire area of the sample's center.

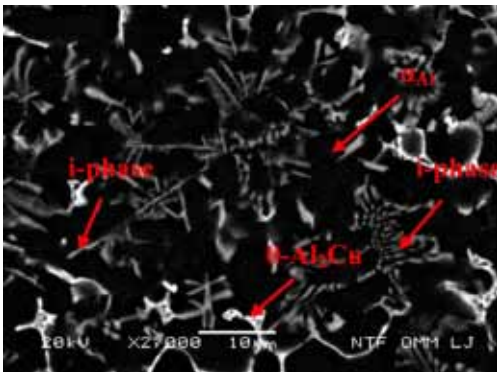Differences in cooling rate at the edge and the center of the sample should be

Figure 4. Microstructure of casting with 2 mm diameter (22MCuKO alloy) – SEM (BSE)
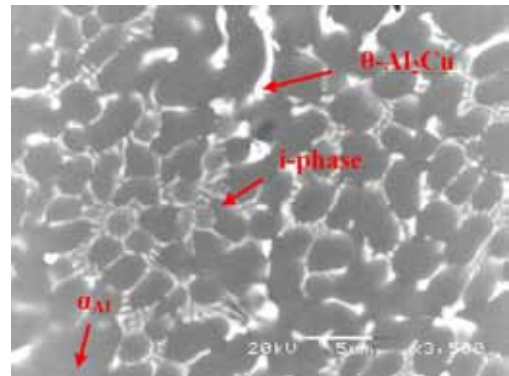

Figure 5. Microstructure of casting with 4 mm diameter (22MCuKO alloy) – SEM (BSE)

evident from measurements of fraction of the i-phase on the edge and in the middle of the sample. Average fraction of the i-phase on the edge of the sample was 6.1 % and then it increased (to 10.1 %), but at some point it started to decrease. In the middle of the sample fraction was 8.5 %. Obviously the points of measurements were not selected appropriately.

Conclusions

Based on the results of the constitution research, estimated cooling rates and fraction measurements of the i-phase, the following can be concluded:

- the addition of the beryllium and copper enables the formation of the quasicrystalls at lower cooling rates than that of the casting processed via melt spinning (where the cooling rates are of the order of 10^6 K s^{-1})
- in addition to the appropriate chemical composition the main influence on the fraction (shape, size distribution and size) of the i-phase is due to the cooling rate
- with increasing cooling rate the fraction of the i-phase increase in general, but the additional further studies and measurements are necessary
- i-phase dendrites in the case of the dendrite morphology with decreasing cooling rate grow, the primary

branches are thicker and in some places already the second start to grow. At the highest cooling rate (edges of the castings with diameter of 2 mm) the i-phase is very small and fine, therefore it is difficult to distinguish its morphology

- i-phase occurs both in primary form such as the part of the quasicrystalline eutectic
- method used for the heat calculations is appropriate for estimating the cooling rate in case of the smaller samples (diameters of 2 mm and 4 mm), as the values agree well with the reference[7] and measurements DAS
- in all the samples inevitable θ-Al$_2$Cu phase occurs. The desire is to eliminate and dissolve it all, which would additionaly contribute to the hardening when heat-treated.

References

[1] Zupanič, F., Bončina, T., Šušteršič, B., Anžel, I., Markoli, B. (2008): Microstructure of Al-Mn-Be melt-spun ribbons. *Mater. Charact., 59.* pp. 1245–1251.

[2] Rozman, N., Zupanič, F., Bončina, T., Grooger, W., Gspan, C., Hofer, F. (2009): Analytical TEM of Al-Mn-Be-Cu alloy, *Materials Science, 3.* pp. 205–206.

[3] Steurer, W., Deloudia, S. (2008): Fascinating quasicrystals. *Acta Crystallographica Section A. A64,*

pp. 1–11.

[4] Bončina, T. (2006): *Karakterizacija kvazikristalnih zlitin Al-Cu-Fe in Al-Mn-Be.* Magistrsko delo. Ljubljana: Univerza v Ljubljani 2006; 72 p.

[5] Spaić, S. (2002): *Fizikalna metalurgija. Zgradba kovinskih materialov. Strjevanje kovinskih talin.* Ljubljana: Univerza v Ljubljani 2002; 328 p.

[6] Bončina, T. (2010): *Stabilization and identification quasicrystalline phases in alloy of Al-Mn-Be.* Ph. D. Ljubljana: University of Ljubljana 2010; 143 p.

[7] Rozman, N. (2011): *Razvoj visokotrdnostnih aluminijevih zlitin s kvazikristali.* Ph. D. Maribor: Univerza v Mariboru 2011; 143 p.

[8] Štrekelj, N. (2011): *Influence of the cooling rate on the constitution of the Al-Mn-Be-Cu alloys.* Diploma work. Ljubljana: University of Ljubljana 2011. 78 p.

Development of intelligent knowledge-based computing environment for controling the proces parameters and nonmetalic inclusions in steels

Razvoj inteligentnega, na znanje oprtega računalniškega okolja za kontrolo procesnih parametrov in nekovinskih vključkov v jeklih

Uroš Krušič[1,*], Milan Terčelj[2], Goran Kugler[2] & Iztok Peruš[2]

[1]Metal Ravne, d. o. o., Koroška cesta 14, SI-2390 Ravne na Koroškem, Slovenia
[2]University of Ljubljana, Faculty of Natural Sciences and Engineering, Aškerčeva 12, SI-1000 Ljubljana, Slovenia

*Corresponding author. E-mail: uros.krusic@metalravne.com

Abstract: An intelligent knowledge-based computing environment for controling the steel production is proposed. CAE non-parametric mathematical model was developed based on the measured industrial data. Analysis of the obtained results reveals that there is a strong correlation between chemical composition of melts, Al blocs for dezoxidation and different supplements added at various stages, and nonmetalic inclusions. Relatively small number of input parameters taken into account in the existing model resulted in large scatter of the obtained results. Use of a higher number of input parameters will reduce the scatter and improve the prediction. It is evident that the standard ISO 4967 systematically overestimates some types of nonmetalic inclusions, which may be the result of a subjective human assessment or deliberately conservative estimate. The nonmetalic inclusions can be most effectively influenced at the early stages of the EAF process. As there is still long way to sufficiently describe the whole phenomenon of nonmetalic inclusions in steels, the results presented in this study are very promissing and they will eventualy lead us to the better models in the future.

Izvleček: Predlagano je inteligentno, na znanje oprto računalniško okolje za kontrolo proizvodnje jekla. Na podlagi izmerjenih industrijskih podatkov je bil razvit neparametrični matematični model CAE. Analiza dobljenih rezultatov je pokazala, da obstaja močna korelacija med kemično sestavo šarže, Al bloki za dezoksidacijo in drugimi dodatki, dodanimi v različnih fazah procesa, in nekovinskimi vključki. Zaradi relativno majhnega števila upoštevanih vhodnih parametrov je raztros rezultatov dokaj velik. Upoštevanje večjega števila vhodnih parametrov bo zagotovo zmanjšalo raztros in izboljšalo napovedi. Očitno je, da standard ISO 4967 sistematično precenjuje nekatere tipe nekovinskih vključkov, kar je lahko posledica subjektivnega vrednotenja posameznikov ali pa namerno bolj konservativne ocene. Na nekovinske vključke lahko najbolj učinkovito vplivamo v zgodnjih fazah EAF-procesa. Čeprav je pred nami še dolga pot, preden bo mogoče v celoti opisati fenomen nekovinskih vključkov, so rezultati, predstavljeni v tem prispevku, zelo spodbudni in nas bodo v prihodnosti pripeljali do boljših modelov.

Key words: steel production, SQL database, non-parametric models, CAE neural network, nonmetalic inclusions

Ključne besede: proizvodnja jekla, SQL-baza podatkov, neparametrični modeli, nevronska mreža CAE, nekovinski vključki

Introduction

Production of steel, which includes many intermediate stages with high energy consumption, is a complex and costly procedure. Optimization of steel manufacturing process is therefore highly desirable. It can be achieved through better in-depth understanding of various influential parameters which determine the technological path of material in the production process. The problem is extremely complex due to the large number of influential parameters and consequently there is still lack of useful comprehensive solutions in the everyday steel production. Luckily, artificial intelligence and modern information and communication technologies now offer better opportunities for solution of this problem.

In recent years we have witnessed an intensive development of both physical and metallurgical models which can adequately describe various processes taking place in steels during their thermo-mechanical processing as well as solutions in the field of artificial intelligence and optimization methods, which are possible by means of the modern computer technology.

Numerous publications demonstrate that the methods of artificial intelligence provide a set of tools with great practical value for complex industrial processes.[1–5] Range of applications of artificial intelligence methods in materials research is wide.[6–10] Practical applications can be found both in research of metallic materials in virtually all phases of their production, such as casting, rolling, forging, heat treatment, etc.[10–16] Especially popular are applications of neural networks, which are becoming an indispensable component of such systems for manufacturing automation and IT solutions that are designed to process control of metallurgical processes.[17–19] Recently, Fazel-Zarandi and Ahmadpour[2] have used neural networks in developing expert system to control the parameters of electric arc furnaces in steel by means of a variety of independent modules, which coordinated the operation with regard to other modules. Zhou[3] used the dynamic neural networks and computer vision to predict the quality of the sintered products. Badheshia and colleagues used the methods of artificial intelligence in the development of materials and to find relations between the various parameters of their production. [6–8, 15, 16] Reviewed literature reveals that neural networks are often used to find the complex relations between the large number of influential parameters within individual processes. Research which address the entire manufacturing process or, where the method of artificial intelligence would be coupled with optimization methods that would allow the search of optimal values of influential parameters, are very rare.

In this paper we present briefly the results of research which was focused on the development of intelligent knowledge-based computing environment for controling and optimizing the real industrial steel production. Due to the complexity of the problem only the solutions of aquirying and managing information from real steel production, development of non-parametric model and analysis of underlying trends in the formation of nonmetalic inclusions, defined by different standards, are presented.

IT SOLUTION FOR INFORMATION MANAGEMENT AND OPTIMIZATION IN STEEL PRODUCTION

General

In practice, a lot of the optimization in steel-making process is still based on »trail and error« procedures and/or expert knowledge of process engineers, who based on their empirical experience of tuning the process parameters control the production. From a theoretical point of view it is the most appropriate to describe the manufacturing processes by means of abstract mathematical models in order to to

represent mathematical relationships. However, due to the problems in the real steel production mentioned in the introduction section, these processes can be most effectively simulated by analogue models based on electronic devices (computers) using the measured data. Whitin this there are two main problems: (1) data aquisition and mathematical presentation of data as well as expert knowledge and (2) development of appropriate analog models with modern computer technology. It is clear that measurements and mathematical models represent mutually interdependent components in optimizing steel production.

Data acquisition in Metal Ravne has been implemented several years ago. DBSteel is an integrated software solution for process control in the steel production. It was implemented by Siemens VAI Metals Technologies. The solution enables comprehensive data management process, quality control, planning process, steel production control per charge, networking and communication with the ERP (Enterprise Resource Planning) systems and to generate various reports.
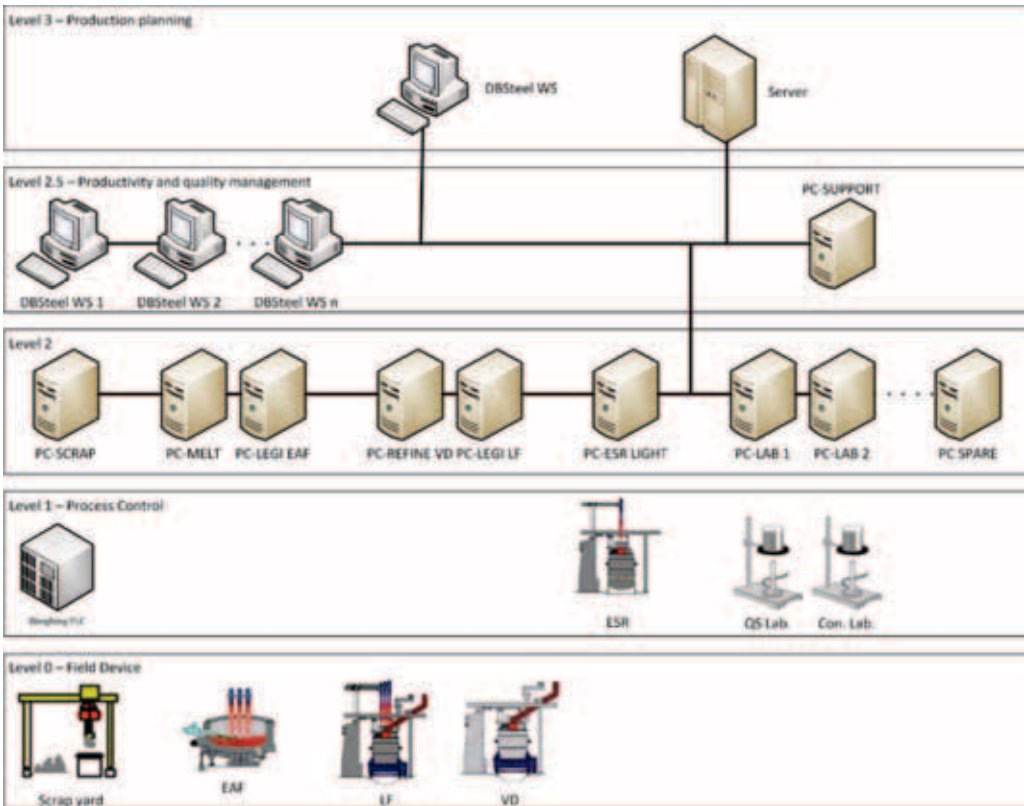

Figure 1. Schematic presentation of the main building blocks of DBSteel integrated software solution.

Client - server environment

The server part consists of a High-Availability (HA) cluster,[20] nine processing computers and fifteen workstations (Figure 1). HA cluster is based on IBM BladeCenter™ technology and is composed of three physical servers, where completely identical combination of 64-bit operating system Windows Server 2008 R2 and relational database Microsoft Windows SQL Server 2008 R2 is installed.

All three servers connected into a HA cluster use database mirroring technique. One of the servers plays the role of principal database server, another server is a mirror site, while the third server provides a smooth transition to the secondary (MIRROR) server in the event of principal server failure.

Processing computers

Figure 1 shows different levels and connection between those levels of the DBSteel integrated software solution. At the zero-level there is a production unit. First level consists of programmable logic controllers (PLC's), e.g. for weighing system. PLC is special computer, that is used for automation of electromechanical processes and designed to operate in heavy industrial conditions (vibration, electrical noise and dust resistant). Processing computers on the second level control/support the production process, while the

workstations on the third level enable the planning of charges.

Processing computers control the following operations:

- PC-scrap supports the preparation of inlay material (scrap metal, overhead cranes, computerized scales). By using the specific software the module operator determines the composition of the charge, reads data from the scale, records inlay material consumption, etc.
- PC-MELT and PC-LEGI EAF support the melting and then alloying process on the electric arc furnace (EAF), respectively. The software is intended to record the various events (for example, charge start time), to record consumption of electricity, recording the results, obtained with CELOX device, etc.
- PC-REFINE VD in PC-LEGI LF support the process of secondary treatment of steel in a vacuum ladle furnace (LF/VD).
- PC-ESR LIGHT supports the electro slag remelting (ESR).
- PC-LAB 1 in PC-LAB 2 are special-purpose computers for supporting the implementation of chemical analysis in the plant and a chemical laboratory. PC-LAB 1 is connected with the spectrometer at the plant site while PC-LAB 2 is connetced with two spectrometers located in the chemical laboratory.
- PC-SPARE is a spare computer that

is ready to replace any of the above eight processing computers in case of their failure.

Data structure

Physical partition of steel-making process is followed by the similar structure of the DBSteel database. Description of the tables revelas that each process is characterized by a specific prefix. Thus, for example, table, which is linked to the processes in the electric arc furnace, gets the prefix »EAF«, table which is linked to vacuum furnaces and ladle gets the prefix »LF/VD«, etc. The key tables are:

- The main table of charges at the EAF
- The table of events at the EAF
- The main table in charges at the LF/VD
- The table of events at the LF/VD

Structure of the databases is well documented. After applying different scripts we got one database for further processing. It contains numerical empirical data which allow a mathematical description of the various phenomena in the steel production process (see Chapter 3).

Matemathical tools for modeling of manufacturing processes

Development of appropriate mathematical models is necessary to optimize the steel production at high-tech level. Today, in addition to the usual physical models, the models which exploit the principles of artificial intelligence, especially neural networks, are widely used. Among the neural networks is the most common use of BP neural networks, which describe the phenomenon on the basis of measured data and obtained results. Unfortunately, the rate of learning for very complex problem with large number of parameters and with large database is relatively slow and depends on settings of the parameters of learning. An additional weakness of these networks for »real-time« production is that the BP network must be constantly retrained with new data supply in order to improve the optimization. We have therefore in this study decided to use CAE neural network, [21–23] which enables faster analyses and is significantly more robust.

MATHEMATICAL MODELING OF INCLUSIONS BY USING CAE NEURAL NETWORK

Any type of nonmetalic inclusion (i.e. type A_d according to the ISO 4967 standard [24]) of a specimen (e.g. charge) is characterized by a sample of observations/experiments on N test specimens. The mathematical description of the observation/experiment on a single specimen is called a model vector. Consequently, the whole phenomenon can be described by a finite set of model vectors

$$\{\mathbf{X}_1,....,\mathbf{X}_n,...,\mathbf{X}_N\} \tag{1}$$

It is assumed that the observation/experiment on one particular specimen can be described by a number of variables, which are treated as components of a model vector

$$\mathbf{X}_n = \{b_{n1}, ..., b_{nl}, ..., b_{nD}, c_{n1}, ...c_{nk}, ..., c_{nM}\} \tag{2}$$

The vector $\mathbf{X}_n$ can be further composed of two truncated vectors $\mathbf{B}$ and $\mathbf{C}$

$$\mathbf{B}_n = \{b_{n1}, ..., b_{nl}, ..., b_{nD}\}$$

and $\mathbf{C}_n = \{c_{n1}, ..., c_{nk}, ..., c_{nM}\} \tag{3a}$

Vector $\mathbf{B}_n$ is complementary to vector $\mathbf{C}_n$ and therefore their concatenation yields the complete data model vector $\mathbf{X}_n$. The prediction vector, too, is composed of two truncated vectors, i.e. the given truncated vector $\mathbf{B}$ and the unknown complementary vector $\hat{\mathbf{C}}$

$$\mathbf{B} = \{b_1, ..., b_l, ..., b_D\}$$

and $\hat{\mathbf{C}} = \{\hat{c}_1, ..., \hat{c}_k, ..., \hat{c}_M\} \tag{3b}$

The problem now is how an unknown complementary vector $\hat{\mathbf{C}}$ can be estimated from a given truncated vector $\mathbf{B}$ and the model vectors $\{\mathbf{X}_1, \ldots, \mathbf{X}_n, \ldots, \mathbf{X}_N\}$, i.e. how the inclusion $\hat{A}_d$ can be estimated from known input parameters and the available data in the database. By using the conditional probability density function, the optimal estimator for the given problem can be expressed as

$$\hat{c}_k = \sum_{n=1}^{N} A_n \cdot c_{nk}, \quad A_n = \frac{a_n}{\sum_{i=1}^{N} a_i}$$

and $\tag{4}$

$$a_n = \frac{1}{(2\pi)^{D/2} w^D} \exp\left[-\sum_{l=1}^{D} \frac{(b_l - b_{nl})^2}{2w^2}\right]$$

where $\hat{c}_k$ is the estimate of the k-th output variable, c_{nk} is the same output variable corresponding to the n-th model vector in the database, N is the number of model vectors in the database, b_{nl} is the l-th input variable of the n-th model vector in the database (e.g. b_{n1}, b_{n2}, b_{n3}, ..., b_{nL}), and b_l is the l-th input variable corresponding to the prediction vector. D is the number of input variables, and defines the dimension of the sample space. Note that Equation (4) requires the input parameters to be normalized, generally in the range from 0 to 1 if we want to use the same width w of the Gaussian function for all of the input variables (dimensions).

The Gaussian function is used for smooth interpolation between the points of the model vectors. In this context the width w is called the "smoothing" parameter. It determines how fast the influence of data in the

sample space decreases with increasing distance from the point whose coordinates are determined by the input variables of the prediction vector.

A general application of the method does not include any prior information about the phenomenon. Equation suggest that the estimate of an output variable is computed as a linear combination of truncated vectors C_n, while the coefficients A_n are non-linear functions of all the input variables (B_n) in the database. Thus, non-linear phenomena can be modeled by this approach. The weights A_n depend on the similarity between the input variables of the prediction vector, and on the corresponding input variables pertinent to the model vectors stored in the database. Consequently, the unknown output variable is determined in such a way that the computed vector, composed of given and estimated data, is most consistent with the model vectors in the database.

An intermediate result in the computational process is the estimated probability density function $\hat{\rho}$ of known input variables

$$\hat{\rho} = \frac{1}{N}\sum_{n=1}^{N} a_n \qquad (5)$$

It helps to detect the possible less accurate predictions due to the data distribution in the database and due to local extrapolation outside the data range. The higher the $\hat{\rho}$ value is, the

more steel ingots (relatively to the total number of test steel ingots in database) with input parameters similar to the input parameters of the prediction vector exist in the database.

In the case of using CAE for the estimation of the inclusions, which depends on, e.g. three input parameters, namely content of oxygen (O) and sulphur (S) in charge on one side and the amount of Al blocs (Al) relative to the total weight of charge on the other side, the equation for a_n can be written as:

$$a_n = \frac{1}{(2\pi)^{3/2} w^3} \exp \qquad (6)$$

$$\left[-\frac{(O - O_n)^2 + (S - S_n)^2 + (Al - Al_n)^2}{2w^2} \right]$$

Results and discussion

Due to the complexity of the entire process of steel-making, in this paper only the problem of nonmetalic inclusions is studied and discussed. Note, that all chemical analyses for different charges, along with information about the plant where the sample was taken from, the grade of the sample, sample number, etc. are stored in DBSteel database as separate entries. Consequently, sample numbers in the range between 1 and 4 indicate charge sample taken during steel processing at EAF, while sample numbers in the range between

5 and 9 indicates charge samples taken during steel processing at LFVD.

Standards used for the determining the inclusion content of steel
Purity of steel is defined by the amount of nonmetallic inclusions. Nonmetallic inclusions can be found practically in any steel. The quantity, chemical composition and distribution of inclusions depends on the manufacturing process of steel. In general, nonmetallic inclu-

sions lower the quality, workability and mechanical properties of steel.

Different test methods for determination of content of nonmetalic inclusions exist (e.g. standards ISO 4967 [24], ASTM M45 [25] – **ISO**, DIN 50 602 [26] – **M** and **K** method). They cover a number of recognized procedures (macroscopic and microscopic methods) for determining the nonmetallic inclusion content of wrought steel. The methods
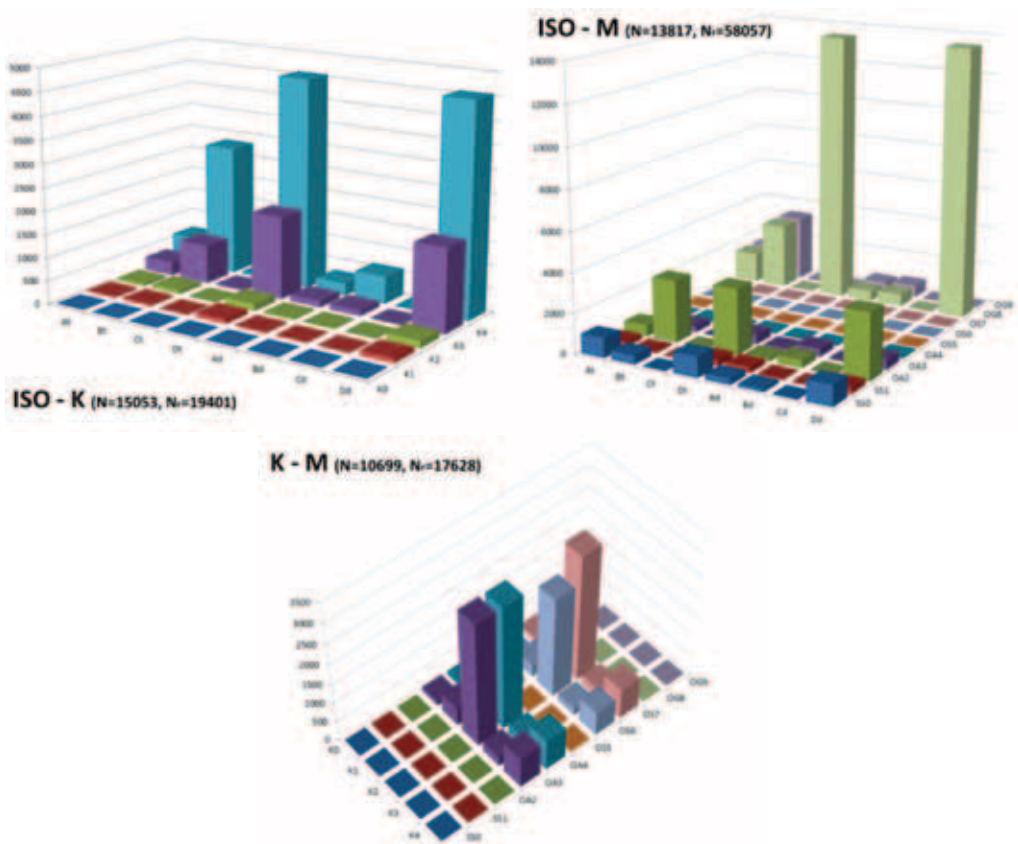

Figure 2. Correlations between different standards, taking into consideration only the incidence but not the absolute value of the inclusions. *N* and *Nr* indicate the number of charges and number of inclusions, respectively, used in the analysis.

are primarily intended for rating inclusions. Constituents such as carbides, nitrides, carbonitrides, borides, and intermetallic phases may be rated using some of the microscopic methods. However, in order to model the phenomena of inclusions mathematicaly (i.e. developing of the non-parametric model), a mathematical representation of such knowledge is neeeded. To this end, we first look for correlations between different standards in order to identify the most appropriate method for modeling inclusionss. The purpose of this study was not to understand precisely the methods and physical background of each type, size and amount of inclusions, but the mathematical formalization of knowledge, contained in different standards.

DBSteel database contains information of the same charges that were inspected using two or three standars simultaneously. Correlations between different standards, taking into consideration only the incidence but not the absolute value of the inclusions, were shown in Figure 2. Note that in one charge different type of inclusions may appear (therefore $Nr \geq N$). Graphs indicate that the standards differ from each other and describe inclusions in different ways. Consequently, customers according to their needs, require consideration of inclusions using the desired standard. Figure 2 indicates that mapping from one standard to another

is more reliable than vice versa (e.g. mapping ISO to K or ISO to M).

Effectivness of the non-parametric CAE model

The effectivness of the CAE model can be estimated by the average prediction error E_k. It is defined for k-th output variable and can be determined with the "leave one out cross validation method". The method computes the prediction of k-th inclusion for every charge sample, whereas the predicted k-th charge sample is excluded from the database. With averaging of the absolute errors of predictions for all N charge samples E_k is calculated as:

$$ E_k = \frac{1}{\overline{c}_k} \sqrt{ \frac{1}{N} \sum_{n=1}^{N} \left(\hat{c}_{nk} - c_{nk} \right)^2 } \qquad (7) $$

where $\overline{c}_k$ is the average of the known k–th outputs of all the model vectors c_{nk} (charge samples) and $\hat{c}_{nk}$ is the prediction of the measured value c_{nk} of the k–th output (inclusion of some type) of the n-th model vector (charge sample).

Figure 3 shows the results of »leave one out cross validation method« for two different smoothing parameters. Studied is the inclusion of type Ad according to the ISO 4967 standard. In the CAE non-parametric model some important chemical elements (C, S, Si, Mn, …), some most influential suplements (FeSi, FeCrC, …), Al blocs and oxygen were

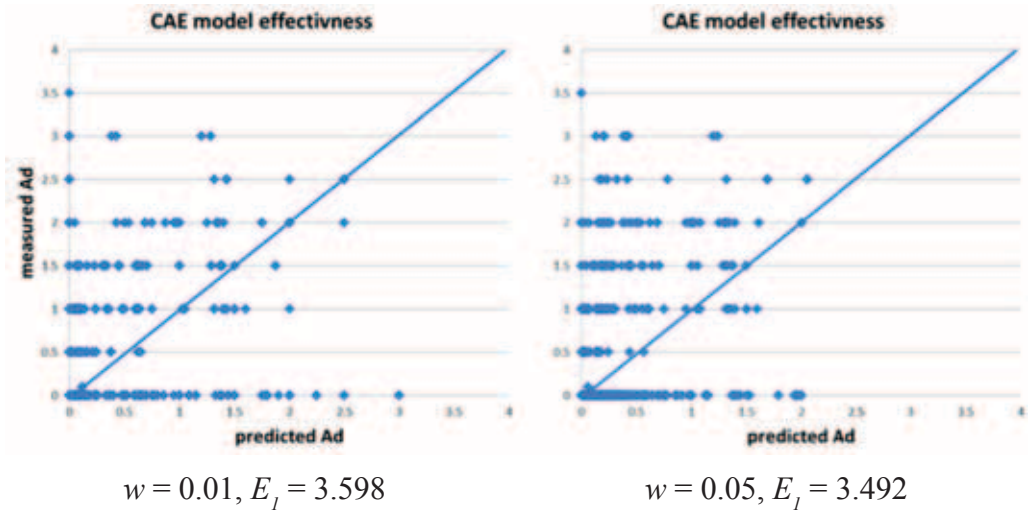$$w = 0.01, \; E_1 = 3.598 \qquad\qquad w = 0.05, \; E_1 = 3.492$$

Figure 3. Results of the »leave one out cross validation method« for inclusion type Ad, using two different smoothing parameters.

taken into account. The obtained results reveal large scatter. It can be concluded that (1) there is high uncertainty in the (subjective) determination of inclusions, and (2) in order to reduce the scatter in the predictions more influential input parameters must be taken into account. Nevertheless, existent model can give a sound qualitative relations between input parameters and different types of inclusions, as shown in the next section. The optimal smoothing parameter was found to amount around 0.05, however, in order to reveal clear qualitative relationships somewhat larger value was used (e.g. 0.1 or 0.2).

Influence of important parameters on inclusions according to the ISO 4867 standard

Due to the limited space only a few selected results are presented and discussed in this paper. In order to show different behaviour in nonmetalic inclusions, results for four different types, namely Ad, At, Dd and Dt are shown and discussed.

Figure 4 reveals that higher content of sulphur increases nonmetalic inclusions of type At and Ad. Its influence is unfavourable, but more for inclusions of type Ad. Influence of oxygen (Figure 5) is very important and amounts up to 5 % of total contribution. In general, more oxygen increases nonmetalic inclusions of type Dd, whereas the influence of Al blocs is relatively small. Note, that use of smaller value of smoothing parameter reveals localy larger influence of Al blocs which may be taken into account when optimization is applied.

Figure 6 reveals the influence of oxygen and Al blocs on nonmetalic inclusions of type Dt. Influence of both parameters is now reversed. Moreover, in absolute terms, both influences are small and relatively insignificant.
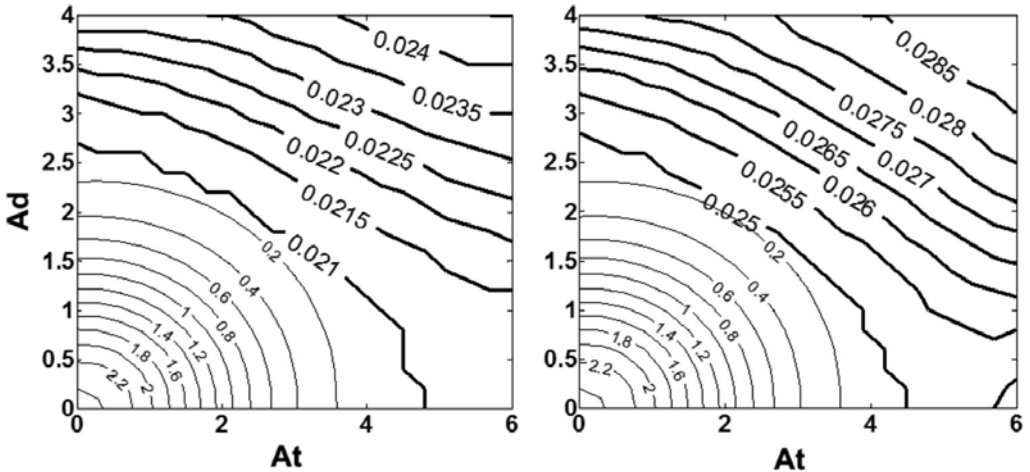

Figure 4. Influence of sulphur (S) after taking first (left) and second (right) charge sample on nonmetalic inclusions At and Ad.

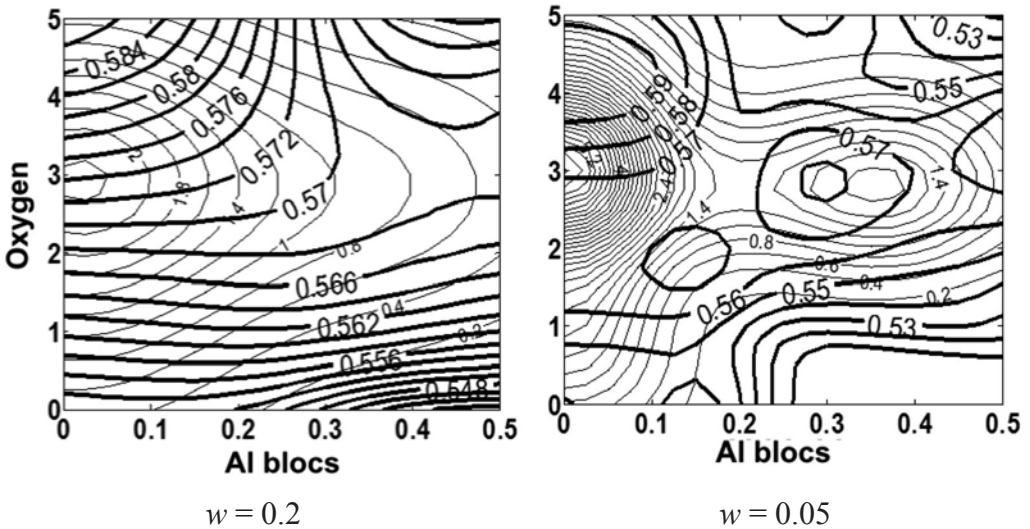

$w = 0.2$ $w = 0.05$

Figure 5. Influence of Al blocs and oxygen (tapping weight in mass fractions $w/\%$) on nonmetalic inclusion Dd after taking second charge sample.

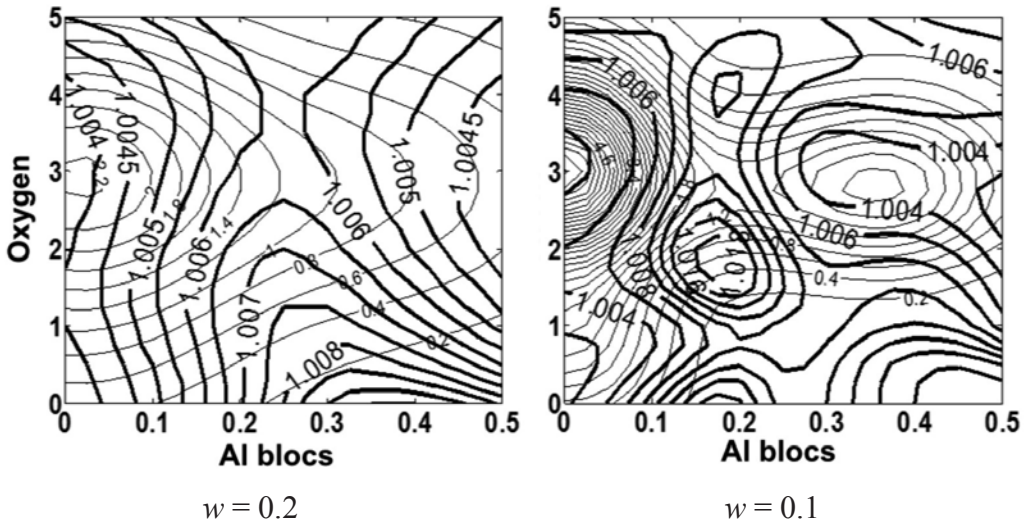$w = 0.2$ $w = 0.1$

Figure 6. Influence of Al aluminium blocs and oxygen (tapping weight in mass fractions w/%) on nonmetalic inclusion Dt after taking second charge sample.

In general, it can be observed the important impact of different input parameters at different stages, suggesting that a specific physical phenomena is associated with a specific type of the nonmetalic inclusion. The results also suggest that some types of inclusions can be influenced more efficiently at earlier stages and some types of inclusions at later stages of the production process.

CONCLUSIONS

In the paper the development of intelligent knowledge-based computing environment for controling the processes in the real industrial steel production was presented. The problem addressed is extremely complex due to the large number of influential parameters. Application of modern information and communication technologies and some artificial intelligence methods enables us to develop and propose one possible solution to this problem.

Within this study the CAE non-parametric mathematical model of nonmetalic inclusions was developed. Analysis of the obtained results lead us to the folowing conclusions:

- There is a strong correlation between chemical composition of melts, Al blocs for dezoxidation and different supplements added at various stages, and nonmetalic inclusions. Relatively small number of input parameters (a limited number of elements of chemical com-

position and a limited number of some most important suplements) taken into account in the existing model reveals large scatter of the obtained results. It is expected that use of a higher number of input parameters will reduce the scatter and improve the prediction.

- It is evident that the standards ISO 4967 and ASTM E45 systematically overestimates the value of smaller At (between 0.5 and 1.5). This probably result from a subjective human assessment or deliberately conservative estimate of nonmetalic inclusions by the producer. It should also be noted that the standard itself has shortcomings which may result in the above overestimations, when it tries to address a physical phenomenon, which is not linear.

- The majority of nonmetalic inclusions can be most effectively influenced at the early stages of the EAF process (e.g. during the time of taking the first or second charge samples). But closer to the end of the process we approach the harder it become to influence the nonmetalic inclusions.

There is still long way to sufficiently describe the whole phenomenon of nonmetalic inclusions in steels. However, the results presented in this study show that the entire process can be fully mathematicaly described and then optimized in order to minimize the nonmetalic inclusions.

Akcnowledgement

References

[1] Schlang, M., Lang, B., Poppe, T., Runkler, T. & Weinzierl, K. (2001): Current and future development in neural computation in steel processing. *Control Engineering Practice*, Vol. 9, pp. 975–986.

[2] Fazel Zarandi, M. H., Ahmadpour, P. (2009): Fuzzy agent-based expert system for steel making process. *Expert Systems with Applications*, Vol. 36 , No. 5, pp. 9539–9547.

[3] Zhou, S. M. (1995): Combining dynamic neural networks and image sequences in a dynamic model for complex industrial production processes. *Expert Systems with Applications*, Vol. 16, No. 1, pp. 13–19.

[4] Canz, T. & Jagdale, S. (1995): Decision support for manufacturing using artificial neural-networks.

Journal of Materials Processing Technology, Vol. 52, No. 1, pp. 9–26.

[5] D'Errico, G. E. (2001): Fuzzy control systems with application to machining processes. *Journal of Materials Processing Technology*, Vol. 109, No. 1–2, pp. 38–43.

[6] Bhadeshia, H. K. D. H. (1999): Neural Networks in Materials Science, *ISIJ International*, Vol. 39, pp. 966–979.

[7] Bhadeshia, H. K. D. H. (2009): Neural networks and information in materials science. *Statistical Analysis and Data Mining*, Vol. 1, pp. 296–305.

[8] Bhadeshia, H. K. D. H. (2009): On the Performance of Neural Networks in Materials Science. *Materials Science and Technology*, Vol. 25, pp. 504–510.

[9] Malinov, S. & Sha, W. (2003): Software products for modelling and simulation in materials science. *Computational Materials Science*, Vol. 28, No. 2, pp. 179–198.

[10] Sha, W. & Edwards, K. L. (2007): The use of artificial networks in materials science based research. *Materials and Design*, Vol. 28, pp. 1747–1752.

[11] Hancheng, Q., Bocai, X., Shangzheng, L. & Fagen, W. (2002): Fuzzy neural network modeling of material properties. *Journal of Materials Processing Technology*, Vol. 122, No. 2–3, pp. 196–200.

[12] Terčelj, M, Turk, R., Kugler, G. & Peruš, I. (2008): Neural network analysis of the influence of chemi-

cal composition on surface cracking during hot rolling of AISI D2 tool steel. *Comput. mater. sci.*, Vol. 42, pp. 625–637.

[13] Večko-Pirtovšek, T, Kugler, G., Peruš, I. Terčelj, M. (2009): Towards improved reliability of the analysis of factors influencing the properties on steel in industrial practice. *ISIJ int.*, Vol. 49, No. 3, pp. 395–401.

[14] Lee, W. B., Cheung, C. F. & Li, J. G. (2001): Applications of virtual manufacturing in materials processing. *Journal of Materials Processing Technology*, Vol. 113, No. 1–3, pp. 416–423.

[15] Bhadeshia, H. K. D. H., Singh, S. B., MacKay, D. J. C., Carey H. & Martin, I. (1998): Neural Network Analysis of Steel Plate Processing, Ironmaking and Steelmaking, Vol. 25, pp. 355–365.

[16] H. K. D. H. Bhadeshia, R. C. Dimitriu, S. Forsik, J. H. Pak & J. H. RyuLi, Y. (2006): Predicting materials properties and behavior using classification and regression trees. *Materials Science and Engineering: A*, Vol. 433, No. 1–2, pp. 261–268.

[17] Monostori, L., Viharos, Z. J. & Markos, S. (2000): Satisfying various requirements in different levels and stages of machining using one general ANN-based process model. *Journal of Materials Processing Technology*, Vol. 107, No. 1–3, pp. 228–235.

[18] Narayanan, V. (1995): Systems for the prediction of process param-

eters. *Journal of Materials Processing Technology*, Vol. 54, No. 1–4, pp. 64–69.

[19]   Perzyk, M., Biernacki, R. & Kochanski, A. (2005): Modeling of manufacturing processes by learning systems: The Bayesian classifier versus artificial neural networks. *Journal of Materials Processing Technology*, Vol. 164–165, pp. 1430–1435.

[20]   SIMATIC IPC847C, Höchste Erweiterbarkeit bei höchster Industriefunktionalität – mit Intel® Core™ Prozessoren (i7, i5, i3), http://www.automation.siemens.com/mcms/pc-based-automation/de/industrie-pc/rack-pc/simatic-ipc847c/Seiten/Default.aspx

[21]   Grabec, I., Sachse, W. (1997): Synergetics of Measurement, Prediction and Control, Springer: Berlin.

[22]   Peruš, I., Poljanšek, K. & Fajfar, P. (2006): Flexural deformation capacity of rectangular RC columns determined by the CAE method.

Earthquake eng. struct. dyn., Vol. 35, pp. 1453–1470.

[23]   Peruš, I. & Dolšek, M. (2009): The error estimation in the prediction of ultimate drift of RC columns for performance-based earthquake engineering. *RMZ – Materials and Geoenvironment*, Vol. 56, No. 3, pp. 322–336.

[24]   ISO 4967, International standard: Steel – Determination of content of nonmetalic inclusions – Micrographic method using standard diagrams, Second Edition, 1998, Geneve, Switzerland.

[25]   ASTM International, E45 – 05: Standard test methods for determining the inclusion content of steel, December 2005, USA; DOI: 10.1520/E0045-05.

[26]   DIN 50 602, Metalographic test methods; microscopic examination of special steels using standard diagrams to assess the content of non-metalic inclusions, September 1985, Germany.

Determination of hot workability and processing maps for AISI 904L stainless steel

Vroča preoblikovalnost nerjavnega jekla AISI 904L ter izračun procesnih map

Peter Fajfar[1],*, Boštjan Bradaškja[2], Boštjan Pirnar[2] & Matevž Fazarinc[1]

[1]University of Ljubljana, Faculty of Natural Sciences and Engineering, Aškerčeva 12, SI-1000 Ljubljana, Slovenia
[2]Acroni, Ltd., Research and Development, Cesta Borisa Kidriča 44, SI-4270 Jesenice, Slovenia

*Corresponding author. E-mail: peter.fajfar@omm.ntf.uni-lj.si

Abstract: Hot workability and microstructural evolution in dependence to deformation conditions for AISI 904L, super-austenitic stainless steel has been investigated on the basis of hot compression tests conducted on a thermo-mechanical simulator, Gleeble 1500D. Processing maps were calculated for various deformation conditions and correlated to the stability maps. An extensive microstructural analysis was conducted and a map of microstructures in correlation to deformation conditions was structured. This will all serve as a basis for better understanding of microstructural processes involved during the production of this steel.

Izvleček: S termomehanskim simulatorjem Gleeble 1500D sta bila preiskovana preoblikovalnost v vročem in razvoj mikrostrukture superavstenitnega nerjavnega jekla AISI 904L. Procesne mape in mape nestabilnosti so bile preračunane za različne stopnje deformacije, prav tako je bila izdelana tudi karta mikrostruktur v odvisnosti od preoblikovalnih parametrov. Taka analiza se uporablja za boljše razumevanje mikrostrukturnih procesov, ki se pojavljajo med vročim preoblikovanjem preiskovanega jekla.

Original scientific paper

INTRODUCTION

AISI 904L is a non-stabilized, low-carbon, high-alloy superaustenitic stainless steel. These types of austenitic stainless steels are known to have very high ductility, formability and exceptional toughness.[1–4] These characteristics are present through a wide temperature range as a result of a single phase structure.

Because of the excellent corrosion resistance AISI 904L is manly used in highly aggressive environments.[5, 6] It has a very good oxidation resistance and retains strength at elevated temperatures.[7] The widespread of use is limited by the production costs on account of high nickel and molybdenum content and can reach high prices on the market compared to similar stainless steels. Thus the knowledge about the processes involved during hot deformation is of a great importance to minimize the processing costs and optimize the processing parameters and insure the uniform characteristics of the end product. The literature overview has shown that no studies of its hot deformation behavior and microstructural evolution during hot deformation were conducted.

The goal of this study was to investigate the hot workability and microstructural evolution during hot deformation, as a basis for process optimization and better understanding of the microstructural processes involved during production of this steel. The uniaxially deformed specimens were metallographically examined using light optical microscopy (LOM).

Gathered data from the experiments was used to calculate the processing maps for different logarithmic deformations and coupled with instability, which can be used in correlation with the microstructure maps to determine the optimal processing parameters during the production of this steel grade.

MATERIALS AND METHODS

The material used in this study is superaustenitic stainless steel AISI 904L. The higher content of copper in the AISI 904L enhances its corrosion resistance to strong reducing acids, e.g., sulphuric acid. Cylindrical specimens with an initial diameter of 8 mm and a height of 12 mm were machined from a 20-mm-thick, rolled, annealed plate, with its chemical composition listed in Table 1.

Table 1. Chemical composition of the AISI 904L stainless steels in mass fractions, (w/ %)

	C	Cr	Ni	Si	Mn	Mo	N	Cu	P	S
AISI 904L	0.0074	19.45	23.31	0.25	1.56	4.19	0.069	1.41	0.019	0.001

A computer-controlled, Gleeble 1500D thermo-mechanical simulator was used for the hot, uniaxial, isothermal compression tests. To reduce the friction between the specimen and the tool, and to avoid their mutual welding, a graphite lubricant foil and a 0.05 mm tantalum foil, respectively, were used. The temperature was measured at the central part of the specimen, using a spot-welded S-type thermocouple.

The testing was performed in the temperature range between 850 °C and 1 200 °C in 50 °C steps and at five different strain rates (0.001 s⁻¹, 0.01 s⁻¹, 0.1 s⁻¹, 1 s⁻¹ and 5 s⁻¹). The specimens were heated to 1 200 °C with a heating rate of 10 K/s, followed by a 5 min soaking time at 1 200 °C. The temperature was subsequently lowered at 3 K/s to the deformation temperature, where it was held for another 5 min before deformation. The maximum true strain was set to 0.9. After the deformation the specimens were rapidly quenched into water (quench time <1 s).

True stress vs. logarithmic strain curves were calculated, taking into account the heat generated due to the high strain rates. The temperature rise was compensated for by applying the method proposed by Liu et al. [9]

The deformed specimens were cut along the mid-plane and metallographically prepared by grinding, polishing and electrolytic etching. Light optical microscopy was used to observe the microstructural features in each sample.
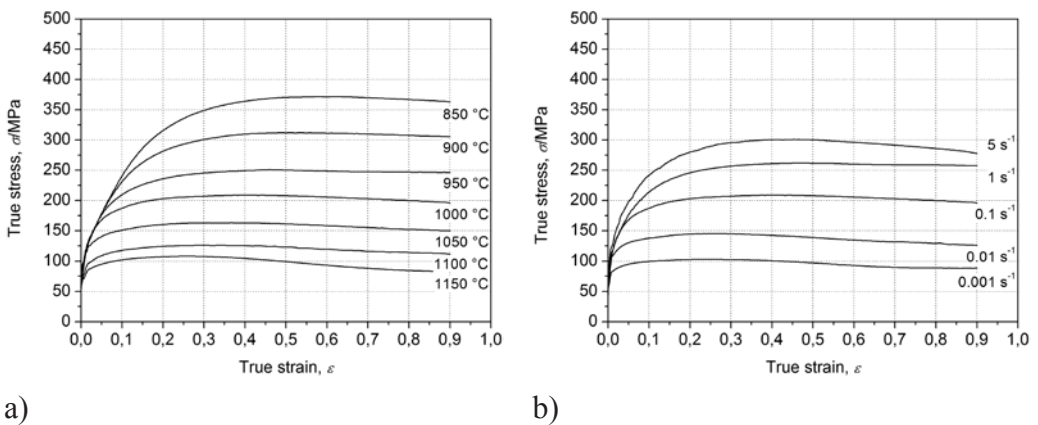

Figure 1. True stress vs. strain curves for the AISI 904L material deformed a) with strain rates of 0.1 s⁻¹ and b) at 1 000 °C.

Results and discussion

Compression tests

Typical true stress vs. trues strain curves are presented in Figure 1 for strain rates of 0.1 s⁻¹ and deformed at 1 000 °C, respectively. After the initial deformation hardening, softening behavior occurs. It is attributed to dynamic recrystallization (DRX), which was later on confirmed by microstructural analysis. The flow curves of the tests performed at higher temperature and lower strain rates (Figure 1a) show steady state behavior after initial softening. This effect is not present at the flow curves of samples deformed below 1 100 °C and at higher strain rate than 1 s⁻¹.

Processing maps

With the use of data, gathered during compression tests, processing maps were calculated and the windows of instable deformations were calculated. Processing maps are developed on the basis of a dynamic material model (DMM) which has been suggested and widely used by the group of Prasad. [10–11] The processing maps of the material can be described as an explicit representation of its response to the imposed process parameters. It is a superimposition of the efficiency of power dissipation and an instability map.

The work-piece under hot deformation conditions works as an essential ener-

gy dissipater for this model. The constituent equation describes the manner in which energy (P) is converted at any instant into two forms, thermal energy (G) making temperature increase and microstructural change caused by transform of metallurgical dynamics (J), which are not recoverable. In general, most of the dissipation is due to a temperature rise and only a small amount of energy dissipates through microstructural changes. The power partitioning between G and J is controlled by the constitutive flow behavior of the material and is decided by the strain rate sensitivity (m) of flow stress as shown in the equation

$$\frac{dJ}{dG} = \frac{\dot{\varepsilon}\, d\overline{\sigma}}{\overline{\sigma}\, d\dot{\varepsilon}} = \frac{\dot{\varepsilon}\,\overline{\sigma}\, d\ln\overline{\sigma}}{\overline{\sigma}\,\dot{\varepsilon}\, d\ln\dot{\varepsilon}} \approx \frac{\Delta \lg\overline{\sigma}}{\Delta \lg\dot{\varepsilon}} = m \quad (1)$$

where ε is true deformation, σ is true stress and $\dot{\varepsilon}$ is strain rate. For an ideal dissipater it can be shown that both quantities J and G are equal in their amount, which means that $m = 1$ and $J = J_{max}$ whereas the efficiency of power dissipation η is given by:

$$\eta = \frac{J}{J_{max}} = \frac{2m}{m+1} \quad (2)$$

The variation of power dissipation with temperature and deformation represents the relative value of energy dissipation occurring through microstructural changes. Microstructural changes, which include a dynamic recovery and dynamic recrystallization, are desired and values for efficiency of

power dissipation η are in such cases in range 0.3–0.4. Lower values for η are less desired and often overlap with area of instable hot deformation (described bellow). Thus lower values for η refer to wedge cracking, void formation at hard particles, dynamic strain ageing and intercrystalline cracking, etc. High values of η refer to formation of new surface related to microcracking.

The instability map is defined by a stability criterion for a dynamic material, where the differential quotient of its dissipative function has to satisfy an inequality condition (ζ), given by equation 3, to allow a stable flow.

$$\xi\left(\overset{\cdot}{\varepsilon}\right) = \frac{\partial \ln(m/(m+1))}{\partial \ln \overset{\cdot}{\varepsilon}} + m > 0 \qquad (3)$$

Areas with values for $\zeta < 0$ are considered as non-stable for hot deformation. These areas refer to adiabatic shear bands, flow localization, Lüder's bands, etc.

The maps, calculated for deformations of 0.1, 0.2, 0.4 and 0.6 are presented in Figure 2. They were calculated for the processing parameters applied during compression tests; for temperature range from 850 °C to 1 150 °C and strain rates 0.001 s⁻¹ to 5 s⁻¹. The dissipation maps are similar at various strains. The instable zone with $\zeta < 0$ (gray region) starts forming at defor-

mation 0.1 in the temperature region around 1 050–1 100 °C, and strain rate of around 0.1 s⁻¹. The instability region grows with the raise of deformation, covering a processing area of strain rates from around 0.01 s⁻¹ to 1 s⁻¹ and temperature range from 1 000 °C to 1100 °C. This processing area should be avoided; strain rates have to be high enough.

From Figure 2 it is clearly seen that instability area overlaps with area with high value for η that although indicates on safe hot forming.

Microstructural analysis
Microstructures of deformed specimens were inspected in the center part of the specimen where the highest deformation was present during compression. The comparison of initial microstructure and the microstructure before deformation is presented in Figure 3. The initial microstructure shows a very evenly distributed, recrystallized microstructure with recrystallization twins present. The measured mean grain size was ≈80 μm. As expected, the grains had grown substantially in the pre-deformation heating stage. This is contributed to the minimization of surface energy through the increase of the grain size. The austenite grains contain annealing twins which are characteristic for the alloys with low stacking fault energy.
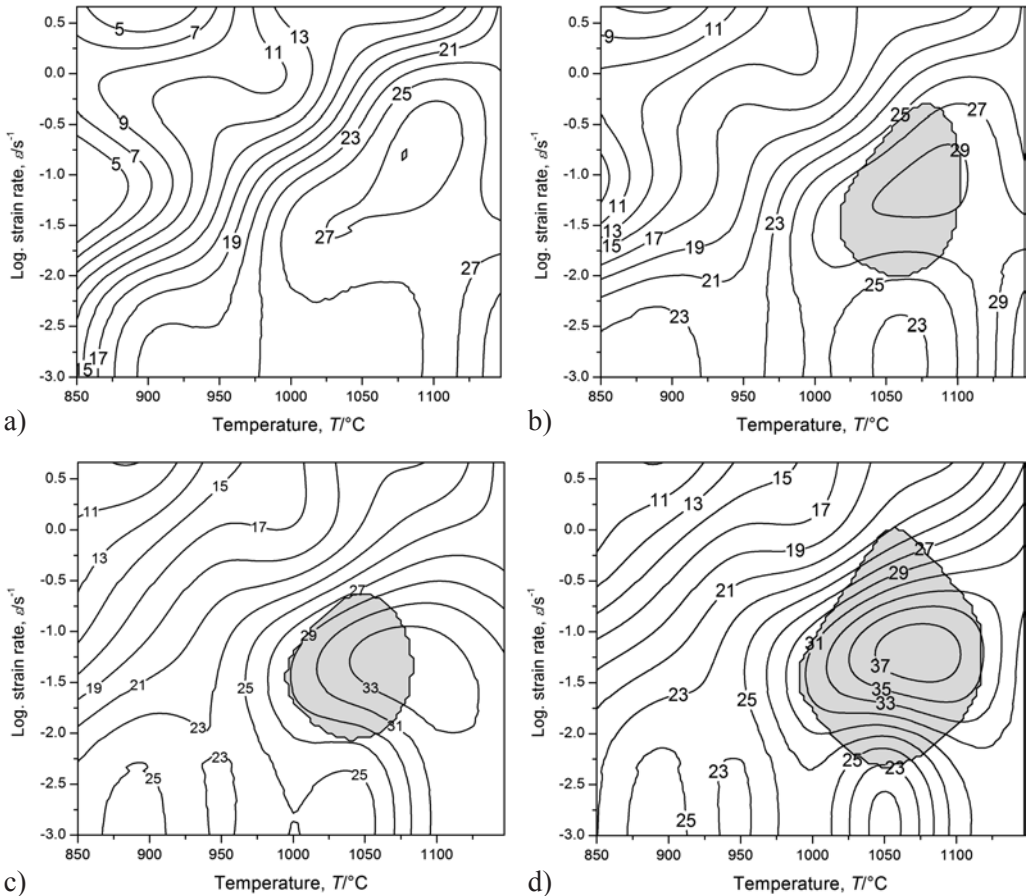
Figure 2. Processing maps for AISI 904L stainless steel, at strains a) $\varepsilon = 0.1$, b) $\varepsilon = 0.2$, c) $\varepsilon = 0.4$ and d) $\varepsilon = 0.6$.
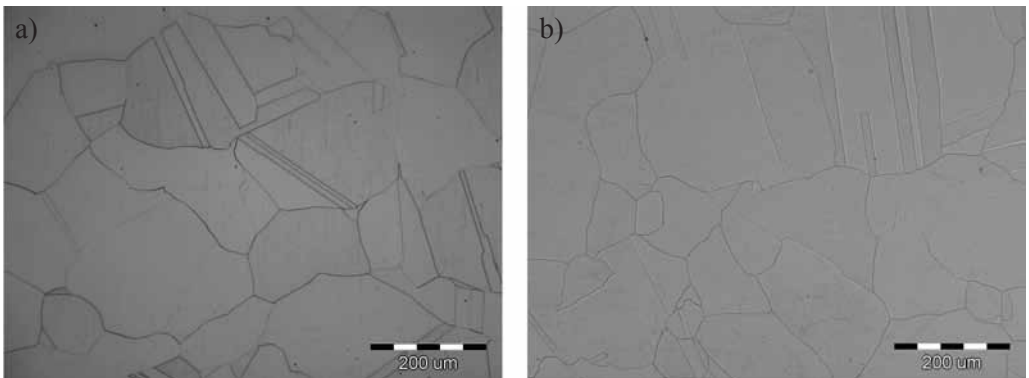

Figure 3. Microstructure of AISI 904L-stainless steel. a) as-received state, b) after soaking at 1 200 °C for 5 min and subsequent water quenching.
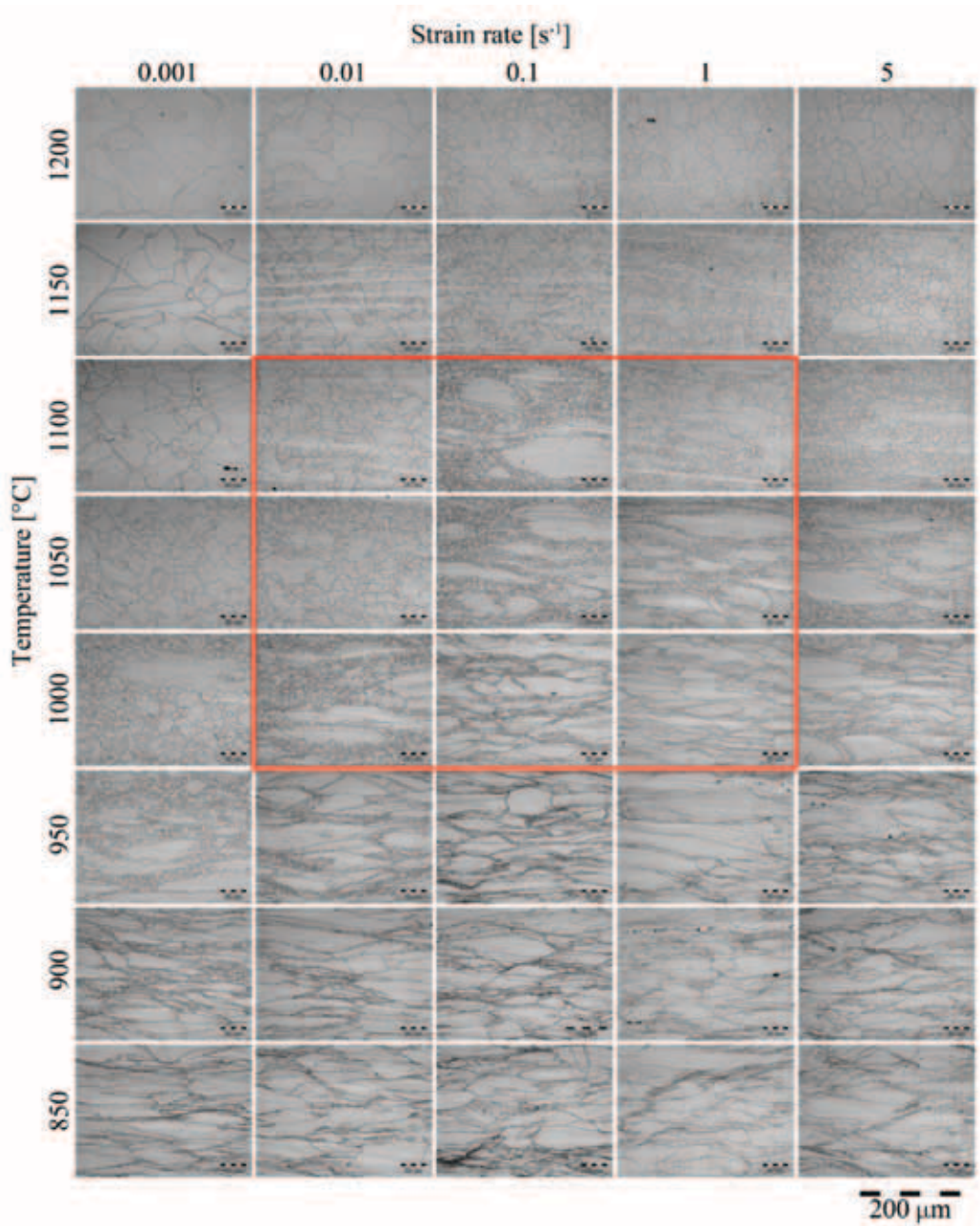
Figure 4. Obtained microstructures after deformation at various strain rates and temperatures. Quenched after deformation to $\varepsilon = 0.9$.

The microstructural map, presented in dependence to processing parameters is presented in Figure 4. No recrystallized grains are to be found in the specimens deformed with higher strain rates (1 s⁻¹ and 5 s⁻¹) and below 950 °C. On the other hand, other specimens did recrystallize some partly, with only necklace type microstructure, with small recrystallized grains around deformed larger grains and some fully recrystallized. Appearance of necklace type microstructure indicates that DRX was not completed. The DRX necklace which follows dynamic nucleation usually takes place in a coarse-grained structure under deformation at low temperature or high strain rates.

The region, marked with red border, shows the region where instability maps predicted low microstructural stability. It can be seen that the grain size is widely distributed, from very small recrystallized grains in necklace to large deformed primary grains. This could cause unstable deformation and as such should be avoided during processing.

Conclusions

Hot deformation behavior of AISI 904L-stainless steel was studied, using thermo-mechanical processing. From the gathered results, the following conclusions can be drawn:

- After initial deformation hardening, softening mechanisms are observed, and steady state flow stress is achieved at the logarithmic strain of 0.9 below the strain rate of 1 s⁻¹ and above 1 100 °C.
- Processing maps, calculated on the basis of compression test show an instability region below 1 s⁻¹ and between 1 000 °C and 1 100 °C.
- Microstructural analysis showed a gradual increase of dynamically recrystallized material with a decrease of strain rate and increase of temperature. A fully recrystallized microstructure is found in specimens deformed with a strain rate of 0.001 s⁻¹ and above 1 050 °C.
- The comparison between results of the map of microstructural evolution and the processing maps are in good agreement, providing useful information for process guidance.
- Highest values for efficiency of power dissipation were obtained around 1 050 °C and strain rate of 0.1 s⁻¹.

References

[1] Belyakov, A., Miura, H. & Sakai, T. (1998): Dynamic recrystallization under warm deformation of a 304 type austenitic stainless steel, *Material Science and Engineering, A*, 255, pp. 139–147.

[2] Deghan-Manshadi, A., Barnett, M.

R. & HODGSON, P. D. (2008): Recrystallization in AISI 304 austenitic stainless steel during and after hot deformation, *Material Science and Engineering, A*, 485, pp. 664–672.

[3]   FRÉCHARD, S., REDJAÏMIA, A., LACH, E. & LICHTENBERGER, A. (2008): Dynamical behavior and microstructural evolution of a nitrogen-alloyed austenitic stainless steel, *Material Science and Engineering, A*, 480, pp. 89–95.

[4]   NEMAT-NASSER, S., GUO, W. G. & KIHL, D. P. (2001): Thermo-mechanical response of AL-6XN stainless steel over a wide range of strain rates and temperatures, *Journal of Mechanical Physics of Solids*, 49, pp. 1823–1846.

[5]   MOAYED, M. H. & NEWMAN, R. C. (2006): Deterioration in critical pitting temperature of 904L stainless steel by addition of sulfate ions, *Corrosion Science*, 48, pp. 3513–3530.

[6]   IVERSEN, A. K. (2006): Stainless steels in bipolar plates—Surface resistive properties of corrosion resistant steel grades during current loads, *Corrosion Science*, 48, pp. 1036–1058.

[7]   LAYCOCK, N. J. & NEWMAN, R. C. (1998): Temperature dependence of pitting potentials for austenitic stainless steels above their critical pitting temperature, *Corrosion Science*, 40, pp. 887–902.

[8]   STAUFFER, A. C., KOSS D. A. & MC-KIRGAN, J. B. (2004): Mechanical Behavior - Microstructural Banding and Failure of a Stainless Steel, *Metallurgical and Materials Transaction: A*, 35A, pp. 1317–1324.

[9]   LIU, J., CHANG, H., WU, R., HSU, T. Y. & RUAN, X. (2000): Investigation on hot deformation behavior of AISI T1 high-speed steel, *Materials Characterization.,* 45, pp. 175–186.

[10]   PRASAD, Y. V. R. K., SASIDHARA, S. (1997): *Hot Working Guide, Compendium of Processing Maps*, ASM - International, OH, USA, 1997, pp. 1–24.

A comparison of parameters below the limit of detection in geochemical analyses by substitution methods

Primerjava ocenitev parametrov pod mejo določljivosti pri geokemičnih analizah z metodo nadomeščanja

TIMOTEJ VERBOVŠEK[1, *]

[1]University of Ljubljana, Faculty of Natural Science and Engineering, Department for Geology, Aškerčeva 12, SI-1000 Ljubljana, Slovenia

*Corresponding author. E-mail: timotej.verbovsek@ntf.uni-lj.si

Abstract: Paper focuses on the analysis of geochemical data with values below the limit of detection (LOD). Such values are treated as text and are difficult to use in further calculations of mean, standard deviation and other statistical parameters. To estimate several methods for substitution of values below the LOD with fractions of LOD (zero, LOD/2, LOD/√2, LOD and *no data* values), a large dataset of generated values with normal and lognormal distributions was tested for different percent of censoring from 1 % to 50 %, plus the censored data of five selected geochemical parameters. Results indicate that the best substitution method is by LOD/√2, as it produces the smallest errors. The greatest errors are found for substitution methods with zero or *no data*. This is valid both for normally and lognormally distributed data. Median is not affected by most methods for censoring level below 50 %. For real geochemical parameters, the interpretation is more complex. For datasets with low amount of censoring (NO_3, O_2), the errors are small. For others (Sr, F, Mn) the errors are larger, as several LODs exist for each parameter and the LOD is sometimes larger than the mean value.

Izvleček: V prispevku je predstavljena in analizirana problematika geokemičnih podatkov pod mejo določljivosti (MD). Ti so obravnavani kot tekst in se s težavo uporabljajo v nadaljnjih statističnih izračunih (povprečje, standardni odklon ipd). Primerjane so bile različne metode nadomeščanja vrednosti pod MD s petimi deleži: nič, MD/2,

MD/√2, MD in vrednosti *brez podatkov*. Sprva je bil analiziran velik nabor generiranih podatkov idealne normalne in lognormalne porazdelitve za različne stopnje okrnjenosti podatkov (od 1 % do 50 %), nato pa še pet izbranih geokemičnih parametrov. Rezultati kažejo, da je najboljše uporabiti metodo nadomeščanja z vrednostjo MD/√2, ker daje najmanjše napake, največje napake pa dajeta metodi nadomeščanja z nič ali *brez podatkov*. To velja tako za normalno in lognormalno porazdeljene podatke. Na mediano ne vpliva večina metod, če je okrnjenih manj kot 50 % podatkov. Za izmerjene geokemične parametre je interpretacija bolj zapletena. Za parametre z manjšim deležem okrnjenosti (NO_3, O_2) so napake majhne, za druge (Sr, F, Mn) pa večje zaradi različnih mej določljivosti za vsak parameter in nekaterih vrednosti MD, večjih od povprečja.

Key words: hydrogeochemistry, limit of detection, statistics
Ključne besede: hidrogeokemija, meja detekcije, statistika

Introduction

Parameters, calculated from geochemical analyses, often lie below some limit which occludes true values. Such a limit is called *limit of detection* (LOD) or *method detection limit* (MDL) and is written with a symbol "<", i.e. "<0.005 mg/L". There are many reasons for laboratories to present the values below the limit, the most obvious being the non-ability of instruments to detect the low concentrations of parameters. Signal from the analyzed parameter can be too small for the instruments to discriminate it from the background noise and several other factors can influence the laboratory to report the values below the limit of detection (Lambert et al., 1991). Limit of detection is usually defined as the level at which a measurement has a 95 % probability of being different than zero (Croghan & Egeghy, 2003), but sometimes in the reports no indication at all is given what a detection limit is (Lambert et al., 1991).

The major problem of such low reported values lies in further statistical analysis of data. First, low concentrations are reported as text values ("<0.005 mg/L") and consequently such values are not recognized as numbers in the analyses. Only in specialized databases (like AquaChem software) it is possible to enter and treat the values as the ones below the LOD. Second, the calculation of statistical moments (mean value, standard deviation ...) is problematic, as low values are truncated or *censored*. Such calcu-

lations are critical when they are used to predict the water quality and one needs to report whether the concentrations of toxic elements lie below or above some critical level.

Several methods exist to "replace" the unknown values below the LOD with such values that the committed errors are minimized when performing the statistical analyses (Chastain, 2007, Gilliom & Helsel, 1986, Glass & Gray, 2001, Gochfeld et al., 2005, Helsel, 1990, Helsel & Cohn, 1988, Helsel & Gilliom, 1986, Smith et al., 2006, Succop et al., 2004), and each method has some advantages and disadvantages:

- Values below the limit of detection are replaced with a *constant of zero (0)*. Calculated mean values are in this case lower than the real ones, as we create a set of artificially low numbers. This approach is not recommended.
- Values are replaced with the values of *limit of detection* (LOD). Consequently, the mean values are higher than the real ones. This approach is also not recommended, as both methods represent the extreme possible values of true mean.
- Values are replaced with some *fraction of LOD*. Usually, the replacement is performed with LOD/2 and LOD/√2 (Croghan & Egeghy, 2003). The error is much lower than in previous methods, and this

approach is very common due to its simplicity. There is no agreement which substitution value is the correct one, for following reasons. Of a great importance is the distribution of data, as replacement with LOD/2 is by some authors (Hornung & Reed, 1990, Succop et al., 2004) recommended for normally distributed data and LOD/√2 for lognormal distribution. Another suggestion is to use the LOD/2 substitution for datasets with much censored data and LOD/√2 for datasets with relatively few data below the detection limit (Glass & Gray, 2001). Substitution with LOD/2 is used in Slovenia for statistical calculations for water quality reports in Decree on groundwater status (Uradni list RS, 25/2009).

- Values are simply *ignored* and are not included in the analysis. Values below the LOD are replaced with *no data* values. Such an approach is not recommended, as calculated mean values are always higher than the real ones (Gochfeld et al., 2005).
- Unknown values are *estimated or extrapolated* from the distribution curve or calculated from regression. These methods are known to perform best, but the distribution of data should be generally known and there is no agreement on the most suitable method. Several methods exist for the estimation (Succop et

al., 2004), and only some can be used for multiple detection limits (Helsel & Cohn, 1988). Compared to these methods, substitution with any fraction values between zero and LOD is generally not recommended, as real data do not have exactly such values (Helsel & Cohn, 1988). However, the usage of substitution methods is still permissible for data with a few censored values (Croghan & Egeghy, 2003).

- Other methods are seldom used. A possible approach is also *not to use any statistical methods at all*, but just to report the values being lower than LOD (Gochfeld et al., 2005). The last two approaches are not presented here, as they require special statistical methods and software and are therefore not comparable to substitution of LOD fractions, discussed in this paper.

The goal of this study is first to analyze the ideal normal and lognormal distribution of generated data with different amounts of censored data (from 1 % to 50 %) and to compare the errors produced in all methods. Secondly, to use the replacement methods on an actual dataset of five geochemical parameters obtained from groundwater analyses and discuss their deviations. Other authors have used some other rather uncommon distributions (bimodal lognormal, gamma and delta; (Gilliom &

Helsel, 1986), but generally lognormal distribution is regarded as more realistic than normal distribution for environmental and geochemical data (Helsel, 2005, Hornung & Reed, 1990).

The novel approach is a systematic comparison of both normal and lognormal distributions (mean and median values) with various substitution methods of replacements of values below the detection limit by five constants: zero, LOD/2, LOD/√2, LOD and *no data* values, all for differently censored data (from 1 % to 50 %), along with a comparison of five geochemical parameters.

Materials and Methods

For the simulation of influence of different detection limits on the statistical calculations, a statistical dataset of normally distributed data was generated first. Data was generated in Microsoft Excel with an internal function NORMINV. Number of data was chosen as $N = 65\,536$, being the maximum possible to calculate further in the program Statistica (Statsoft, Inc.) for the calculations and histograms. Mean value was chosen as 1.00 and standard deviation as 0.25. These data were later transformed to create a lognormal distribution.

Values were later censored at different levels, first by discarding the low-

est 1 % data. These were replaced with values of 0, LOD/2, LOD/√2, LOD and with blank values (*no data*). Datasets with censored 5 %, 10 %, 25 % and 50 % were analyzed as well (Figure 1). Some authors have used data with up to 60 % of censored values (Hornung & Reed, 1990), up to 80 % censored values (Gilliom & Helsel, 1986) or even more than 90 % (Glass & Gray, 2001), but any conclusion based on the analysis of such dataset can be considered as highly inaccurate.

Beside the mean value, the comparison of medians is also presented, as this statistical value is often used in nonparametric statistics for non-normally distributed data.

For the analysis of real geochemical data, a subset of geochemical monitoring data (kindly provided by Slovenian Environmental Agency) for groundwaters in karstic and fractured aquifers was used. Analyses have been performed in years 1990–2009, according to national monitoring program and Decree on groundwater status (Uradni list RS, 25/2009). Number of analyses was $N = 942$, and from available dataset, the following five were chosen for the analysis: NO_3, O_2, Sr, F and Mn. Selection was based on two criteria; first that the percentage of censored data was approximately the same as the vales of generated data (from 1 % to 50 %), with values of NO_3: 0,5 %, O_2: 5 %, Sr: 17 %, F: 25 % and Mn: 45 %, with intention to compare the real data
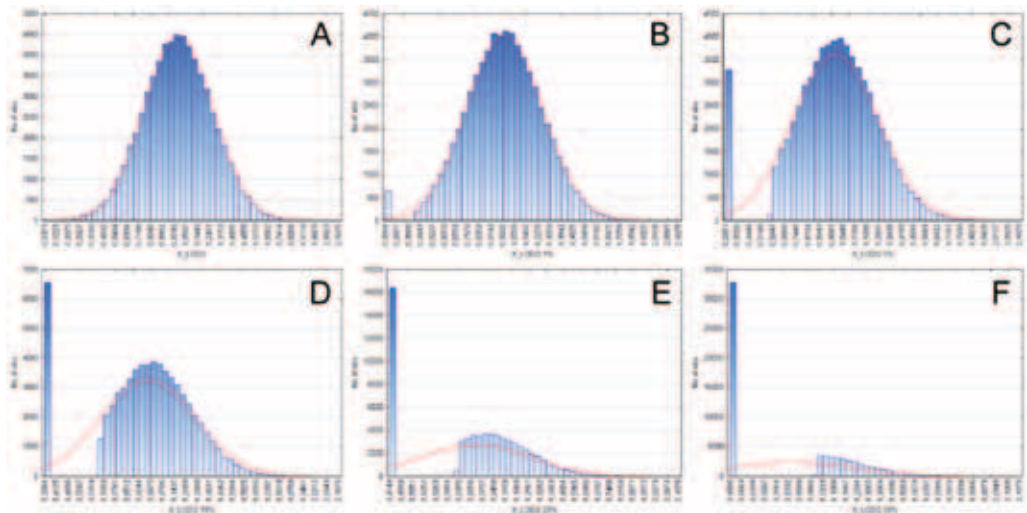

Figure 1. Histograms for generated ideal normal data ($N = 65\ 536$) with data below the detection limit substituted by LOD/2 and censored for: A: no censoring, B: 1 %, C: 5 %, D: 10 %, E: 25 %, F: 50 % of all data.

with generated ones. Secondly, the actual number of data must have been high, at least 70 % of all analyses (NO_3: $N = 942$, O_2: $N = 942$, Sr: $N = 678$, F: $N = 858$, Mn: $N = 942$).

Regarding the analyzed parameters, it must be mentioned that from year 2003 on some major ions (Ca^{2+}, Mg^{2+}, HCO_3^-, ...) are missing from the analyses, as they are not anymore required to analyze according to Rules on drinking water (Uradni list RS, 19/2004). This is a major information loss, as geochemical modeling cannot be performed with such missing data, and the cost of including these parameters into a complete analysis is relatively small.

Results and discussion

Analysis of normally distributed generated data (Figure 1A, Table 1) clearly shows that the replacement of censored data with values of LOD/$\sqrt{2}$ is the best among all substitution methods, as the error is lowest for this approach for all censoring levels (1 %, 5 %, 10 %, 25 % in 50 %). Error is here represented as a ratio between the calculated mean value and true mean value (1.00), in percent. Average error is –1.7 % for normal distribution (Table 1). Replacement with zero produces the greatest errors and should be avoided. Other methods lie in between and also should not be used.

Replacement of values below the limit of detection with LOD/$\sqrt{2}$ underestimates the true mean value only slightly, substitution by LOD/2 produces greater underestimation and substitution by zero the greatest underestimation, which can be seen by the greatest deflection of the curve in Figure 2A. Contrarily, the replacement with LOD or *no data* values overestimated the true mean values.

Similar conclusions are found for the lognormally distributed data (Figure 2B), where the distribution with LOD/$\sqrt{2}$ is again considered the best (average error is only 0.2 % for this method) and therefore recommended method for the substitution, and replacement with *no data* values behaves as the worst method. From the comparison of curves for both distributions, the major difference lies in the fact which method performed worst. For normal distribution, this is substitution by zero and for lognormal distribution, the substitution by *no data* values. The reason lies in the skewness of data, as much more data lies on the left side of the histogram for the lognormal data. As seen from both figures, error is steeply increasing with the percentage of censored data, up to 40 % when a half of data are censored. The increase is not linear and this holds for all methods.
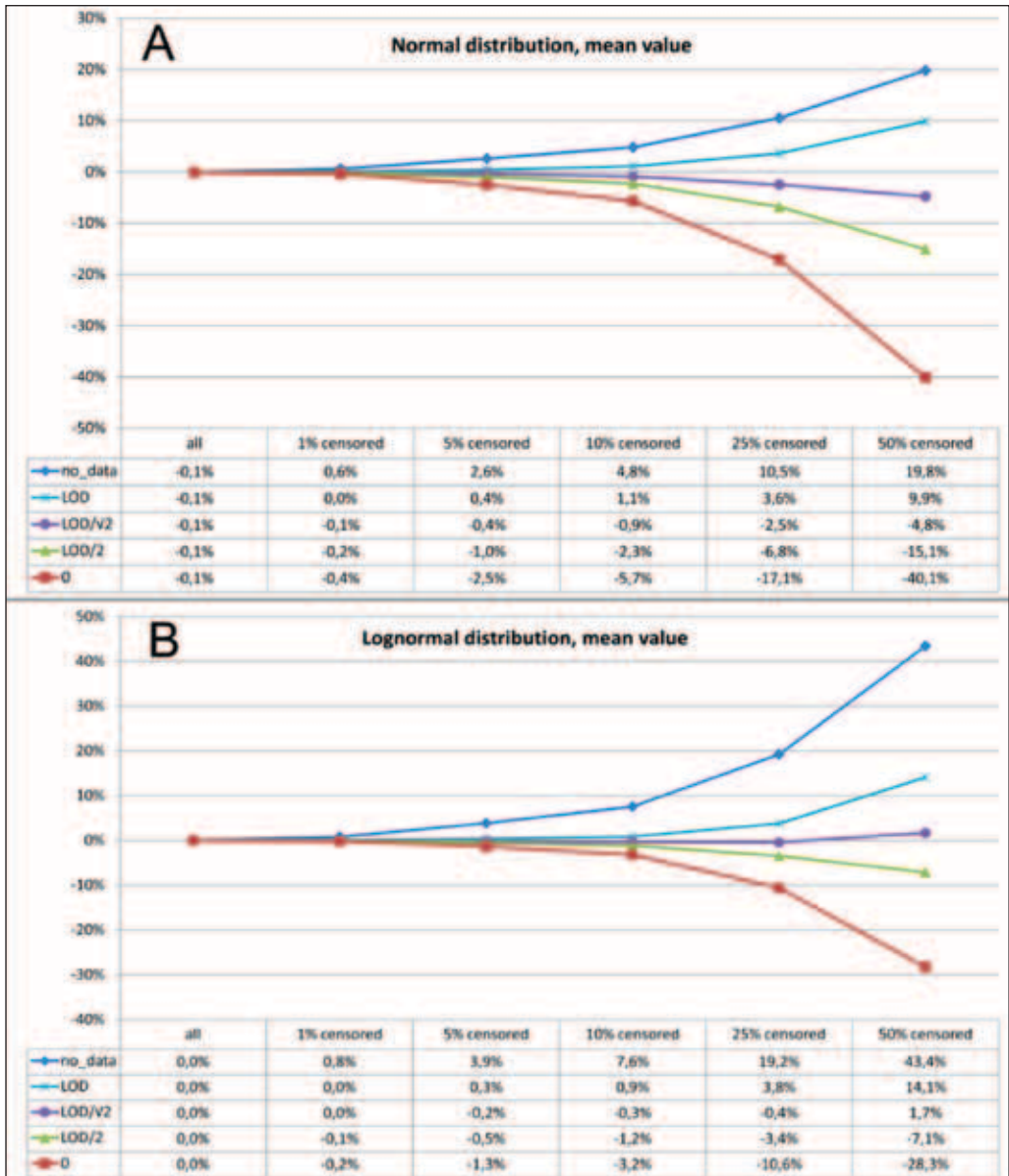
A. Normal distribution, mean value

	all	1% censored	5% censored	10% censored	25% censored	50% censored
no_data	-0,1%	0,6%	2,6%	4,8%	10,5%	19,8%
LOD	-0,1%	0,0%	0,4%	1,1%	3,6%	9,9%
LOD/√2	-0,1%	-0,1%	-0,4%	-0,9%	-2,5%	-4,8%
LOD/2	-0,1%	-0,2%	-1,0%	-2,3%	-6,8%	-15,1%
0	-0,1%	-0,4%	-2,5%	-5,7%	-17,1%	-40,1%

B. Lognormal distribution, mean value

	all	1% censored	5% censored	10% censored	25% censored	50% censored
no_data	0,0%	0,8%	3,9%	7,6%	19,2%	43,4%
LOD	0,0%	0,0%	0,3%	0,9%	3,8%	14,1%
LOD/√2	0,0%	0,0%	-0,2%	-0,3%	-0,4%	1,7%
LOD/2	0,0%	-0,1%	-0,5%	-1,2%	-3,4%	-7,1%
0	0,0%	-0,2%	-1,3%	-3,2%	-10,6%	-28,3%

Figure 2A, 2B. Errors (ratios between the calculated mean value and true value in %) for replacement of values with no data, zero, LOD/2, LOD/√2 and LOD. A. Normal data, mean values. B. Lognormal data, mean values.
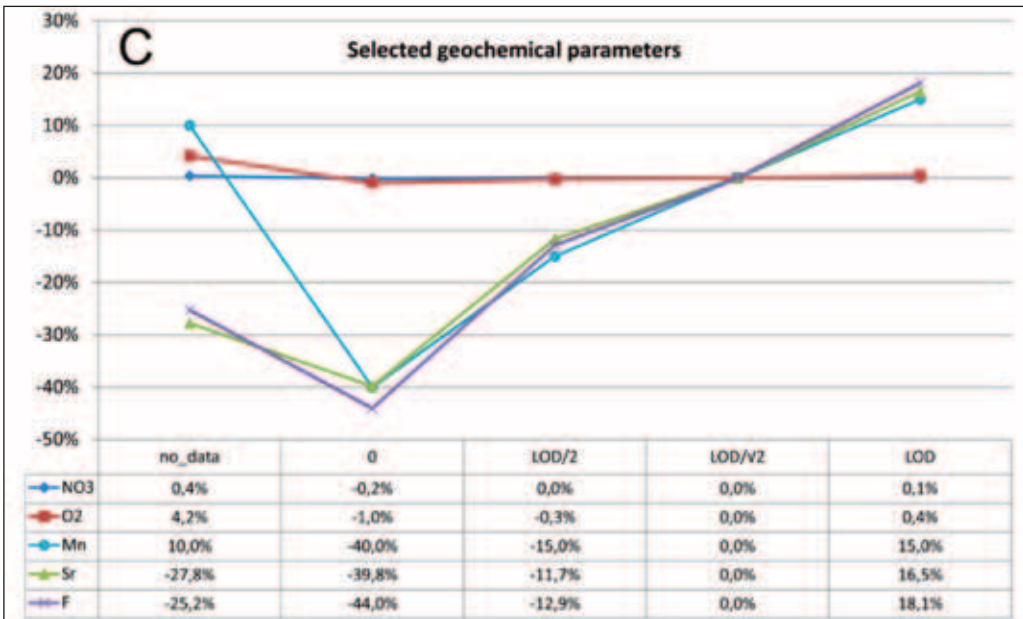
Figure 2C. Errors (ratios between the calculated mean value and true value in %) for replacement of values with no data, zero, LOD/2, LOD/√2 and LOD. C. Errors for selected geochemical parameters: NO₃, O₂, Sr, F and Mn.

From the results of geochemical data (Figure 2C) it is obvious that there are vast differences both among the methods and among the parameters. As the true mean values for all populations are not known (they are influenced by censored values), all comparisons are normalized to the results of method of LOD/√2, as it turned out to be the most accurate. Major differences are visible between the group of NO₃ and O₂ and the group of Sr, F and Mn. Differences within the first group are very small (mostly below 1 %), and very big in the second (up to 40 %). There are several reasons for such behavior compared to generated ideal datasets:

- The detection limits in presented real dataset are often bigger than the values themselves (taking into account only uncensored data). For example, limit of detection for strontium is equal to 500 µg/L, but the mean value of uncensored data is equal to 101 µg/L. Any substitution of LOD/2, LOD/√2 or LOD thus gives much bigger values than the average, so the estimated means are much higher and obviously unacceptable for any further calculations. Censored values should be obviously smaller than the mean. Such an example of a large deviation for strontium is evidently pre-

sented in the histogram in Figure 3. The left histogram (Figure 3A) is based on all data with no censored values (*no data*), and the right one (Figure 3B) for the same data with inclusion of values substituted by LOD/$\sqrt{2}$. A clear peak is visible for the latter data, with values much above the mean values. Such substitution cannot be used as it overestimates the mean by a great value.

• A large fraction of parameters Sr, F and Mn are highly censored, so the estimation of mean values is more problematic than the estimation of less censored NO_3 and O_2.

• Data distribution can also cause some deviations from the ideal datasets. Distributions were not tested for normality by special methods, but were visually estimated from histograms and are mostly lognormal.

• For some parameters, there exist several limits of detection in different time periods. Consequently, different substitutions can influence the statistical calculations. A possible approach to overcome such problem (Helsel & Cohn, 1988) is to use the largest limit of detection for all censored data, but the information about the lower limits is lost in such cases.

Again, the greatest deviations are found for replacements with zero or *no data* values, and this is much more pronounced for parameters Sr, F and Mn. For NO_3 and O_2, the difference between the methods is very small, which can be attributed to very small censoring levels (0.5 % and 5 %).
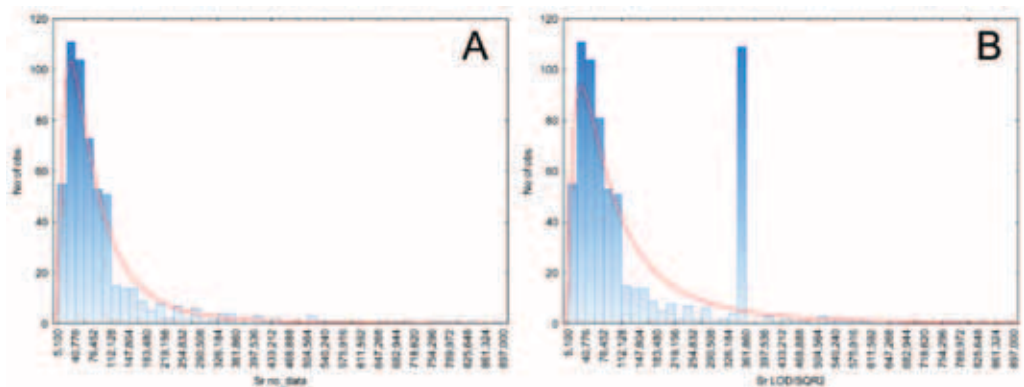

Figure 3. A. Histogram of strontium distribution with substitution of no data values. B. Histogram of strontium distribution with visible outliers, created by substitution of LOD/$\sqrt{2}$.

Table 1. Average method errors for all censored data - mean and median values for normal and lognormal distributions.

Method and distribution	no data	0	LOD/2	LOD /√2	LOD
mean values - normal distribution	7.7 %	−13.2 %	−5.1 %	−1.7 %	3.0 %
mean values - lognormal distribution	15.0 %	−8.7 %	−2.4 %	0.2 %	3.8 %
median - normal distribution	5.9 %	0 %	0 %	0 %	0 %
median - lognormal distribution	157.1 %	0 %	0 %	0 %	0 %

Table 1 summarizes the results for produced errors committed by several substitution methods for mean values and medians, for both normal and lognormal distributions. Replacement with LOD/√2 gives the best results, the replacement with LOD/2 or LOD causes larger deviations and replacements with zero or *no data* the highest errors. Interesting fact is that the median value is not sensible to any method of substitution except for replacement by blank values (ignoring the censored data). In all other cases, there is no deviation from the true data. The reason for such behavior is relatively obvious, as median is by definition the value separating the higher half of the sample from the lower half. Consequently, for data censored up to 50 %, there is no difference between the medians for different methods. For higher censored values, the median is nevertheless increasingly influenced by higher censoring level.

Based on presented results, it is therefore recommended that no more than about 20 % of data should be censored, if one should keep the error relatively small - below few percent for both lognormal and normal methods for substitution with LOD/√2 for the ideal data and somewhat larger value (but still permissible) for natural data.

Conclusions

From the presented results it is clear that the substitution of data below the limit of detection is complex and still not adequately used. For substitution of different fractions of LOD, based on results of this study, the method of LOD/√2 is recommended, as the committed errors are the lowest. Other methods perform worse, with replacement with LOD/2 or LOD causing larger deviations and replacements with zero or *no data* the highest deviations. Real data present a challenge, due to problems with multiple limits of detection, unknown distributions and other factors, but still the substitution with LOD/√2 is recommended if neither of such factors is known. Median is not sensible to replacement method except for the replacement with *no data* values, up to 50 % of the censored data and can be used as a reported value, like the mean.

Substitution with estimation of missing data below the detection limit can be obtained by more complex statistical methods, like the maximum likehood estimation or various regressions (not used in this paper), but for such, the distribution of data should generally be known. A better method is to analyze the samples again (perhaps in another laboratory) or use another method, to avoid the censored values as much as possible.

Acknowledgments

REFERENCES

CHASTAIN, J. R. (2007): Censored Data: What's The Average Of Unknown Values. Chastain-Skillman, Inc.

CROGHAN, C. W. & EGEGHY, P. P. (2003) Methods of Dealing with Values Below the Limit of Detection using SAS, paper presented at the *Southeastern SAS User Group*, City, 22–24 September, 2003.

GILLIOM, R. J. & HELSEL, D. R. (1986): Estimation of Distributional Parameters for Censored Trace Level Water Quality Data: 1. Estimation Techniques – *Water Resources Research,* Vol. 22, No. 2, pp. 135.

GLASS, D. C. & GRAY, C. N. (2001): Estimating mean exposures from censored data: exposure to benzene in the Australian petroleum industry – *The Annals of occupational hygiene,* Vol. 45, No. 4, pp. 275–82.

GOCHFELD, M., BURGER, J. & VYAS, V. (2005) *Statistical Analysis of Data Sets with Values Below Detection Limits.* Report for (Piscataway, New Jersey).

HELSEL, D. R. (1990): Less than obvious - statistical treatment of data below the detection limit – *Environmental Science & Technology,* Vol. 24, No. 12, pp. 1766–1774.

HELSEL, D. R. (2005): More than obvious: Better methods for interpreting nondetect data – *Environmental Science & Technology,* Vol. 39, No. 20, pp. 419a–423a.

HELSEL, D. R. & COHN, T. A. (1988): Estimation of descriptive statistics for multiply censored water quality data – *Water Resources Research,* Vol. 24, No. 12, pp. 1997.

HELSEL, D. R. & GILLIOM, R. J. (1986): Estimation of Distributional Parameters for Censored Trace Level Water Quality Data: 2. Verification and Applications – *Water Resources Research,* Vol. 22, No. 2, pp. 147.

HORNUNG, R. W. & REED, L. D. (1990): Estimation of Average Concentration in the Presence of Nondetectable Values – *Applied Occupational and Environmental Hygiene,* Vol. 5, No. 1, pp. 46–51.

Lambert, D., Peterson, B. & Terpenning, I. (1991): Nondetects, Detection Limits, and the Probability of Detection – *Journal of the American Statistical Association,* Vol. 86, No. 414, pp. 266–277.

Smith, D., Silver, E. & Harnly, M. (2006): Environmental samples below the limits of detection – comparing regression methods to predict environmental concentrations. http://www.lexjansen.com/wuss/2006/Analytics/ANL-Smith.pdf

Succop, P. A., Clark, S., Chen, M. & Galke, W. (2004): Imputation of data values that are less than a detection limit – *Journal of Occupational and Environmental Hygiene,* Vol. 1, No. 7, pp. 436–441.

Uradni list RS (19/2004): Pravilnik o pitni vodi = Rules on drinking water, Ljubljana.

Uradni list RS (25/2009): Uredba o stanju podzemnih voda = Decree on groundwater status, Ljubljana.

Compositional appraisal and quality implications of a metacarbonate deposit occurring in parts of southeastern Nigeria

Presoja sestave in njenega vpliva na kakovost metakarbonatne kamnine iz nahajališča v jugovzhodni Nigeriji

Bassey Edem Ephraim[1, *]

[1]University of Calabar, Department of Geology, P. M. B. 1115 Calabar, Nigeria

*Corresponding author. E-mail: basifrem@yahoo.com

Abstract: Metacarbonate deposits occurring in Nsofang and environs in the Ikom area of southeastern Nigeria are low grade dolomitic marble. Field and compositional attributes of the marble have been used to establish the material's suitability for identified end-product uses. Thin-section optical microscopy, X-ray powder diffraction and bulk rock chemistry agree with the fact that carbonate phases dominate the modal mineralogy of the rock. Dolomite is clearly the dominating phase and calcite the subordinate, while silicates constitute the accessory phases. The mineralogical composition reflects the possible attainment of peak metamorphic conditions that is equivalent to, at most, the greenschist facies metamorphism. Geochemical and comparative data show that the Nsofang marble displays lower CaO and elevated MgO, LOI and trace elements compositions, compared to similar carbonate – bearing rocks occurring in other parts of Nigeria and elsewhere. Also, computed CaO/MgO ratio of the marble appears relatively lower and some of the trace elements display significant positive relationships with the insoluble residue contents of the Nsofang marble. All these attributes degrade the quality of the marble, making it unsuitable for many conventional applications. However, certain compositional features, such as elevated MgO composition and low total sulphur contents can impact positively on the applicability of the Nsofang marble. Accordingly, the marble can be relied upon as compensators for magnesium deficiencies in the agricultural

---

Original scientific paper

industry, and in the sourcing of magnesium oxide for the chemical industry as well as when used as dimension stones. Furthermore, with adequate beneficiation, the Nsofang marble can also be adapted for use as MgO + C refractories for electrical arc furnace (EAF) linings.

Izvleček: Metakarbonatna kamnina v nahajališčih Nsofanga in okolice na območju Ikoma v jugovzhodni Nigeriji je dolomitni marmor nizke stopnje metamorfoze. Na podlagi terenskih in kemičnih lastnosti tega marmorja je bila opredeljena njegova primernost kot surovina za določene namene. Rezultati preiskave zbruskov pod optičnim mikroskopom, rentgenske difrakcijske analize prahu in kemijske analize kamnine pričajo o tem, da prevladujejo v mineraloški sestavi kamnine karbonatne faze. Prevladujoč glavni mineral je dolomit, stranski pa kalcit, medtem ko so silikatni minerali akcesorni. Mineraloška sestava nakazuje verjetnost pogojev metamorfoze, ki ustreza vsaj faciesu zelenih skrilavcev. Geokemijski in primerjalni podatki pričajo o tem, da se sestava marmorja iz Nsofanga odlikuje po nižjem CaO in visokih MgO, LOI in slednih prvinah v primerjavi s podobnimi karbonate vsebujočimi kamninami iz drugih delov Nigerije in od drugod. Tudi izračunani količnik CaO/MgO tega marmorja je razmeroma nizek, medtem ko so nekatere sledne prvine statistično značilno pozitivno korelirane z vsebnostjo netopnega ostanka v Nsofanškem marmorju. Vse navedene lastnosti slabo vplivajo na kakovost marmorja, ki zato ni ustrezen za marsikatero običajno uporabo. Vendar pa nekatere lastnosti sestave, tako visoka vsebnost MgO in nizka celotnega žvepla utegnejo ugodno vplivati na njegovo uporabnost. Tako ga je mogoče uporabljati kot protisredstvo ob pomanjkanju magnezija v kmetijstvu, kot vir magnezijevega oksida v kemični industriji in kot arhitektonski kamen. In slednjič, marmor iz Nsofanga je mogoče uporabiti po ustrezni predelavi tudi za izdelavo MgO + C ognjevzdržnih materialov za obloge v električnih obločnih pečeh (EAF).

Key words: metacarbonate, composition, geochemistry, Nigeria
Ključne besede: metakarbonat, sestava, geokemija, Nigerija

Introduction

Although metacarbonate deposits, such as marble, occur abundantly in Nigeria, and furnish the raw material needed for the rapidly expanding building and other industries, their compositional features have not been widely investigated and documented. The few contributions on composi-

tional and quality attributes of marble deposits in Nigeria, include those of AGE (2008), DANLADI (1993), DAVOU & ASHANO (2009), EMOFURIETA & EKUAJEMI (1995) and EMOFURIETA et al. (1995). On the other hand, much more work appears to have been done on investigations of dimensional properties of prospects. OJO et al. (2003) focused on the determination of the lateral and depth extents of the Takalafia marble, situated close to the Federal Capital Territory of Nigeria. ODEYEMI et al. (1997) considered ground gravity and magnetic surveys in an effort to evaluate the economic significance of the Ikpeshi marble. FOLAMI & OJO (1991) worked on the geophysical study of the southern part of Igarra with the intent of mapping concealed Ore deposit in the form of marble.

Much as the dimensional features of metacarbonate bodies are important, the compositional properties are also required, especially in the economic valuation of a prospect. The relevance of mineralogical and chemical investigations cannot be overemphasized when assessing the suitability of metacarbonate rocks for specific usage.

In southeastern Nigeria, metamorphosed carbonate deposits was recently discovered in Nsofang and environs in the Ikom area, and no published data exist yet on this deposit. There is the need to explore the deposit in sufficient

details, and such investigation should normally include physical evaluation, compositional assessments, and geophysical exploration. The present contribution focused on the compositional appraisal of the metacarbonate rock, and the intension is to reveal the industrial quality of the material, based on available compositional data. However, no effort is made in the present study to interpret the compositional features of the rock to reflect petrogenetic history of the deposit since this aspect constitutes another area of research. The impetus for the present research was derived from the need to be actively involved in the growth and development of the hitherto dormant solid minerals sector of Nigeria.

Description of Study Area
The area of investigation is situated southeast of Ikom in the southeastern region of Nigeria (Figure 1), and delimited by latitude 5°40′ and 6°00′ North and longitude 8°35′ and 8°50′ East within the Nigerian topography sheet 315 (Ikom NW). Geologically, most parts of the area can be classified as parts of the Mamfe embayment, a predominantly sedimentary deposits comprising sandstones, mudstones, shales, limestones, micro-conglomerates, polygenic conglomerates having thickness of about 2000 m (OLADE, 1975) associated with basic volcanic and undifferentiated basement rocks (Figure 1). In recent times, metacar-

bonates, which occur as lensoid bodies within the low to very low grade metamorphosed and unmetamorphosed sedimentary sequences near Nsofang village, have also been revealed as parts of the lithologic components of the embayment. The metacarbonate body is delimited by latitude 5°44′ and 5°47′ North and longitude 8°38′ and 8°42′ East. The deposits are generally low-lying, with slightly elevated portions in some locations, while their surfaces are rugged, possibly due to the influence of weathering. Some of the exposure appears foliated with steep dips and vari-

able strike orientation. Also, joints are common and assume cross or east – west orientations.

Methods of Study

Both petrographic and chemical analyses were undertaken in the study of the Nsofang metacarbonates. The petrographic study comprised both thin section optical microscopy and X–ray diffraction investigations. Unweathered rock samples collected during fieldwork and traversing of various metacarbonate outcrops, within the prospect region, were utilized for the various
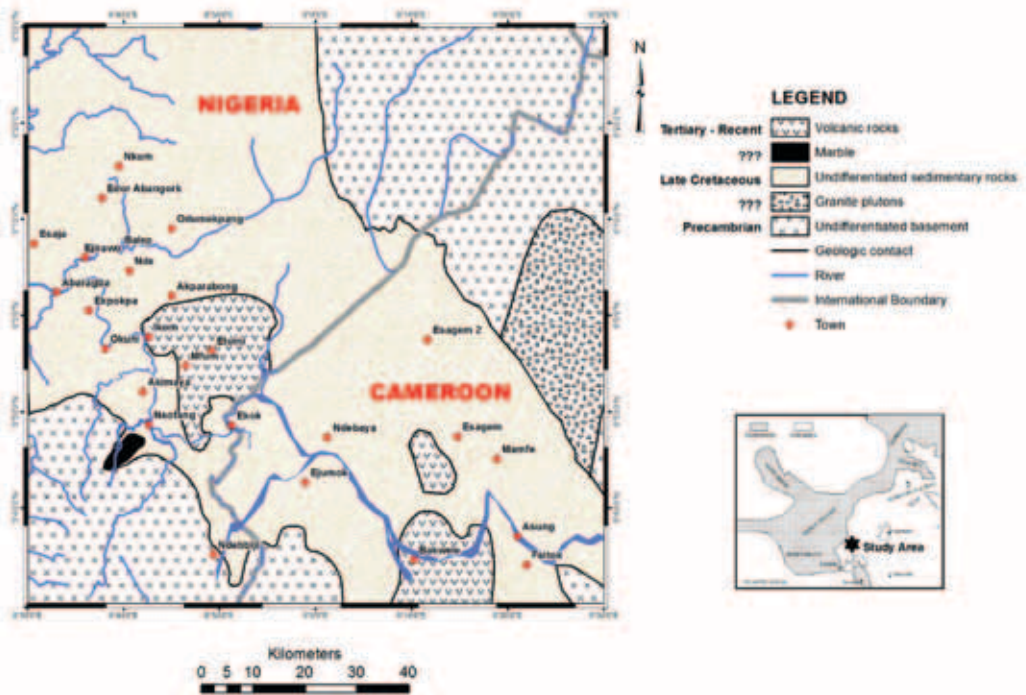

Figure 1. Geologic map of Southeastern Nigeria and Western Cameroon, showing the location of Nsofang marble within the Mamfe embayment of southeastern Nigeria

analyses. Systematic sampling was hampered by irregular exposure of the rocks, weathering and thick forestation. Nevertheless, a total of eleven representative metacarbonate rock samples were considered fresh and appropriate for the analysis. The rock samples, weighing 0.5–1.5 kg, were reduced and finely chipped. The sample chips were thoroughly cleaned, crushed with a "jaw-crusher", split by quartering and finely ground. All sample preparations and treatments were done at the Thin–Section Workshop of Department of Geology, University of Calabar, Calabar- Nigeria. Thin sections were also prepared in the same venue.

Data thus obtained from the thin section examinations were supported with X-ray diffraction (XRD) information. The XRD analyses were carried out on powdered samples, and the XRD patterns were obtained under the following conditions: $CuK_{\alpha 1}$ radiation (0.154059 nm) with 30 kV, 30 mA energy and graphite monochromatic. XRD study was considered most useful in the discernment of individual mineral components of cryptocrystalline phases and in differentiation of calcite and dolomite since this was almost impossible with the thin sections.

The chemical analysis was done at Acme Analytical Laboratories, Vancouver BC, Canada under the analysis code 4A4B, a lithium metaborate/ tetraborate fusion ($LiBO_2/Li_2B_4O_7$) ICP/ES whole – rock package and trace element ICP/MS package which is unique for the scope of elements and detection limits. The two packages are combined for Code 4A02 and Code 4B02. Essentially, the prepared samples were mixed with $LiBO_2/Li_2B_4O_7$ flux, and the crucibles fused in a furnace. The cooled beads were dissolved in ACS grade nitric acid. Loss on ignition (LOI) was determined by igniting a sample split before measuring weight loss. Total carbon and total sulphur were analyzed by high temperature (LECO) combustion. Each analysis was done in duplicate, and reproducibility found to be within ±2 %. Also, analyses of standard materials indicate that the methods adopted give results that are generally accurate to within ±10 %.

RESULTS AND INTERPRETATIONS

Mineralogy and petrography
In hand specimen, the carbonate rock is characterized by a fairly homogeneous texture, uniform hardness and good resistance to abrasion. The investigated samples, which are mostly unweathered, commonly exhibit off – white to greyish colour, unimodal grain size distribution pattern and distinct linear and planar fabric produced by variation in coloration. The grain sizes are mostly fine to medium.

Table 1. Mineralogical compositions, based on XRD data, of metacarbonate rocks of Nsofang, Ikom area of Southeastern Nigeria

	Major	**Minor**	**Trace**
L_{11}	dolomite	calcite	quartz – phlogopite – talc
L_{21}	dolomite – calcite	–	quartz – phlogopite – talc
L_{31}	dolomite	calcite	quartz – phlogopite – talc

The microscopic features, as observed through optical microscopy and XRD (Table 1) show a dominantly carbonate mineralogy. The various carbonate phases could not be differentiated during microscopic examinations, because the investigated thin sections were not stained with alizarin or other relevant chemical. However, the XRD data (Table 1) revealed that the metacarbonate is predominantly dolomitic with calcite as subordinate in most cases, and quartz, talc, phlogopite and probably muscovite constituting the accessory phases. The microscopic study also shows that the rock is heteroblastic with grains of different sizes forming mortar fabric. Most often, medium grained ($\approx$1.0–2.0 mm) calcite or dolomite, having deformed twinning lines, are observed surrounded by fine grained (<1.0 mm) dolomite or calcite crystals. The boundaries of the medium crystals are usually sutured to minerals, particularly phlogopites and occasionally muscovite, formed hypidioblastic to idioblastic weakly – deformed flakes that occur mostly as small inclusions within the medium grained calcite and dolomite grains. However, it must be emphasized that all the accessory phases, put together, exhibit an abundance that rarely exceeds 1 %.

Geochemical compositions and comparisons

The chemical compositions of the metacarbonate rocks are listed in Table 2, together with relevant statistical data. Characteristic is the high content of CaO (29.85–51.67 %, av. 35.79 %), MgO (3.88–21.25 %, av. 16.70 %) and LOI (40.8 %–46.50 %, 44.41 %). Very high is also the total carbon concentration (11.31–12.97 %, av. 12.28 %) while the total sulphur concentrations are generally below detection limit of 0.02 %. The SiO_2 contents range from 0.82–6.21% with a mean value of 2.31 %, the Al_2O_3 contents from 0.03–1.01% and an average value of 0.22 %. The contents of TiO_2, MnO, Na_2O and probably K_2O are all low. Fe_2O_3 and P_2O_5 contents range from <0.04–0.36 % and from 0.02–0.1 % respectively. The data clearly fall within the limiting values known for carbonate rocks (CHERNEVA et al., 2009; DAVOU & ASHANO, 2009; DEELMAN, 2008; EMOFURIETA et al., 1995; LEAKE et al., 1975).

Table 2. Geochemical composition and relevant data of metacarbonate rocks of Nso-fang, Ikom area of Southeastern Nigeria

	L_{11}	L_{12}	L_{13}	L_{21}	L_{22}	L_{23}	L_{31}	L_{32}	L_{41}	L_{42}	L_{43}	Statistics	
												Mean	St. Dev.
Major elements oxides, total C, total S and estimated mineral compositions in mass fractions, wt/%													
SiO_2	6.21	4.08	3.26	1.08	2.74	0.82	1.6	1.43	1.03	1.37	1.82	*2.31*	*1.649*
TiO_2	0.06	<0.01	<0.01	0.01	<0.01	0.01	<0.01	0.01	<0.01	<0.01	<0.01	*0.01*	*0.015*
Al_2O_3	1.01	0.03	0.03	0.24	0.15	0.15	0.3	0.25	0.14	0.06	0.06	*0.22*	*0.278*
Fe_2O_3	0.36	<0.04	<0.04	0.08	0.08	0.08	0.08	<0.04	<0.04	<0.04	<0.04	*0.08*	*0.094*
MnO	0.01	0.01	<0.01	0.01	0.02	0.02	0.02	<0.01	0.01	<0.01	<0.01	*0.01*	*0.005*
MgO	20.42	21.25	20.56	12.6	21.09	20.14	18.43	11.43	3.88	16.35	17.52	*16.70*	*5.415*
CaO	30.26	30.1	30.94	41.09	29.85	31.67	33.78	41.88	51.67	36.94	35.55	*35.79*	*6.793*
Na_2O	<0.01	<0.01	<0.01	0.01	0.01	0.01	0.04	0.02	<0.01	<0.01	<0.01	*0.01*	*0.009*
K_2O	0.49	<0.01	<0.01	0.03	0.06	0.06	0.03	0.02	0.02	0.03	0.03	*0.07*	*0.140*
P_2O_5	0.05	0.05	0.06	0.02	0.15	0.14	0.14	0.13	0.02	0.04	0.02	*0.07*	*0.054*
LOI	40.8	44.1	44.8	44.6	45.4	46.5	45.2	44.5	43.1	44.9	44.6	*44.41*	*1.459*
TOTAL	99.68	99.69	99.73	99.77	99.56	99.6	99.63	99.72	99.93	99.76	99.67	-	-
Total C	11.31	12.16	12.17	12.46	12.18	12.97	12.37	12.61	12.14	12.45	12.21	*12.28*	*0.407*
Total S	<0.02	<0.02	<0.02	<0.02	<0.02	<0.02	<0.02	<0.02	<0.02	<0.02	<0.02	*<0.02*	*0.000*
CaO/ MgO	1.48	1.42	1.50	3.26	1.42	1.57	1.83	3.66	13.32	2.26	2.03	3.07	-
Calcite	3	1	4	42	1	7	15	46	83	25	20	-	-
Dolomite	93	97	94	58	96	92	84	52	18	75	80	-	-
Trace elements in μg/g													
Ba	190	22	6	33	78	70	37	37	19	57	52	*55*	*49.91*
Cs	3.9	0.2	<0.1	0.2	0.4	0.3	0.2	0.2	0.1	0.3	0.4	*0.6*	*1.11*
Rb	17.8	0.5	0.3	0.8	2.7	2.2	0.9	0.7	0.6	1.2	1.5	*2.7*	*5.08*
Sr	59.1	53.8	60.1	167.7	97.4	95.6	100.1	181.4	552.3	115.8	112.6	*145.1*	*141.16*
Nb	1.5	0.2	0.1	0.3	0.2	0.3	0.2	0.2	0.1	<0.1	<0.1	*0.3*	*0.40*
Pb	0.9	0.4	0.5	0.7	0.6	0.5	0.7	0.8	1.1	0.3	0.5	*0.6*	*0.23*
Zr	35.7	4.1	6.7	7.7	14.9	15.1	7.8	12.4	3.8	5.4	12.8	*11.5*	*9.03*
Cd	0.2	0.2	0.7	0.3	0.2	0.1	0.3	0.3	0.1	0.3	0.3	*0.3*	*0.16*
Cu	0.9	0.7	1.6	0.6	1	0.6	2.7	1.5	12.1	0.2	0.2	*2.0*	*3.42*
Ni	0.3	<0.1	0.8	3.9	1.2	1.7	1.3	3.5	1.6	1.1	1	*1.6*	*1.19*
U	0.5	1.3	3	0.8	0.3	0.3	0.6	0.6	2.3	2.3	1.8	*1.3*	*0.95*
Y	5.7	2.7	2	1.8	0.6	0.7	1.4	2	1	0.7	0.6	*1.8*	*1.49*
Zn	9	5	6	8	4	5	7	6	3	5	4	*5.6*	*1.80*

The major elements geochemical and relevant data of the metacarbonate rocks have been compared with average values of carbonate – bearing rocks occurring in Nigeria and elsewhere in Table 3. As shown in Table 3, the CaO composition of the investigated metacarbonate rock is low, compared to that of Mfamosing limestone (Ekwueme, 1995), Ashaka limestone (Tadco Consulting Engineers, 1989), Jakura marble (Ofulume, 1993), Ososo marble, Akure marble (Emofurieta & Ekuajemi, 1995), metacarbonate rocks from the Zambezi mobile belt of Zambia (Munyanyiwa & Hanson, 1988), Jabal Farasan marble deposit of Saudi Arabia (Qadhi, 2008), Dalradian Connemara marble in western Ireland (Yardley, 1977), metacarbonate rocks of northwest Konya in Turkey (Eren, 1993) and marble with carbonatite-like geochemical signature of the Bohemian Massif in Czech Republic (Houzar & Novak, 2002). It is only in the Guyuk limestone of northeastern Nigeria (Gabako & Tedra, 1994), marble occurring east of the Federal Capital Territory (Davou & Ashano, 2009) and the Igbeti marble (Emofurieta & Ekuajemi, 1995) that comparatively lower CaO values are observed. Ironically, these are the only deposits having MgO concentration that are higher than that of the Nsofang rocks. All other deposits displayed relatively lower MgO concentration (Table 3). SiO_2 and LOI components of the investigated rocks are comparable to those of Ashaka limestone (Tadco Consulting Engineers, 1989) and metacarbonate rocks of northwest Konya in Turkey (Eren, 1993) while the Jakura marble (Ofulume, 1993) only differ by its slightly depleted SiO_2 composition. No other LOI values are lower than that of the metacarbonate rocks of Nsofang and environs.

Generally, the overall major elements geochemistry data of the Nsofang marble is comparable to those of marble occurring east of the Federal Capital Territory (Davou & Ashano, 2009) and the Igbeti marble of Emofurieta & Ekuajemi (1995), both in southwestern Nigeria.

The concentrations of trace elements in the rock, also shown in Table 2, are not as low as expected, and values for Sr and Ba are highly variable. Interesting are the relatively high concentrations of Ba (6–190 × 10^{-6}, av. 55 × 10^{-6}), Sr (53.8–552.3 × 10^{-6}, av. 145.1 × 10^{-6}), Rb (0.3–17.8 × 10^{-6}, av. 2.7 × 10^{-6}) and probably Zr (3.8–37.7 × 10^{-6}, av. 11.5 × 10^{-6}) at a markedly predominance of Sr. Other components, notably, Zn (av. 5.6 × 10^{-6}), Pb (av. 0.6 × 10^{-6}), Cu (av. 2.0 × 10^{-6}), Cd(av. 0.3 × 10^{-6}), Ni (av. 1.6 × 10^{-6}), U (av. 1.3 × 10^{-6}) and Y (av. 1.8 × 10^{-6}) show moderate concentrations.

Table 3. Comparison of averages chemical data of metacarbonate rocks of Nsofang in Ikom area of southeastern Nigeria with carbonate – bearing rocks occurring in other part of the world and MgO/CaO ratio values

	1	2	3	4	5	6	7	8	9	10	11	12	13	14
SiO_2	2.31	0.38	16.20	7.30	2.40	0.50.5	0.49	1.18	0.44	1.98	11.69	10.61	1.91	11.18
TiO_2	0.01	0.004	0.17	–	0.01	0.00	–	–	–	0.01	0.01	0.07	0.04	0.05
Al_2O_3	0.22	0.07	0.43	2.78	0.92	0.07	0.03	0.10	0.07	0.83	0.09	4.30	7.33	0.65
Fe_2O_3	0.08	0.1	12.5	1.18	0.04	0.04	0.07	0.07	0.04	0.26	0.02	2.97	0.01	1.10
MnO	0.01	–	–	–	0.009	0.00	0.002	0.003	0.002	0.01	0.00	0.22	–	0.02
MgO	16.70	0.3	26.89	–	19.60	0.42	20.70	1.75	0.32	2.75	4.38	2.01	8.78	5.36
CaO	35.79	54.87	8.78	47.70	31.82	54.92	28.94	53.64	55.33	50.89	48.71	41.90	45.39	45.30
Na_2O	0.01	0.03	–	–	0.05	0.02	0.01	0.02	0.03	0.06	0.00	1.38	0.26	0.13
K_2O	0.07	0.03	–	–	0.007	0.03	0.03	0.01	0.001	0.01	0.01	0.56	–	0.29
P_2O_5	0.07	–	–	–	0.045	0.00	–	–	–	0.01	0.15	0.21	–	0.04
LOI	44.41	–	32.05	38.66	44.09	43.37	–	–	–	–	35.74	–	42.66	35.56
CaO/MgO	3.07	182.90	0.33	–	1.62	130.76	1.40	30.65	172.91	18.51	11.12	20.85	5.17	8.45

1. Average chemical data of metacarbonate rocks of Nsofang, ikom area of southeastern Nigeria (present work).
2. Average chemical data of Mfamosing limestone, (EKWUEME, 1995)
3. Average chemical data of Guyuk limestone, northeastern Nigeria (GABAKO & TEDRA, 1994)
4. Average chemical data of Ashaka limestone, (TADCO, 1989)
5. Average chemical data of marble, east of the Federal Capital Territory (DAVOU & ASHANO, 2009)
6. Average chemical data of Jakura marble, southwestern Nigeria (OFULUME, 1993)
7. Average chemical data of Igbeti marble, southwestern Nigeria (EMOFURIETA & EKUAJEMI, 1995)
8. Average chemical data of Ososo marble, southwestern Nigeria(EMOFURIETA & EKUAJEMI, 1995)
9. Average chemical data of Akure marble, southwestern Nigeria (EMOFURIETA & EKUAJEMI, 1995)
10. Average chemical data of metacarbonate rock from the Zambezi mobile belt of Zambia (MUNYANYIWA & HANSON, 1988)
11. Average chemical data of Jabal Farasan marble deposit in Saudi Arabia (QADHI, 2008)
12. Average chemical data of marble in the Dalradian Connenera of Western Ireland (YARDLEY, 1977)
13. Average chemical data of metacarbonate rocks in northwest Konya, Turkey (EREN, 1993)
14. Average chemical data of marble with carbonatite-like geochemical signature of the Bohemian massif, Czech Republic (HOUZAR & NOVAK, 2002)

DISCUSSIONS

Characterization and quality implications

The results of the chemical analyses (Table 2) reflect the paragenesis determined by X-ray powder diffraction (XRD) (Table 1), and observed by optical microscopy on thin sections. In particular, the very high concentrations of LOI, CaO, MgO and total carbon (Table 2) corroborate mineralogical observations that the carbonate phases are the dominating phases in the investigated rock, which agree with the broad classification of the rock as a carbonate. Dolomite is clearly the dominating phase, with calcite as subordinate while silicates, notably quartz, talc and phlogopite constitute the accessory phases of the rock (Table 1). The mineralogical composition of the metacarbonate rock indicate that peak metamorphic conditions equivalent to, at most, the greenschist facies (BLATT & TRACY, 1995) was most likely attained. Given the overall field, petrographic, mineralogical and geochemical data, the metacarbonate rocks of Nsofang in Ikom area of southeastern Nigeria can best be classified as low grade dolomitic marble.

The quantitative identification of CaO, Fe_2O_3, MgO and SiO_2 in the Nsofang marble is important in the characterization of the quality and hence the usability of the material. Technically, following ROSEN et al. (2005, 2007), Nsofang marble qualify as pure marble. However, the fact that CaO and LOI composition of the marble, taken together, constitute less than 80 % in most cases (Table 2), points to the presence of significant concentration of components and phases that are not compatible with the purity required of marble for various important applications. CHERNEVA et al. (2009) observed that most of the marble of the Arda Tectonic unit in the Central Rhodope in Bulgaria classified as pure marble are calcite dominated, low in MgO content and display high CaO/MgO ratio. In contrast, the Nsofang marble is dolomite dominated with an MgO contents that are relatively high, reaching a peak of 21.25 % in sample L_{12} and displaying an overall average of 16.62 % (Table 2). Furthermore, the computed CaO/MgO ratio values of the marble (Table 2), which vary between 1.42–13.30 with a mean of 3.07, is quite low when compared to those of deposits of other localities (Table 3), notably, those of Mfamosing limestone, (EKWUEME, 1995), Jakura marble (OFULUME, 1993), Ososo marble (EMOFURIETA & EKUAJEMI, 1995), Akure marble (EMOFURIETA & EKUAJEMI, 1995), metacarbonate rock from the Zambezi mobile belt of Zambia (MUNYANYIWA & HANSON, 1988), Jabal Farasan marble deposit in Saudi Arabia (QADHI, 2008), Dalradian Connenera in western Ireland (YARDLEY, 1977), metacarbonate rocks in northwest Konya in

Turkey (Eren, 1993) and marble with carbonatite-like geochemical signature of the Bohemian massif, Czech Republic (Houzar & Novak, 2002) (Table 3).

In considering these attributes, indication is that the Nsofang marble is tainted, and MgO appear to be the major component that reduces the purity of the marble. SiO_2 also constitute a source of contamination, even though, its concentration in the marble is frequently less than 2 %. Other contaminants, notably Fe_2O_3, Al_2O_3, Na_2O and K_2O are present in small proportion with overall average values that is often less than 1 % (Table 2). The ''impure'' nature of the Nsofang marble can also be sufficiently mirrored by the slightly elevated abundance of trace elements (Table 2) since, according Chernerva et al., (2009), impure marbles of the Arda Tectonic unit in the Central Rhodope in Bulgaria are richer in trace elements than the pure marbles.

Economic aspects
High chemical purity of >97 % $CaCO_3$ compositions and LOI values <3 % are required for a carbonate materials to be considered suitable for used in the manufacture of lime (Boynton, 1980; Ofulume 1993; Ofulume et al., 2009, Power, 1985), and lime that is manufactured for fluxing in steelmaking is expected to exhibit at least 52 % CaO (about 92.8 % $CaCO_3$) (British Standard Institute, 1982). Similarly,

materials to be adopted for use as fillers suitable for the production of paper coatings, paints, rubber and plastics are expected to be of high chemical purity and to display maximum possible calcium carbonates content and minimum acid insoluble composition (Howse, 1994; Qadhi, 2008).

In the light of the foregoing, the Nsofang marble fall short of the specifications of materials to be used as flux and also lack the requirements for its application as raw material in the manufacture of lime and fillers. In particular, the relatively low CaO contents (mean concentration of 35.79 %) of the Nsofang marble, together with the presence of acid insoluble minerals (such as quartz with a maximum content of 6.21 %) fall short of the requirements for adoption of the marble for these usages. Also, the high LOI values of between 40.8 % and 46.5 %, exhibited by the Nsofang marble is considered unacceptable, since LOI of materials to be processed for lime or flux in the Basic Oxygen Furnace (BOF) is expected to be less than 3 % (Ofolume, 1993). Excessive LOI values can have significant effects in reducing potential for scrap melting which may lead to uncontrolled foaming or stopping (Anderson & Vernon, 1971).

Furthermore, a simple comparison of the chemical data of Nsofang marble with the compiled chemical specifica-

tion of a number of industries that consume raw marble (Emofurieta & Ekuajemi, 1995) indicate that the Nsofang marble may also not be appropriate for application in the cement, ceramics and glass industries. Nevertheless, despite these shortcomings, the Nsofang low grade dolomitic marble can be adapted for a variety of other uses, notably, as aggregate in mortar and concrete of the construction industry and as an abrasive product for the polishing of certain metals. Most importantly, the elevated concentration of MgO in the marble can be exploited for use as compensators for magnesium deficiencies in the agricultural industry, especially for neutralizing acidic soils for farming purposes, and may also be relevant in the sourcing of magnesium oxide for the chemical industry as well as in the production of chrome-based products. In addition, with appropriate beneficiation, the elevated MgO, moderate total carbon, and low Al_2O_3 and SiO_2 composition of the Nsofang marble can be harnessed for application as MgO + C refractories for electrical arc furnace (EAF) linings.

Impurities, such as pyrite and marcasite are undesirable in marbles to be used as dimension stones because on oxidation they can produce stains which is of particular concern for exterior work (Howse, 1994). Thus, the low total sulphur composition of the marble, which most likely reflects the absence of sulphur-bearing minerals such as pyrite and marcasite (FeS_2) can be exploited in the application of the marble as dimension stones. Also, with favorable physical attributes, the marble could be considered as a potential source of terrazzo chips and landscaping material and may be suitable for use as a decorative stone. Furthermore, when pulverized and ground to specified mesh size, the Nsofang marble can also be used as low grade carbonate fillers, for use in putty, caulking, sealing, venyl floor covering, carpet backing, asphaltic products and adhesives.

Conclusion and Recommendations

Metacarbonate deposit occurring in Nsofang area of southeastern Nigeria has been classified as low grade dolomitic marble, based on inherent compositional, petrographic and field attributes. The marble is characterized as tainted because of its relatively low CaO contents and CaO/MgO ratio, and elevated MgO, LOI and trace elements composition. The observed compositional features of the marble have suggested a number of applications for the marble, but these are by no means exhaustive. More uses would still be revealed when physical attributes, notably bulk specific gravity and bulk density, water absorption, apparent porosity, reflectance/chromaticity, including brightness, decrepitation, me-

chanical strength tests, notably principle schmidt hammer rebound, uniaxial compression strength test and strength point load index as well as surface area and reactivity, are determined. Subsequent research should also incorporate geophysical techniques so that the extent of the prospect can be adequately defined for reserve estimation purposes.

Acknowledgements

References

Age, T. (2008): Preliminary evaluation of BIF and marble deposits of the area south of Muro Kasa, Northcentral Nigeria. *Continental Journal of Earth Sciences*, 3, pp. 47–52.

Anderson, L. C. & Vernon, J. (1971): Quality and production of lime for basic Oxygen steel making. *The Quarry Manager's Journal, Institute of Quarrying Transaction,* pp. 169–175.

Blatt, H & Tracy, R. J. (1995): Petrology: Igneous, sedimentary and metamorphic. W. H. Freeman and Company, New York, 529p.

Boynton, R. S. (1980): Chemistry and technology of lime and limestone. Wiley Inter Science, 482p.

British Standard Institute (1982): British Standard Institute Specification for limestone for fluxing in steel plants (IS: 10345).

Cherneva, Z. Geogieva, M., Stoilkova, T., Petrova, A. & Hekimova, S. (2009): Geochemistry of metacarbonate rocks from the Arda tectonic unit in the central Rholdope, Bulgaria. Abstracts *of National Conference, Geosciences 2009*.

Danladi, R. (1993): Geological and compositional studies of Burum (FCT) and Kwakuti (Niger State) marble. M. Sc. Thesis, Ahmadu Bello University, Zaria, 114p

Davou, D. D. & Ashano, E. C. (2009): The chemical characteristics of the marble deposits east of Federal Capital Territory (FCT), Nigeria. *Global Journal of Geol. Sciences*, Vol. 7, No. 2, pp. 189–198.

DEELMAN, J. C. (2008): Low-temperature formation of dolomite and magnesite: A comprehensive revision Version 2.3, Compact Disc Publications, Eindhoven, The Netherlands.

EKWUEME, B. N. (1995): The Precambrian geology of Oban Massif, Southeastern Nigeria. In: Ekwueme, B. N., Nyong, E. E and Petters, S. W. (eds), *Geology Excursion guide to Oban Massif, Calabar flank and Mamfe embayment, Southeastern Nigeria*. Dec – Ford Publishers Ltd., Calabar, pp. 1–13.

EMOFURIETA, W. O. & EKUAJEMI, V. O. (1995): Lime products and economic aspects of Igbetti, Ososo and Jakura Marble Deposit in SW – Nigeria. *Journal of Mining and Geology*, Vol. 31, No .1, pp. 79–89.

EMOFURIETA, W. O; IMEOKPARIA, E. G. & AYUK, M. A. (1995): Geochemistry of marbles and Calc-silicate rocks in the Igarra Schist belt Southwestern Nigeria. *African Journal of Science and Technology*, Vol. 7, No. 2, pp. 17–26.

EREN, Y. (1993): Eldes-Gökçeyurt-Derbent-Sögütözü (Konya) Arasinin jeolojisi, Unpublished *Ph.D*., Selçuk University, Konya, 224p.

FOLAMI, S. L. & OJO, J. S. (1991): Gravity and magnetic investigations over marble deposits in the Igarra area, Bendel State. *Journal of Mining and Geology*, Vol. 27, No. 1, pp. 49–54.

GABAKO, D. K. & TEDRA, P. R. (1994): The suitability of Guyuk limestone for the manufacture of Portland cement. 30th Annual Conference of the Nigerian Mining and Geoscience Society, Jos, Nigeria.

HOUZAR, S. & NOVAK, M. (2002): Marbles with carbonatite-like geochemical signature from variegated units of the Bohemian Massif, Czech Republic, and their geological significance. *Journal of the Czech Geological Society,* Vol. 47, No. 3–4, pp.103–110.

HOWSE, A. E. (1994): Industrial potential of the silver mountain marble deposit, western Newfoundland. Current Research, Newfoundland Department of Mines and Energy, Geological Survey Bruvch, Report 94-1, pp. 225–232.

LEAKE, B. E., TANNER, P. W. G. & SENIOR, A. (1975). The composition and origin of Connemara dolomitic marbles and ophicalcites. *Ireland Journal of Petrology*, Vol. 16, pp 237–277.

MUNYANYIWA, H. & HANSON, R. E. (1988): Geochemistry of marble and calc-silicate rock in the Pan-African Zambezi belt, Zambia. *Precambrian Research*, Vol. 38, pp. 177–200.

ODEYEMI, I. B., OLORUNNIWO, M. A. & FOLAMI, S. L. (1997): Geological and geophysical characteristics of the Ikpeshi marble deposit, Igarra area, southwestern Nigeria. *Journal of Mining and Geology*, Vol. 33, No. 2, pp. 63–79.

OFULUME, A. B. (1993): An assessment of the calcination of the suitability of the Jakura marble for use as a flux in steelmaking. *Journal of Mining and Geology*, Vol. 29, No. 1, pp. 1–8.

OFULUME, A. B., ORAZULIKE, D. M. & HARUNA, I. V. (2009): An assessment of the calcination characteristics of the Mfamosing limestone for commercial lime production. *Global Journal of Geological Sciences*, Vol. 7, No. 2, pp. 171–180.

Ojo, J. S., Olorunfemi, M. O., Folami, S. L., Omosuyi, G. O., Abiola, F. J. & Enikanselu, P. I. (2003): Geophysical investigation of marble occurrence in Takalafia area, around Abuja, Central Nigeria. *Global Journal of Geological Sciences*, Vol. 1, No. 1, pp. 51–62.

Olade, M. A. (1975): Evolution of Nigeria's Benue Trough (Aulacogen): A tectonic model. *Geological Magazine*, Vol. 112, No. 6, pp. 93–103.

Power, T. (1985): Limestone specification – limiting constraints on the market. Industrial Minerals, October, pp. 65–84.

Qadhi, T. M. (2008): Testing Jabal Farasan marble deposit for multiple industrial applications. *The Arabian Journal for Science and Engineering*, Vol. 33, No. IC, pp. 79–97.

Rosen, O., Desmons, J. & Fettes, O. (2007): Metacarbonate and related rocks – In Provisional recommendations by the IUGS Subcommission on the systematics of metamorphic rocks. Web version of 01.02.07. www.bgs. as.uk/scmr/home.html.

Rosen, O., Fettes, O. & Desmons, J. (2005): Chemical and mineral compositions of metacarbonate rocks under regional metamorphism conditions and guidelines on rock classification. Russian Geology and Geophysics, Vol. 46, No. 4, pp. 351–360.

Tadco Consulting Engineers (1989): Geological Survey report for Guyuk limestone, Gongola State Government, Nigeria. *Industrial feasibility Report*, 2, 214p

Yardley. B. W. D. (1977): Relationships between the chemical and modal composition of metapetites, Ireland. *Lithos*, Vol. 10, pp. 235–242.

Hydrochemistry of the near shore marine bay, Calabar river (South-eastern, Nigeria)

Hidrokemične razmere v priobalni vodi morskega zaliva ob izlivu reke Calabar v jugovzhodni Nigeriji

EKWERE, A. S.[1, *], EDET, A.[1] & UKPONG, A. J[1]

[1]University of Calabar, Department of Geology, Nigeria

*Corresponding author. E-mail: zerratta77@yahoo.com

Abstract: A study to assess the current hydrochemical status of the rapid developing marine bay of the Calabar River, south-eastern Nigeria, was carried out. The waters have pH values ranging from slightly acidic to slightly alkaline and defined as generally fresh based on TDS values (<1000 mg/L). Analysis reveals an abundance sequence of Na>Ca>Mg>K and Cl>SO$_4$>HCO$_3$>NO$_3$ for cations and anions respectively. Averages were Ca^{2+} (15.15 mg/L), Mg^{2+} (2.93 mg/L), Na$^+$ (21.27 mg/L) and K$^+$ (2.86 mg/L) while for the anions it was Cl$^-$ (156.99 mg/L), SO$_4^{2-}$ (27.85 mg/L), HCO$_3^-$ (14.98 mg/L) and NO$_3$ (0.551 mg/L). The waters belong to the Na-Ca-Cl field on the Piper diagram plot, indicating influence of atmospheric precipitation. Trace elements Fe, Mn, Pb, Zn, Cu, Cd, Cr, Ni and Co show levels within world averages and acceptable limits. Hydrochemical modelling shows heavy metals to exist mainly in free mobile states, chlorides, sulphates, carbonates and hydroxides bound under prevailing pH-Eh conditions at unsaturated levels. Chemical contents and mineral phases are adjudged to be sourced from mineral dissolution, salinization and minimal anthropogenic input.

Izvleček: Raziskava je bila opravljena z namenom oceniti sedanje hidrokemične razmere v naglo spreminjajočem se okolju morskega zaliva ob izlivu reke Calabar v jugovzhodni Nigeriji. Vrednosti pH vode nihajo med rahlo kislimi do rahlo alkalnimi. Vodo je mogoče splošno oceniti za sladko glede na vrednosti TDS (celotna raztopljena snov <1000 mg/L). Analiza razkriva naslednji zaporedji kationov in anionov:

Original scientific paper

Na>Ca>Mg>K in Cl>SO_4>HCO_3>NO_3. Povprečna koncentracija Ca^{2+} je 15,15 mg/L, Mg^{2+} 2,93 mg/L, Na^+ 21,27 mg/L in K^+ 2,86 mg/L in anionov Cl^- 156,99 mg/L, SO_4^{2-} 27,85 mg/L, HCO_3^- 14,98 mg/L in NO_3 0,551 mg/L. Vode pripadajo Na-Ca-Cl-polju v Piperjevem diagramu, kar nakazuje vpliv atmosfernih padavin. Sledne prvine Fe, Mn, Pb, Zn, Cu, Cd, Cr, Ni in Co so na ravni svetovnih povprečij in v sprejemljivih koncentracijah. Hidrokemijsko modeliranje kaže, da so težke kovine navzoče pretežno v prostih mobilnih specijah kot kloridi, sulfati, karbonati in hidroksidi, ki so v sedanjih razmerah pH-Eh v nezasičenih koncentracijah. Vir raztopljenih snovi in mineralnih faz so raztapljanje mineralov, salinizacija in minimalen antropogeni vpliv.

Key words: river, trace element, mineral species, geogenic, Calabar, Nigeria

Ključne besede: reka, sledne prvine, mineralne specije, geogeno, reka Calabar, Nigerija

Introduction

Rivers transport more than just water from land to sea as river basins are not inert. River chemistry and particulate load reflect natural and human processes within the watershed. The progression of a river along its course leads to interaction with a variety of geological types and it may have input from aquifers not visible on the surface anywhere in the locality.

In most developing communities, increase in human population geared by the quest for good water supply, irrigation, fish production, recreation and navigation has resulted in enormous pressure and stress on reservoirs. This is readily identified by variation of the natural chemistries of reservoirs as well as heavy metal contamination. However-

er two major sources have been identified as possible sources of metal loads in rivers in proximity to urbanised areas. These are natural sources from rock weathering within the catchment and anthropogenic sources derived from human activities (Abrahim & Parker, 2002). Mustapha (2008), reckon water quality deterioration in reservoirs as related to excessive nutrient inputs, eutrophication, acidification, heavy metal contamination, organic pollution and obnoxious fishing practices.

Indiscriminate disposal of industrial and urban waste into river catchment plays a major role in most environmental problems. Associated presence of nutrients and heavy metals especially at elevated levels, leads to accumulation in tissues of organisms. These metals are not readily assimilated for

growth or excreted, resulting in amplifications of their concentrations along the food chain and exposure of humans at the apex to the risk of metal poisoning (AKPAN et al., 2002).

Physico-chemical properties have been used to assess water quality in reservoirs (DJUKIC et al., 1994). This gives a good impression of the status, productivity and sustainability of such water bodies.

The estuarine Marine Bay of the Calabar River, south-eastern Nigeria, has experienced a significant increase in activities in recent times. These human perturbations include fishing, shipping, recreation, aquaculture etc. Discharge of effluents into the river basin has been recognized as an integral part of these operations. These apparently will culminate into stresses on the status of the water quality with time. The present study aims to ascertain the potability of the near-shore waters of this marine bay and provide data set for future environmental and resource management issues.

DESCRIPTION OF STUDY AREA

The study area belongs to what has been described as Calabar urban (EDET et al, 2003), situated between latitude 4º15'–5º15' North and longitude 8º5'–8º25' East (Figure 1). The study area receives an average rainfall of about 254 mm annually within two distinct seasons; dry and wet seasons. Mean annual air temperature and relative humidity are 26.8 ºC and 84.6 % respectively. Geologically the study area is composed of Tertiary and Quaternary sediments referred to as Coastal Plain Sands of the broader Niger Delta basin (SHORT & STAUBLE, 1967). This formation consists of alternating sequence of gravel, sand, silt, clay and alluvium which are derived from the adjoining Precambrian Basement and Cretaceous rocks.

The Precambrian basement (Oban Massif) complex is made up of migmatites-gneisses, granites, schists, para-schists, pegmatites and a host of other ultramafic rock suites (EKWUEME, 2003).

The Cretaceous sedimentary geologic unit is known as the Calabar Flank and is built up of limestones, sandstones, shales and marls (REIJERS, 1996).

Geomorphologically, the study area is of a coastal setting with surface elevations ranging from less than 10 m in the southern part to about 80 m in the north.

MATERIAL AND METHODS

A total of twenty (20) water samples were collected from locations along the near shore of the marine bay. The

sampling locations included but were not limited to sites in proximity to marine related human activities within the study area (Table 1). This was to assess possible impacts of anthropogenic activities on water chemistry. The sampling period was June–July 2009 at the peak of the wet season.

Physical parameters (pH, temperature, TDS, Eh and conductivity) were measured in the field using standard equipment: PHT-027 multi-parameter water quality probe. Major and trace element contents were determined by atomic absorption spectrophotometer (AAS), model UNICAM 939. The anion contents of samples were determined by colorimetric method using UNICAM UV2 spectrophotometer. All instrumental analyses were carried out in the quality control laboratory of the Aluminium Smelter Company of Nigeria (ALSCON), Ikot Abasi, Nigeria.

Saturation indices and mineral phases were determined using the VISUAL MINTEQ computer program. The em-
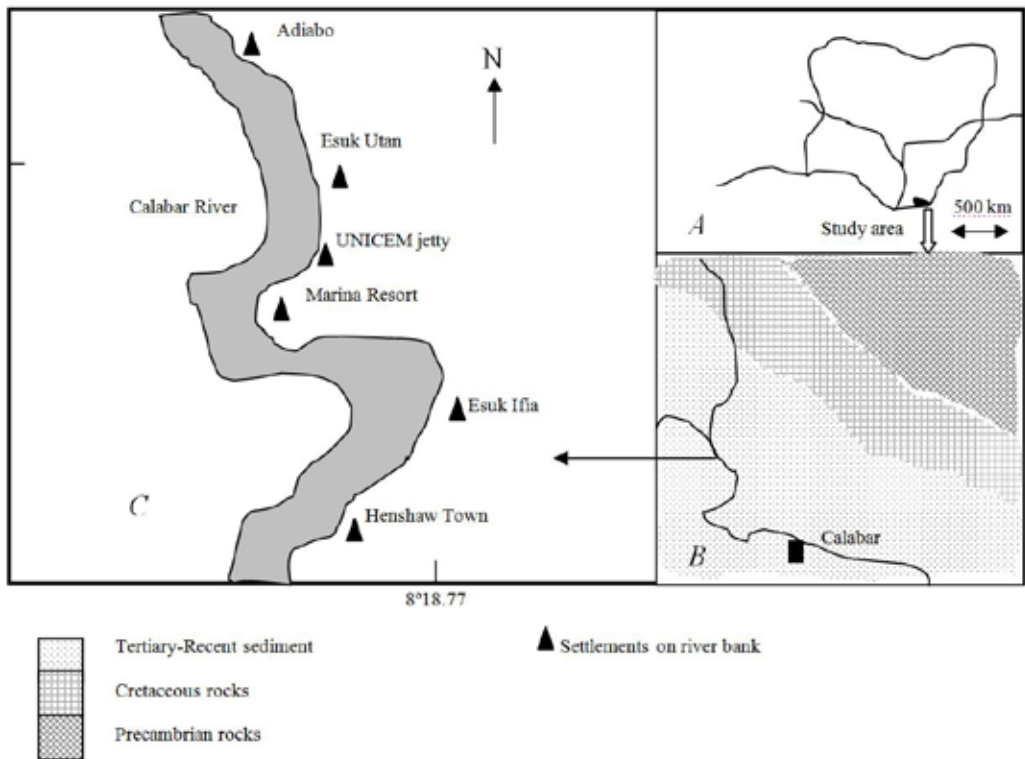
Figure 1. Map of Calabar and environs including sampled river. [*A*] Index map of Nigeria, [*B*] geologic map, [*C*] Calabar River; modified after EDET & WORDEN (2009)

Table 1. Some sampling locations with active potential sources of contamination.

Location	Surrounding Activities
Henshaw town beach	Sand mining, wood processing, domestic waste disposal
Esuk Ifia (marina)	Boat jetty, wood processing, out-board engine repairs, abandoned boats
Marina Resort	Tourist/leisure park, boating, food waste and effluent disposal
Inland Water Authority	Jetty, boat repairs
UNICEM jetty	Jetty, hauling of cement, boating
Esuk Utan	Sand mining, boating, domestic waste disposal, wood processing
Tinapa	Jetty, boating, waste disposal, oil/crude carrying vessels
Adiabo bridge	Boating, domestic waste disposal
Ibonda (NPA Port)	Boating and boat repairs, shipping, waste disposal
Creek Town beach	Boating, domestic waste disposal, wood processing

ployment of VISUAL-MINTEQ as modelling tool was due to its extensive database of mineral and aqueous species for interpretation purposes.

Results and discussion

Table 2 outlines the descriptive statistics for physico-chemical and trace elements contents of samples in comparison to world averages and acceptable standards. Table 3 shows the correlations between major cations and anions as a means of establishing probable controls of chemical characteristics.

Physical properties

The temperature of the sampled waters ranged from 27–29 ºC with a mean of 28.5 ºC (Table 2). These values are consistent with mean air temperatures as they coincide with period of sampling and diurnal temperature

variations within the locality (Edet & Worden, 2009).

The pH values ranged from 3.48–7.60 with an average of 6.27. The lowest pH of 3.48 was recorded at one of the most active sites (Esuk Utan) along the shore with great potency for pollution. The rest of the locations revealed pH values of slightly acidic – slightly alkaline with a greater percentage within the 6.5–8.5 WHO recommended standard.

Electrical conductivity (EC) data showed a range of 460–2,240 µS/cm with an average of 1 080 µS/cm. the values were generally below the 1,400 µS/cm WHO limit, except for the site with the maximum value. Comparison of EC data from Edet & Worden (2009) shows the values are within background levels, reflecting minimal or absence of pollution effects.

Total dissolved solids (TDS) ranged from 320–1140 × 10⁻⁶ with an average value of 745 × 10⁻⁶. With reference to quality, about 60 % of the sampled waters are freshwater with TDS values <1,000 mg/L (FREEZE & CHERRY, 1979). The rest of the waters were within the lower limits of brackish water (TDS 1,000–10,000 mg/L). There was an observed direct relationship between TDS and EC data, reflecting equilibrium of abundance of free ions in water relative to soluble content (HEM, 1986).

The redox potential values (Eh), ranged from 9–97 mV with a mean of 42 mV. These values are well within the baseline data as reported by EDET et al. (2003) and significant variation in future may indicate pollution effects.

Chemical characteristics

As revealed from mean values, the relative abundance sequence of the major cations was Na > Ca > Mg > K. Sodium concentration varied from 4.65–33.16 mg/L with a mean of 21.27 mg/L. From observations all the values were within the baseline data as reported by EDET et al. (2003), below world average and within the WHO limits.

Calcium had concentrations of 7.07–22.46 mg/L and a mean of 15.15 mg/L. The mean value is in proximity to world average of 15.0 mg/L (TUREKIAN, 1977) and all values were below the WHO limits.

Magnesium and potassium exhibited ranges of values within local baseline data, global averages and below WHO standards with means of 2.93 mg/L and 2.86 mg/L respectively (Table 2).

The relative dominance of Na reflects the mixing of seawater with the freshwater within the estuarine coastal area. Ion exchange processes for seawater cations (especially Na and Mg) for Ca are prevalent at exchange sites with Ca^{2+} going into solution (EDET & WORDEN, 2009). The effect of this would probably be more defined with an assessment based on tidal regimes within the study area.

Sources of Ca and Mg are attributed to the weathering of anorthite, pyroxene and amphibole from the overlying Oban massif in the northern parts of the study area (EDET et al., 2003, EKWERE, 2010). Mineral dissolution incepted by precipitation and weathering of hydroxyl-apatite, fluorite, dolomite, calcite, sylvite, epsomite, mirabilite and halite (which are present in the catchment geology) are also probable sources of these cations (EKWERE 2010).

However, the contributions of rainfall through marine input of sea salts (BERNER & BERNER, 1996) cannot be ruled out as high precipitation levels is characteristic of this marine coastal setting.

Assessment of anion concentrations shows that chloride varied from 118.10–234.10 mg/L with a mean of 156.99 mg/L. All the concentration values of Cl were above the baseline data of EDET et al., (2003) but below the WHO limit of 250 mg/L. The Cl contents in the waters are attributable to seawater incursion into the fresh coastal waters as well as precipitation influence. River runoff dominated by precipitation is proportionally high in Cl (recycled salt) and low in total concentration.

Sulphate concentration ranged between 12.10–52.40 mg/L with an average value of 27.88 mg/L. the concentration levels were within the local baseline and below the WHO limit (table 2). Sulphate concentrations are attributed to natural accentuation from pyrite (FeS) within this estuarine setting (EDET & WORDEN, 2009).

The bicarbonate (HCO_3) concentration levels varied from 10.56–24.32 mg/L with a mean value of 14.98 mg/L. The concentrations were within the local baseline and below world average value (Table 2). The dominant source of HCO_3 is the dissolution of carbonate rocks within the Cretaceous sediments which forms part of the catchment geology of the study area.

Nitrate had concentration values ranging from 0.298–0.862 mg/L with a mean of 0.551 mg/L. This shows that all values were below the WHO maximum permissible limit of 10 mg/L. The main source of nitrate in the water is the use of nitrogenous fertilizers for agricultural purposes as well as the indiscriminate dumping of human and animal waste into the environment. These are anthropogenic and though not posing any threat to health status, monitoring is duly advised.

Ammonium concentration ranged from 1.12–3.73 mg/L with a mean of 2.54 mg/L. These concentration levels are the result of agricultural land scrubbing, human and animal waste disposal into the environment.

Heavy metal trend
Assessment of heavy metal data (Table 2) shows that iron and manganese had mean values of 0.95 mg/L and 0.16 mg/L respectively with ranges within world average (TUREKIAN, 1977) but slightly above WHO limits. The relatively more toxic elements; Pb, Zn, Cu, Cd, Cr, Co and Ni, had mean values of 0.004, 0.054, 0.051, 0.004, 0.071, 0.004 and 0.026 mg/L respectively. These values were within world averages and WHO limits.

Contents of trace elements reflect a dominant influence of rock weathering processes, as mineral phases laden with these elements constitute the rocks within the overlying basement

and Cretaceous sediments (Ekwere, 2010). However, though minimal, the effects of anthropogenic activities can contribute to concentration levels of these potentially toxic elements.

Hydrochemical facies and variable projections

A plot of the data for the major cations and anions on the Piper (1944) diagram (Figure 2) shows that the waters fall within the Na – Ca - (Mg) – Cl field. This is in line with relative abundance sequence as revealed from the data set. The recognized water type is defined to be a major constituent of atmospheric precipitation (Davis & De Weist, 1966).

Bivariate correlation analysis was also employed to assess relations between variables. From the correlation matrix (Table 3), Ca^{2+} exhibits a strong positive correlation with Mg^{2+} and Na^+ ($r > 0.70$) and moderate correlation with NO_3^- ($r = 0.50–0.70$). Magnesium (Mg^{2+}) has a strong positive correlation with Na^+. These relationships between the major exchangeable cations Ca-Mg-Na represent effects of dissolution and precipitation reactions and concentration effects (Ekwere, 2010). Moderate correlation between Na^+, K^+ and Cl^- suggests evaporite dissolution and seawater mixing effects with the coastal freshwaters. The entire scenario reflects a dominance of geogenic influence over water chemistry than anthropogenic.

Two factorial axes *F1* and *F2* (Table 4) were determined through factor analysis using the STATISTICA computer program, extracting 31.22 % and 17.13 % respectively of total data variance and accumulating to 48.35 %. Classification of factor loadings is described as 'strong', 'moderate' and 'weak', corresponding to absolute values of >0.75, 0.75–0.50 and 0.50–0.30, respectively (Liu et al., 2003). However for this study, factor loadings greater than 0.60, were considered significant.

Factor 1 (Ca, Mg, Na, Cl, SO_4 and Mn) projected a maximum of variables and defined by the majority of parameters that describe water quality. These are contents in calcium (0.676), magnesium (0.906), sodium (0.876), chloride (0.750) and on the negative pole sulphate (–0.805) and manganese (–0.662). This axis defines water of strong salinities and charged in suspended matter (Ben Garali et al., 2011). The composition of this factor reflects natural weathering from water-rock interactions in geo-matrix of the basement and inputs from primitive saline waters of Cretaceous limestones of the Calabar Flank (Ekwere, 2010).

Factor 2 (HCO_3, Cr, K and Zn) appears erratic in composition but apparently indicates dissolution effects of mineral phases that constitute the rocks of the catchment geology. The dissolution of carbonate rocks from the Calabar Flank

Table 2. Comparison of physico-chemical parameters with baseline data, world average and WHO (2001) standards

Stat	Temp	EC	TDS	pH	Eh	Ca	Mg	Na	K
Mean	28.75	1080	745	6.27	42	15.15	2.93	21.27	2.86
Min	28	460	320	3.48	9.0	7.07	0.78	4.65	1.08
Max	29	2240	1140	7.60	97	22.46	4.02	33.16	6.11
SD	0.42	578.90	340.63	1.21	29.80	4.94	1.01	9.45	1.47
BLD		41–264		4.0–6.0	31–143	1.73–4.76	0.51–6.10	9.05–48.2	1.3–3.6
WA			120[a]			13.4[b]	3.4[b]	5.2[b]	1.3[b]
SW			35,000			412	1,280	10.780	399
WHO		1,400	1000	6.5–8.5		200	100	250	12

Stat	Cl	SO$_4$	HCO$_3$	NO$_3$	NH$_4$	Fe	Mn
Mean	156.9	27.85	14.98	0.55	2.54	0.95	0.16
Min	118.1	12.10	10.56	0.30	1.12	0.13	0.003
Max	234.1	52.40	24.32	0.86	3.73	2.19	0.712
SD	40.34	11.51	4.05	0.21	0.92	0.60	0.25
BLD	0.78–69.9	0.18	12.2–18.3	1.3–2.7			
WA	5.8[b]	8.3[b]	52[b]			100[a]	15[a]
SW	19,350	2,710	123				
WHO	250	400		50		0.3	0.1

Stat	Pb	Zn	Cu	Ni	Cd	Cr	Co
Mean	0.004	0.054	0.051	0.026	0.004	0.071	0.004
Min	0.002	0.023	0.014	0.003	0.001	0.006	0.001
Max	0.007	0.104	0.086	0.083	0.016	0.211	0.007
SD	0.002	0.023	0.036	0.023	0.003	0.052	0.002
BLD							
WA	3.0[a]	20[a]	3.0[a]	1.5[a]	0.03[a]	1.0[a]	0.1[a]
SW							
WHO	0.05	5.0			0.005	0.05	

Temp (°C), EC (μs/cm), Eh (mV), TDS (× 10^{-6}), cations, anions and heavy metals (mg/L)
BLD-Baseline data (EDET et al., 2003)
WA-World Averages   [a] (TUREKIAN, 1977)
                         [b] (MEYBECK, 1979)
SW-Sea Water (MILLERO, 1996)
WHO-World Health Organization (2001)

and ultra-mafic rocks from the basement are visible in this factor loading.

Hydrochemical modelling

The modelling package VISUAL-MINTEQ was used to calculate distributions of aqueous species and mineral saturation indices using the measured water compositions. The employment of VISUAL-MINTEQ as a complimentary interpretation tool was to assess chemical species of dissolved component, saturation indices and hazard prognosis. Results for selected parameters for the sampled waters are presented in Table 5.

Mineral equilibrium calculations for water are useful in predicting the presence of reactive minerals in water sys-
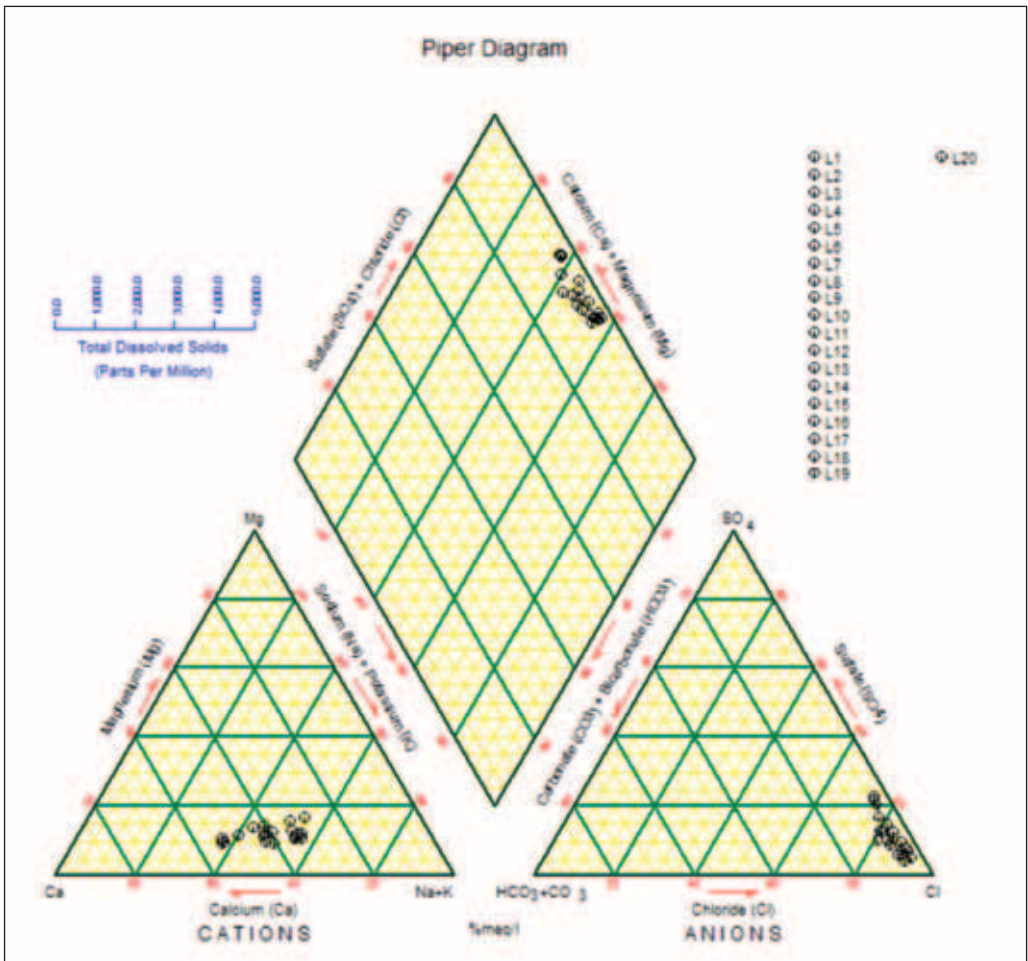
Figure 2. Piper trilinear diagram of sampled waters

tem and estimating mineral activity; (TAYLOR et al, 1996; DEUTSCH, 1997 and ZHU et al, 2008).The solution is considered to be in equilibrium with regards to a particular mineral if the saturation index (SI) = 0. It is considered to be undersaturated if SI < 1 and oversaturated if the SI > 1.

Metals can exist in water as many aqueous species and the type(s) of species can affect mineral solubility, adsorption/desorption behaviour and possibly bioavailability. The predicted predominant aqueous species from hydrochemical modelling are given below for the metals measured and detected in the water samples.

Iron
Iron existed as Fe^{2+}, $FeOH^+$, $FeCl^+$, $FeSO_{4(aq)}$ and $FeHCO_3$. Despite the many possible aqueous species for iron, the predominant ones were invariably predicted to be Fe^{2+} and $FeSO_{4(aq)}$ (melanterite) constituting 86 % and 8

Table 3. Correlation matrix for major constituents of water

	Ca	Mg	Na	K	HCO_3	Cl	SO_4	NO_3	NH_4
Ca	1	0.74	0.83	0.44	0.23	0.28	−0.56	0.50	−0.29
Mg		1	0.90	0.52	0.18	0.62	−0.76	0.46	−0.48
Na			1	0.61	0.17	0.58	−0.63	0.40	−0.25
K				1	0.45	0.70	−0.24	−0.16	−0.07
HCO_3					1	0.09	−0.45	−0.17	−0.49
Cl						1	−0.44	0.31	−0.05
SO_4							1	−0.55	0.62
NO_3								1	−0.21
NH_4									1

Table 4. Factor loadings of chemical parameters

	Factor 1	Factor 2
	Ca 0.676 Mg 0.906 Na 0.876 Cl 0.750 SO_4 −0.805 Mn −0.662	HCO_3 −0.648 Cr −0. 851 K −0.713 Zn −0.674
Eigenvalue	5.619	3.082
% total variance	31.22	17.13
Cumul. Eigenval Cumul. %	5.619 31.22	8.701 48.35

Table. 5 Major chemical species of trace elements.

Element	Dominant species	mass fraction, $w/\%$
Fe	Fe^{2+} $FeSO_{4(aq)}$	86.0 8.0
Mn	Mn^{2+} $MnSO_{4(aq)}$	92.0 3.0
Ni	Ni^{2+} $NiSO_{4(aq)}$ $NiHCO_3$	88.0 6.0 3.0
Pb	Pb^{2+} $PbCl^-$ $PbSO_4$	64.0 9.0 6.0
Zn	Zn^{2+} $ZnSO_{4(aq)}$	95.0 3.0
Cu	Cu^{2+} $CuOH^+$ $CuCO_{3(aq)}$	86.0 5.0 4.0
Cd	Cd^{2+} $CdCl^-$	71.0 23.0
Cr	$CrOH^-$	92.0
Co	Co^{2+}	90.0

% respectively of the species. Under the prevailing Eh-pH condition, Fe^{2+} is immobile. Its mobility will further be hindered in the area by precipitation as Fe oxides (hematite, magnetite), oxyhydroxides (goethite) and other co-precipitating metal phases (Edet et al, 2004).

Manganese
Manganese exhibited various species in the water including, Mn^{2+}, $MnCO_{3(aq)}$, $MnCl^-$, $MnSO_{4(aq)}$ and $MnHCO_3^-$. Mn is non-toxic and the dominant phase was the ionic Mn^{2+} accounting for over 92 % in the waters. Lesser to this was $MnSO_{4(aq)}$ constituting about 3 %. Under the present pH- Eh of the waters, Mn^{2+} is immobile posing no problem in the area.

Nickel
The following species of Ni were identified through modelling, Ni^{2+}, $NiOH^+$, $NiCl^+$, $NiSO_{4(aq)}$, $NiCO_{3(aq)}$ and Ni-HCO_3^+. Ni^{2+} was the most dominant constituting 88 %, $NiSO_{4(aq)}$ (retgersite) about 6 % and $NiHCO_3^+$ 3 %. Ni^{2+} compounds are non-toxic (Reimann & Caritat, 1998) and its immobility un-

der the present pH-Eh condition, Ni does not pose any threat to the waters in the study area.

Lead

Species of lead (Pb) included, Pb^{2+}, $PbOH^+$, $PbCl^+$, $PbCl_{(aq)}$, $PbSO_{4(aq)}$, $PbCO_{3(aq)}$ and $PbHCO_3^+$. Though aqueous lead is predicted to be distributed amongst several species Pb^{2+} made up about 64 %, $PbCl^-$ 9 %, while $PbSO_{4(aq)}$ (anglesite) and $PbHCO_3$ were 6 % each. The distributions of the species show no marked difference for the different locations. Pb^{2+} appears to be mobile but however poses no problem of contamination as Pb is low (mean 0.004 mg/L) and $PbCO_3$ will restrict its mobility (EDET et al, 2004).

Zinc

Species of zinc included Zn^{2+}, $ZnOH^+$, $ZnCl^+$, $ZnSO_{4(aq)}$, $ZnCO_{3(aq)}$ and $ZnHCO_3^+$. Zn^{2+} made up about 95 % of the species. Far less but next to this was $ZnSO_{4(aq)}$ (bianchite) constituting only about 3 %.

Copper

Various species of copper were revealed and included Cu^{2+} (86 %), $CuOH^+$ (5 %), $CuCO_{3(aq)}$ (4 %), $CuSO_{4(aq)}$ (3 %) and $Cu(OH)_2^{2+}$, $Cu(OH)_{2(aq)}$, $CuCl^+$, $CuNH_3^{2+}$ and $CuHCO_3^+$. The speciation of copper is controlled by pH, redox, chlorinity, sulphate and total copper concentrations.

Cadmium

Cadmium existed as various species but major constituents included, Cd^{2+}, $CdCl^+$, $CdOH$, $CdCl_{2(aq)}$, $CdSO_{4(aq)}$, $CdHCO_3^+$ and $CdCO_{3(aq)}$. The speciation of cadmium is dependent on pH, chlorinity, sulphate and total cadmium concentrations. However Cd^{2+} was dominant with 71 % and $CdCl^-$ with 23 %. At present pH-Eh condition, Cd^{2+} which is toxic and carcinogenic is immobile and if present in high concentrations may be precipitated, thus reducing its danger potential.

Chromium

Chromium with minimal concentrations in most samples, exhibited a predominance predicted to be $CrOH^-$ with about 92 % of total composition. The only other specie was Cr^{2+}. This potentially toxic element is immobile posing no threat to water quality as its content was low at a mean of 0.071 mg/L.

Cobalt

Cobalt (Co^{2+}), $CoOH^+$, $CoCl^-$, $CoSO_{4(aq)}$, $CoCO_{3(aq)}$ and $CoHCO_3^+$ were the species of cobalt identified. Co^{2+} predominated with over 90 % of total composition.

Mineral saturation states were calculated as part of the output from the modelling program as a means of indicating what minerals might be dissolving or precipitating into or from the water and controlling its composition. The cal-

Table 6. Oversaturated mineral species

Mineral species	Chemical composition	Saturation index
Brochantite	$CuSO_{4(aq)}$	1.423
Malachite	$CuCO_{3(aq)}$	1.449
Ni-hydroxide	$Ni(OH)_2$	1.413
Tenorite	$Cu.H^+(H_2O)$	2.302

culations are based on an equilibrium model, so the results are only an indication, as kinetic factors may inhibit approach to equilibrium.

The modelling reveals that majority of the species of the metals (hydroxides, carbonates, sulphates, chlorides and bicarbonates) were under-saturated. However a few species were above equilibrium at very low levels of oversaturation (Table 6). These include aqueous Cu-sulphate (brochantite), Cu-carbonate (malachite), hydrous copper (tenorite) and hydroxides of Ni and Fe.

Free metal species are the most bio-available and toxic form of trace elements that exist in natural water (APTE et al., 1995). Considered metals exist as free ions and are relatively mobile under prevailing Eh-pH conditions. However their low concentrations in addition to the presence of limiting mineral phases (carbonates and sulphates) reduce the risk of their contamination to the waters.

CONCLUSION

The waters of the marine bay of the Calabar River exhibit a compositional abundance sequence of Na>Ca>Mg>K for cations and Cl>SO_4>HCO_3>NO_3 for anions. The waters are characterised as Na-Ca-Cl, indicating influence of saline water incursion and lesser effects of atmospheric precipitation. The water characteristics also reflect mixing of waters of multiple geogenic origin; Ca-Mg-HCO_3 and Ca-Na-Cl waters from the basement and Cretaceous geologic units north of the study area (Ekwere, 2010). Heavy metals (Fe, Mn, Pb, Zn, Cu, Cd, Cr, Ni and Co) generally show ranges within world averages and acceptable limits. Speciation modelling shows that metals exist as ions, chlorides, sulphates, carbonates and hydroxides, largely at unsaturated levels. Mineral dissolution and salinization are the main controls of water chemistry.

REFERENCES:

ABRAHIM, G. & PARKER, R. (2002): Heavy metal contaminants in Tamaki estuary: impact of city development and growth, Auckland, New Zealand. *Environmental Geology*, Vol. 42, pp. 883–890.

AKPAN, E. R., EKPE, U. J. & IBOK, U. J. (2002): Heavy metal trends in the Calabar River, Nigeria. *Environmental Geology*, Vol. 42, pp. 47–51.

APTE, S. C., BENKO, W. I. & DAY, G. M. (1995): Partition and complexation of copper in the Fly River, Papua, New Guinea. J Geochem. Explor. 52:67–79

BEN GARALI, A., OUAKAD, M. & GUEDDARI, M. (2011): Geochemistry of Bizert lagoon affluent water, Northern Tunisia: principal component analysis. *Arab. Jour. Geosci.,* Vol. 4, pp. 475–481.

BERNER, E. K. & BERNER, R. A. (1996): Global environment: water, air and geochemical cycles. Upper Saddle River, NJ. Prentice Hall, Inc.

DAVIS, S. N. & DE WEIST, R. J. M. (1966): Hydrogeology. New York: John Wiley & Sons.

DEUTSCH, W. J. (1997): Groundwater geochemistry, fundamentals and applications to contamination. Lewis Press, New York.

DJUKIC, N., MALETIN, S., PUJIN, V., IVANC, A. & MILAJONOVIC, B. (1994): Ecological assessment of water quality of Tisze by physico-chemical and biological parameters. *Tisze Szeged*, Vol. 28, No. 1, pp. 37–40.

EDET, A. E., MERKEL, B. J., & OFFIONG, O. E. (2003): Trace element hydrochemical assessment of the Calabar Coastal Plain Aquifer, SE Nigeria using statistical methods. *Environmental Geology*, Vol. 44, pp. 137–149.

EDET, A. E., MERKEL, B. J., & OFFIONG, O. E. (2004): Contamination risk assessment of fresh groundwater using the distribution chemical speciation of some potentially toxic elements in Calabar (southern Nigeria). *Environmental geology*, Vol. 45, pp. 1025–1035.

EDET, A. & WORDEN, R. H. (2009): Monitoring of the physical parameters and evaluation of the chemical composition of river and groundwater in Calabar (south-eastern Nigeria). *Environ. Monit. Assess.*, Vol. 157, pp. 243–258.

EKWERE, A. S. (2010): Hydrogeological and Hydrogeochemical Framework of the Oban Massif, south-eastern Nigeria. PhD Thesis, Dept. of Geology, University of Calabar, Calabar, Nigeria.

EKWUEME, B. N. (2003): The Precambrian geology and evolution of the Southeastern Nigerian basement complex. University of Calabar Press 135p.

FREEZE, R. A. & CHERRY, J. A. (1979): Groundwater, 2nd edition (604pp). New Jersey: Prentice Hall.

HEM, J. B. (1986): Study and interpretation of chemical characteristics of natural water. *US Geological survey water supply paper*, Vol. 2245, pp. 263.

LIU, C. W., LIN, K. H., KUO, Y. M. (2003): Application of factor analysis in the assessment of groundwater quality in a Blackfoot disease area in Taiwan. *Sci. Total Environ.*, Vol. 313 (1–3), pp. 77–89.

MEYBECK, M. (1979): Concentration des

eaux fluvales en elements majeurs et apports en solution aux oceans. *Revue de Géologie Dynamique et de Géographie Physique*, Vol. 21, pp. 215–246.

MILLERO, F. J. (1996): Chemical oceanography. Boca Raton, FL: CRC Press.

MUSTAPHA, M. K. (2008): Assessment of the water quality of Oyun reservoir, Offa, Nigeria, using selected physicochemical parameters. *Turkish Journal of Aquatic Sciences*, Vol. 8, pp. 309–319.

PIPER, A. M. (1944): A graphic procedure in the geochemical interpretation of water analysis. *Am. Geophys. Union Trans.*, Vol. 25, pp. 914–923.

REIMANN, C. & CARITAT, P. (1998): Chemical elements in the environment. Fact sheets for the geochemist and environmental scientist. Springer, Berlin Heidelberg New York, 398pp.

SHORT, K. C. & STAUBLE, A. J. (1967). Outline of geology of Niger Delta. *AAPG Bulletin*, Vol. 52, pp.761–779.

TAYLOR, J. R., WEAVER, T. R., MCPHAIL, D. C., & MURPHY, N. C. (1996): Characterization and impact assessment of mine tailings in the King River System and delta, Western Tasmania. Final Rept: Project No. 5 Mt. Lyell Remediation Res. and Demonst. Program.

TUREKIAN, K. K. (1977): Geochemical distribution of elements. *Encyclopaedia of Science and Technology*, 4th edition. New York: McGraw Hill.

WHO, (2001): Guidelines for drinking water quality, 3rd edn. WHO/EO/20.1. WHO, New York, 283 pp.

ZHU, G. F., SU, Y. H., & FENG, Q. (2008): The hydrochemical characteristics and evolution of groundwater and surface water in the Heihe River Basin, northwest China. *Hydrogeology Journal*, Vol. 16, pp. 167–182.

Modernization of technological process and equipment at floor level roadways execution in Velenje coal mine

Modernizacija tehnoloških procesov in opreme pri gradnji jamskih prog v Premogovniku Velenje

Evgen Dervarič[1],*, Željko Vukelić[1], Milan Medved[2]

[1]University of Ljubljana, Faculty of Natural Sciences and Engineering, Aškerčeva 12,
SI-1000 Ljubljana, Slovenia
[2]Velenje Coal Mine, Partizanska 78, SI-3320 Velenje, Slovenia

*Corresponding author. E-mail: evgen.dervaric@ntf.uni-lj.si

Abstract: In the period from 2008 to 2010 Premogovnik Velenje (Velenje Coal Mine) carried out an extensive research and development project on modernization of technological processes, materials and equipment needed in construction of the floor level roadways. The main purpose of this research project was a comprehensive update of all key processes in construction of roadways, which contribute to increasing advances in highly productive extraction by divergent method of mining, especially in the working phase of dismantling the steel arch support units on the accession lines during extraction. In the technological process of building floor level roadway elements such as a steel arch supports, wooden panels, composite bolts, composite nets and various insulating coatings that prevent the formation of oxidation processes are used for support. The bright roadway diameter lines represent the modified steel arches shape where the cross section ranges from 13 to 18 m^2. Due to technological changes and new support elements a new appropriate shape of the roadway profile was constructed, tested and introduced. As well, new screw clamps, wire clamps for screw clamps and the new struts for connecting steel arch line frame supports were introduced. Analysis and the load bearing capacity tests of supports were carried out with intention of re-installing. There were several experiments, on the surface and underground, on materials and technologies which are used for isolation procedures. Experimental results during the construction phase were rather excellent, the situation will

---

Original scientific paper

be monitored further on in 2011, so a comprehensive technical evaluation could be defined. In case of equipment an extensive work has been done. A new conveyer, a mobile conveyor belt with continuous lengthening, won all the parameters which enable continuous operation without physical assistance. New feeder bars were introduced. In the field of equipment development the research was primarily aimed on complete mechanization and automation of all phases of roadway construction work and thus greatly improved security, technical and economic parameters. In this paper all the important achievements in the floor level roadways construction are presented.

Izvleček: Premogovnik Velenje je v letih od 2008 do vključno 2010 izvedel obsežen razvojno-raziskovalni projekt pri modernizaciji tehnoloških procesov, materialov in opreme pri gradnji etažnih jamskih prog. Temeljni cilj razvojnega projekta je bil celovita posodobitev vseh ključnih procesov gradnje jamskih prog, ki bistveno pripomorejo k povečanju napredkov na visokoproduktivnih odkopih z odstopajočim načinom odkopavanja, predvsem pri delovni fazi demontaže jeklenega ločnega podporja v pristopnih progah ob napredovanju odkopa. V tehnološkem procesu gradnje jamskih prog se uporabljajo podgradni elementi v obliki jeklenega ločnega podporja, lesenega opaža, kompozitnih mrež in kompozitnih sider ter različnih izolacijskih oblog, ki preprečujejo nastanek oksidacijskih procesov. Svetli premer jamske proge so modificirani profili dimenzij od 13 m² do 17 m². Na področju tehnoloških sprememb in novih podgradnih elementov je bil konstruiran, preizkušen in uveden nov ustreznejši profil gradnje jamskih prog. Poleg tega so bile uvedene nove vijačne objemke, žične spone za vijačne objemke in nove veznice za povezovanje okvirjev jeklenega ločnega podporja. Izvedena je bila analiza in preizkusi nosilnosti ločnega podporja, ki je namenjeno za ponovno vgradnjo. Na področju materialov in tehnologij izdelave izolacijskih oblog je bila izvedena vrsta poizkusov na površini in v jami. Rezultati poizkusov so bili v fazi gradnje dobri, stanje bomo spremljali še ob prehodu odkopa ob koncu leta 2011 in tako podali celovito tehnično oceno. Na področju opreme za delovišča je bilo opravljeno obsežno delo. Uveden je bil nov napredovalni stroj, pomični transporter, trak s kontinuiranim daljšanjem, osvojeni so bili vsi parametri avtomatizacije odvozov, ki omogočajo obratovanje odvoza brez posadk. Uveden je bil novi podajalnik lokov. Na področju opreme je bilo razvojno-raziskovalno delo usmerjeno predvsem v popolno mehanizacijo in avtomatizacijo vseh delovnih faz procesa gradnje jamskih prog in tako močno izboljšanih

varnostnih, tehničnih in ekonomskih parametrov. V prispevku smo celovito predstavili vse dosežke pri gradnji jamskih prog.

INTRODUCTION

The starting point of the face development and open-up work is dictated by extreme thickness and geometry of the Velenje coal seam. As these conditions are unique in the world, it has not been possible to select an optimum mining method for years.

Coal extraction is carried out from the hangingwall to footwall of the seam, and it is based on the retreating mining method. This means that it is necessary to prepare all the roadways before starting to extract the coal. As the face advances, the roadways are simultaneously liquidated.

Development constructions, which enable access to the deposit and coal exploitation, are driven partly in the rock mass and mainly in the coal seam. At present, there are about 50 km of roadways driven in the coal deposit. A great concentration of roadways is typical, and all roadways are driven in the exploitation area that ensures nowadays the planned output (4 000 000 t per year) of the coal mine. With regard to the mining system and the mining output it is necessary to drive about 7 km of roadways a year. The designing of individual floor levels and the sequence of extraction from hangingwall towards the footwall of the seam it is usually limited to the floor level working heights of 15 m. The designing method is conceived so that the level of coal seam exploitation is a maximum one. Each floor level is confined by two drift roads used for airing and for the transportation of coal and material.

A great number of underground structures in a limited exploitation field and their interaction during the exploitation process demand a systematic designing approach in order to achieve the necessary stability of the underground constructions.

While designing and driving the roadways the basic principle is taken into consideration, namely roadways have to remain stable without being additionally maintained or repaired during their life period. This demand can be

fully satisfied only by systematic evaluation of geological and geotechnical conditions, by evaluating other factors which have a significant influence on designing and roadway drivage, and by verification and improving the existent roadway drivage procedures. The qualitative and quantitative parameters collected in this way represent a good basis for the selection of optimal technically technological and economically most favourable solutions which can be used at designing method, support elements and at roadway drivage.

Influencing factors in building underground structures

Building floor level roadways at PV is affected by many factors[1], which are mutually intertwined, they can be defined as follows:
- natural,
- planning,
- designing,
- technological and
- organizational.

Natural factors
Natural factors are set out in layer of coal and other materials where facilities are made. These are mainly:
- depth,
- depth inside the layer,
- geomechanical properties,
- tectonics and faults,
- microstructural properties,
- content of gas,
- water content,
- ash content,
- oxidation process susceptibility,
- and others.

Planning factors
Planning factors are determined by the method of planning and executing works. These are mainly:
- timeliness of preparation works before starting mining,
- the timely start of construction of the roadways,
- assurance of all resources (material, equipment, team),
- the adequacy of planning according to the number construction teams,
- interactions between the structures in terms of planning face out.

Designing factors in terms of required lining capacity
Designing factors are determined by load bearing capacity of the lining. These are mainly:
- distance from the hangingwall of the seam,
- distance from the old works,
- interaction of the roadways and the longwall face in terms of design,
- location of the roadway in the coal layer,
- method of excavation.

Technological factors
Technological factors occur in all phases of construction works during

the roadway drivage procedures. These are mainly:

- cutting and preparing the space for the new section,
- supporting,
- building a fire covering and back filling,
- coal transportation,
- material delivery,
- energy supply,
- water drainage,
- ventilation,
- factors affecting the security of the working area.

Organizational factors

Organizational factors are related to the organization of work and contractors in the construction of underground objects. These are mainly:

- corresponding numerical and structural ensemble of performers,
- appropriate knowledge and practical skills of operators,
- adequate motivation of contractors,
- an appropriate organization of working time,
- an appropriate organized execution of the various stages of technological process.

In separate groups the presupposed influential parameters were selected on the basis of mathematical analysis. The link between natural, designing and technological conditions is worked out in the form of a mathematical model. The right choice and selection of influential parameters was confirmed by comparing the measured convergence with the convergence calculated on the basis of model.

The research of natural, designing and technological conditions resulted in the elaboration of systematization of supporting methods, and in the calculation of the supporting load bearing capacity and of the combination of supporting elements.

Categorisation of geological and geotechnical conditions and the necessary supports load bearing capacity is dealt with separately for three basic groups (trunk, access, gate) of underground roadways.

Underground structures and execution methods

PV underground structures are divided into three groups[3]:

- the main or trunk underground roadways,
- important or access underground roadways and
- floor level or gate objects (allowed convergence 20 %).

Trunk roadways

Trunk roadways are designed at safety pillar distance totalling 120 m. The allowed common convergence ensuring permanent roadway stability is

estimated at 5 %. In order to ensure the stability of the roadways we have to select the support system with load bearing capacity of at least 450 kPa at 8,35 MPa compressive strength, at least 500 kPa at 5,43 MPa compressive strength, and at least 650 kPa at 3 MPa compressive strength.

Access roadways

They are designed at safety pillar distance which totals 50 m for such roadways. The allowed common convergence of access roadways is 10 %. To ensure the stability at this convergence the load bearing capacity of the supporting system has to total 300 kPa at 8,35 MPa compressive strength, at least 350 kPa at 5,43 MPa compressive strength, and at least 450 kPa at 3MPa compressive strength.

Gate roadways

Besides taking over the influences caused by face advance during the roadway drivage, gate roads have to take load also dynamic tensions developing in front of the active coal face. So the worst case is considered in the categorisation, namely when the face crosses over the roadway. The allowed convergence still enabling the use of roadway is 20 %. To ensure this stability we have to select the support system with load bearing capacity totalling at least 150 kPa at 8,35 MPa uniaxial compressive strength, at least 200 kPa at 5,43 MPa compressive strength, and

at least 300 kPa at 3MPa compressive strength.

Roadway drivage

Technological procedures of driving roadways depend on the use and the life period of roadway. Gate roads are developed exclusively in the coal seam, their life period is on average 1 year. They are supported by girders and wooden struts. The density of building in girders is from 0,83 of girders set per one meter of roadway to 2,5 of set per one meter of driven roadway. As additional supporting measures anchor systems with composite and rope bolts are used, or the isolation of roadway frame with backfilling mixtures made of electrofilter ash functioning at the same time as prevention against the oxidation processes in roadways. Successful use of backfilling mixtures has decreased the range of coal mine fires by more than 95 %, whereas the reconstructions of roadways has been almost completely reduced.

Access roads are supported in a similar way as gate roads, the minimum density of building in girders amounts to 1,66 of set per one meter of driven roadway. Besides this, different anchor systems are included in supporting the roadways. Trunk roadways are supported by girders, bolts, and shotcrete. The life period of this roadways is up to 10 years.

Technological procedures of trunk roadway drivage are represented by the driving technology using concrete or shotcrete combined with anchoring systems. The life period of trunk roadways is more than 10 years, and even to the very end of coal mine exploitation.

Technology of building gate roadways with steel arches, isolation and backfilling the frame with fly ash mixtures

The basic feature of the technology[2] is primarily linked on supporting roads with a steel arch supports and filling edge lines with different mixtures of fly ash. This kind of technology is basicaly used in execution of floor level roadways and also in making access roadways with a shorter life time. By filling voids between wooden panels and the coal in particular security against the development of oxidation processes in coal and the stability of the road is improved.

Excavation of profile is achieved by using roadheader. Profile cutting is usually performed in three phases, which are divided onto the ceiling, side and floor of profile. Step advancement depends of the conditions at working area, ranging from 0.8 m to 1.6 m.

Roadway support consists of steel arches supports and wooden panels placed successively after each phase of the cutting profile of a roadway. There are severe types of steel arches support profiles used, they consist of 6 or 7 modified profiles.

The advantage of the modified (bell shaped) profile can be determined by providing the same support quality as a circular profile and also offers space advantages in terms of required usable area of the constructed roadway and in phase of excavation

The designed profile area is between 13 m^2 and 18 m^2. The over all design profile radius is 2 200 mm or 2500 mm. In accordance with increase of a profile the length and the overall weight of support system increases. At present we use K 24 steel arch supports, 24 kg/m weight.

In the past, several types of steel arches supports were tested. In 2011, we installed TH29 steel arches support. First results of the experiment show that this kind of support could be a good choice in replacing the existing K24 steel arches support. Joints in steel arches support units are interconnected with body clamps. Due to the studies and research of capacity of the clamp, the result is that screw clamps which have been tested and implemented had a better performance. Their advantage is represented by a greater strenght of screw clamps, easier remove and when overstressed, it does not fail instantly. Clamp is shown in Figure 1.
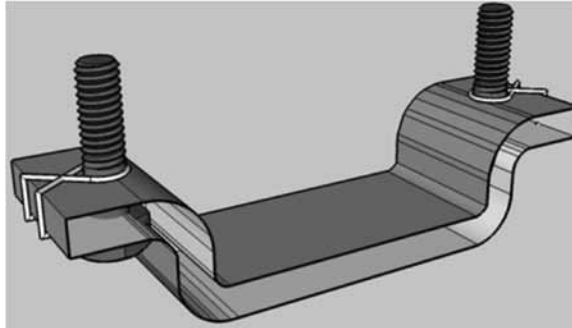
Figure 1. Screw Clamp

Figure 2. Strut for connecting steel frames of arch support units
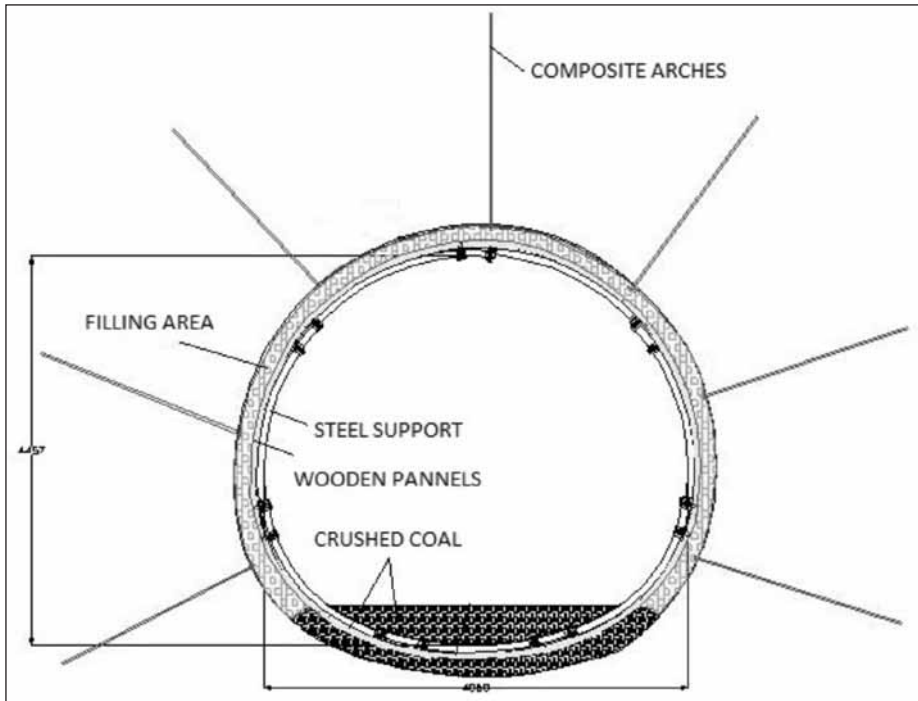
Figure 3. Cross section of the roadway

To achieve greater stability of roadways steel arches are interconnected on four sides with struts. By replacing the clamp it was necessary to design a new strut, which is shown in Figure 2.

It is possible to combine steel arch support with other types of anchors or bolts. To protect the head wall during construction phase of roadway (from falling pieces of coal) we temporary use composite bolts, which are combined with wooden paneling. For anchoring in the roadway we use steel anchors, composite bolts and plain strand cables. Composite bolts are used in gate roads of the longwall face panel because steel anchors can not be cut by shearer. Composite bolts provide similar load bearing capacity as steel anchors. As using composite bolts the advancement of the longwall face rapidly increases because of the ability of the longwall shearer to cut them. Loading of bore holes for composite bolts is carried out with artificial quick-setting materials. With composite bolts we managed to reduce the overall installation of steel arches supports because the distance between two sets of support is longer. (from 0.4 m to 0.6 m in some cases 0.75 m)

Wood turned out to be the most effective material for framework of the roadway, it provides sufficient support for the pressure of shotcrete filling mixture and it is easier to remove when necessary. Using this technology wood is economically accepted. For execution of framework we use oak panels, acacia and pine trees, thickness of the panels ranges from 40 mm to 100 mm. As an alternative material for the framework, it is possible to use a composite mash, which is processed in order of good connection with shotcrete materials for outdoor insulation paneling.

With the aim of preventing leakage of thin mixture at filling voids between the framework and the outside material layers it is necessary to seal the framework. It is done by making a thin lining over the entire surface of the roadway.

Two procedures at the same time are provided, excavation and supporting on one hand and isolating and filling-in on the other. Disposition of a roadway is shown in Figure 3.

The results of geotechnical research show that the interaction between installed liner and surrounding materials is efficient when the filling-in of space between them is carried out right after the installation of the liner.[6] According to those researches PV changed the roadway excavation procedure and the installation of the necessary liner support.

The excavation area of the roadway face is more extensive because of the addi-

tional installation of shotcrete fly ash filling. Radius of the roadway increases by 150 mm. However, this method is not suitable for the roadway excavation in faulted coal layers where cracking begins right after cutting out the profile.

After cutting the roadway, face steel supports are installed into the segments. Then we install composite mash which is covered with fabrics. The fabrics prevent from the leakage of fly ash filling mixture. Another alternative is installation of wooden panels, where the outer layer is fabrics with the same assignment as before. When the framework in length between 0.8 m and 1.6 m is finished we immediately fill-in with fly ash filling mixture from the bottom to the top of the framework. Fly ash filling is distributed through high pressure pipelines from the mixing device through the pump to the side. The overall density of the thick filling material consists of a mixture of fly ash, lime, cement, clay, and water in accordance to appropriate recipe.[5]

Filling-in is carried out on a distance of 30 m to 50 m from the roadway face. We use a thinly mixture of fly ash and water.

Development and technological improvements of equipment used in construction of the roadway

Analysis of equipment at the roadway excavation side showed that it is nec-essary to achieve greater efficiency and humanization of the technology, and that a comprehensive renewal of equipment is necessary. GPK road-header was an appropriate solution for the construction of roadways in PV, but it was technologically obsolete. Removal of coal from the roadway excavation site has been edited by a chain conveyor, which length was manually increased or decreased, similar to the belt conveyor. It was also necessary to allocate workers at each conveyor intersection. This method of removal has proven to be economically unap-propriate solution. Accordingly the delivery of the materials to the site was arranged by diesel locomotives and monorail transportation and it was proper solution. Delivery of material to the excavation site has been edited by hand, which represented a lot of hard physical work to be carried out for the employees. In Figure 4 there is a drawing of equipment prior to the techno-logical modernization.

Update of the existing and in development of new equipment for the construction of roadways has been linked to all stages of technological processes. The update was made on the cutting roadway face with the new roadhead-er, on installation of support elements with steel sets of feeding equipment and drilling rig for drilling anchor bore-holes, on the crushing and conveying system with a continuous extension of
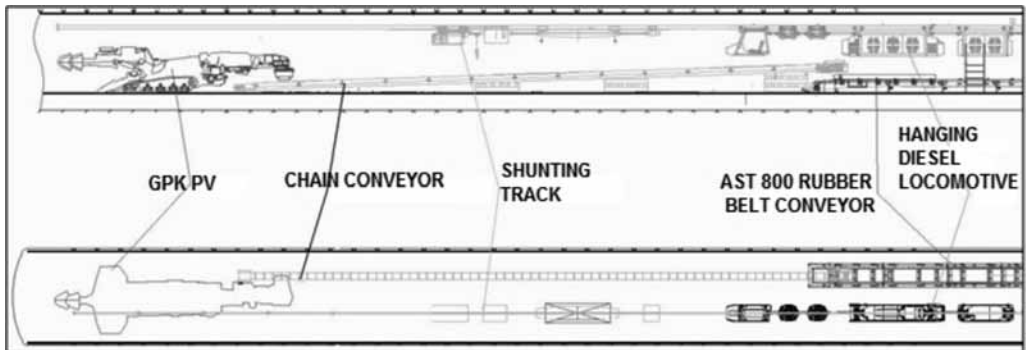
Figure 4. Disposition of equipment on site (before the update)

the transport. The system of roadway excavation has been fully automated. In this paper, we briefly summarize the achievements in the development of equipment in technological processes. [4]

New GPK PV roadheader is the product of Coal Mine Velenje which meets the requirements of the technological process of roadway building from 13 m^2 to 18 m^2. Electrical equipment for the roadheader has been developed in cooperation with Bartec company. Hydraulic steering system is our own Coal Mine Velenje development result. Steel base structure was built by Russian manufacturer.

Hazemag MCS 27 crushing and conveying system equipped with a continuous extension of the transportation is the product of collaboration between our own experts and the German manufacturer Hazemag. It serves to crush and transport coal between the roadway

Figure 5. Automating removal excavations from roadway site

excavation machine and belt conveyor. Crushed coal is transported by a chain conveyor to a belt conveyor. Hazemag MCS 27 crushing and conveying system with a continuous extension of the transportation is self-advanced unit pulled behind belt conveyor 800 AST transporter with a belt width of 800
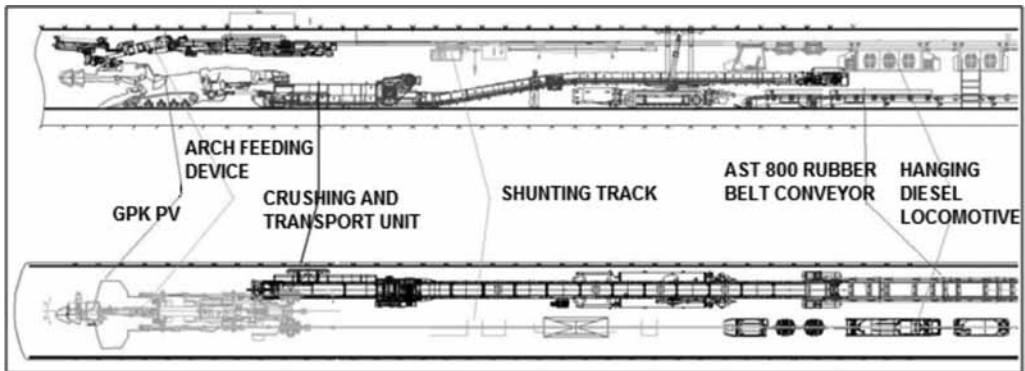
Figure 6. Disposition of equipment at excavation site (after comprehensive techno-logical renovation)

mm designed for conveying coal from excavation site. Conveyor consists of the main steel segments, the drive and convey unit. The unit has ability of continuous belt conveyor lengthening.

Removal of the excavated material with the use of Hazemag unit is fully automated by implemented steering sistem Mincos. Figure 5 shows the control unit.

For updated delivery and installation of material has been developed a new steel sets feeding equipment PL 08 PV. Development of this equipment is the result of collaboration between experts in Coal Mine Velenje and companies DBSS (steel works) and Bartec (steering system). The GTA company has developed a mobile drilling unit for drilling boreholes in the roadway face and anchoring boreholes around the roadway liner. In Figure 6 there is a drawing of equipment at the roadway

excavation site undergoing update of equipment and facilities.

Conclusion

In the years from 2008–2010 there has been an extensive research development in roadway excavation. Update of the existing and development of new equipment for the construction of roadways has been linked to all stages of technological process. Numerous applications of research developments improved all stages of technological processes of roadway excavation. It is absolutely necessary to continue the research development in the future.

References

[1]   Dervarič, E. (1997): Rock categori-zation for roadway support design and roadway development. Dis-

sertation thesis, Ljubljana.

[2]   DERVARIČ, E., KEMPERLE, C., HACE, M. (1994): Fire prevention system at Velenje coal mine. Pasamehmetoglu, A. Günhan. *Mine planning and equipment selection 1994.* Brookfield: A. A. Balkema, Rotterdam; 895–898.

[3]   DERVARIČ, E. (1997): Roadway drivage designing and development model at Velenje coal mine. Panagiotou, G. N., Sturgul, J. R. *Mine simulation: proceedings of the First international symposium on mine simulation via the INTERNET / 2–13 December 1996.* (1997) Rotterdam, A. A. Balkema, 90.

[4]   VUKELIČ, Ž., DERVARIČ, E., LIKAR, J., KOLENC, M., ČIŽMEK, D., POHOREC I., MAYER, J., SOTLER, B. (2010): *Izgradnja etažnih jamskih prog v Premogovniku Velenje. (*2010)*: raziskovalno-razvojni projekt: Poročilo o delu za leto 2010.* Ljubljana: Univerza v Ljubljani, NTF-OGR.

[5]   TERNIK, P., MARN, J., KANDUTI, D., DERVARIČ, E. (2001): The power law as a model for an electrostatic filter ash and water mixture. *Stroj. Vestn.*, 47(6), pp. 248–262.

[6]   LIKAR, J., DERVARIČ, E., MEDVED, M., ČADEŽ, J., JEROMEL, G. (2006): Some methods of analysing caving processes in sublevel coal mining. *RMZ-mater. geoenviron.*, Vol. 53, No. 2, pp. 203–220.

Author`s Index, Vol. 58, No. 4

Author`s Index, Vol. 58

RMZ MATERIALS AND GEOENVIRONMENT
Contents
Volume 58, 2011/1, 2, 3, 4

INSTRUCTIONS TO AUTHORS

RMZ-MATERIALS & GEOENVIRONMENT (RMZ- Materiali in geookolje) is a periodical publication with four issues per year (established 1952 and renamed to RMZ-M&G in 1998). The main topics of contents are Mining and Geotechnology, Metallurgy and Materials, Geology and Geoenvironment.

RMZ-M&G publishes original Scientific articles, Review papers, Preliminary notes, Professional papers **in English**. In addition, evaluations of other publications (books, monographs,...), In memoriam, Professional remarks and reviews are welcome. The Title, Abstract and Key words in Slovene will be included by the author(s) or will be provided by the referee or the Editorial Office.

* Additional information and remarks for Slovenian authors:
Only Professional papers, Publications notes, Events notes, Discussion of papers and In memoriam, will be exceptionally published in the Slovenian language.

Authorship and originality of the contributions. Authors are responsible for originality of presented data, ideas and conclusions as well as for correct citation of data adopted from other sources. The publication in RMZ-M&G obligate authors that the article will not be published anywhere else in the same form.

Specification of Contributions

RMZ-M&G will publish papers of the following categories:

<u>Full papers</u> *(optimal number of pages is 7 to 15, longer articles should be discussed with Editor prior to submission). An abstract is required.*
- **Original scientific papers** represent unpublished results of original research.
- **Review papers** summarize previously published scientific, research and/or expertise articles on the new scientific level and can contain also other cited sources, which are not mainly result of author(s).

- **Preliminary notes** represent preliminary research findings, which should be published rapidly.
- **Professional paper**s are the result of technological research achievements, application research results and information about achievements in practice and industry.

Short papers (the number of pages is limited to 1 for Discussion of papers and 2 pages for Publication note, Event note and In Memoriam). No abstract is required for short papers.

- **Publication notes** contain author's opinion on new published books, monographs, textbooks, or other published material. A figure of cover page is expected.
- **Event notes** in which descriptions of a scientific or professional event are given.
- **Discussion of papers (Comments)** where only professional disagreements can be discussed. Normally the source author(s) reply the remarks in the same issue.
- **In memoriam** (a photo is expected).

Supervision and review of manuscripts. All manuscripts will be supervised. The referees evaluate manuscripts and can ask authors to change particular segments, and propose to the Editor the acceptability of submitted articles. Authors can suggest the referee but Editor has a right to choose another. **The name of the referee remains anonymous.** The technical corrections will be done too and authors can be asked to correct missing items. The final decision whether the manuscript will be published is made by the Editor in Chief.

The Form of the Manuscript

The manuscript should be submitted as a complete hard copy including figures and tables. The figures should also be enclosed separately, both charts and photos in the original version. In addition, all material should also be provided in electronic form on a diskette or a CD. The necessary information can conveniently also be delivered by E-mail.

Composition of manuscript is defined in the attached Template

The original file of Template is available on RMZ-Materials and Geoenvironment Home page address:

http://www.rmz-mg.com

References - can be arranged in two ways:
- first possibility: alphabetic arrangement of first authors - in text: (Borgne, 1955), or
- second possibility: [1] numerated in the same order as cited in the text: example[1]

Format of papers in journals:
> LE BORGNE, E. (1955): Susceptibilite magnetic anomale du sol superficiel. *Annales de Geophysique*, 11, pp. 399–419.

Format of books:
> ROBERTS, J. L. (1989): Geological structures, *MacMillan*, *London*, 250 p.

Text on the hard print copy can be prepared with any text-processor. The electronic version on the diskette, CD or E-mail transfer should be in MS Word or ASCII format.
Captions of figures and tables should be enclosed separately.
Figures (graphs and photos) and tables should be original and sent separately in addition to text. They can be prepared on paper or computer designed (MSExcel, Corel, Acad).
Format. Electronic figures are recommended to be in CDR, Al, EPS, TIF or JPG formats. Resolution of bitmap graphics (TIF, JPG) should be at least 300 dpi. Text in vector graphics (CDR, Al, EPS) must be in MSWord Times typography or converted in curves.
Color prints. Authors will be charged for color prints of figures and photos.
Labeling of the additionally provided material for the manuscript should be very clear and must contain at least the lead author's name, address, the beginning of the title and the date of delivery of the manuscript. In case of an E-mail transfer the exact message with above asked data must accompany the attachment with the file containing the manuscript.

Information about RMZ-M&G:

Editor in Chief prof. dr. Peter Fajfar (phone: ++386 1 4250-316) or

Secretary Barbara Bohar Bobnar, univ. dipl. ing. geol. (phone: ++386 1 4704-630),

Aškerčeva 12, 1000 Ljubljana, Slovenia

or at E-mail addresses:

peter.fajfar@ntf.uni-lj.si,

barbara.bohar@ntf.uni-lj.si

Sending of manuscripts. Manuscripts can be sent by mail to the **Editorial Office** address:

- RMZ-Materials & Geoenvironment
  Aškerčeva 12,
  1000 Ljubljana, Slovenia

or delivered to:

- **Reception** of the Faculty of Natural Science and Engineering (for RMZ-M&G)
  Aškerčeva 12,
  1000 Ljubljana, Slovenia
- E-mail - addresses of Editor and Secretary
- You can also contact them on their phone numbers.

These instructions are valid from August 2009

NAVODILA AVTORJEM

RMZ-MATERIALS AND GEOENVIRONMENT (RMZ- Materiali in geookolje) – kratica RMZ-M&G - je revija (ustanovljena kot zbornik 1952 in preimenovana v revijo RMZ-M&G 1998), ki izhaja vsako leto v štirih zvezkih. V reviji objavljamo prispevke s področja rudarstva, geotehnologije, materialov, metalurgije, geologije in geookolja.

RMZ- M&G objavlja izvirne znanstvene, pregledne in strokovne članke ter predhodne objave samo v angleškem jeziku. Strokovni članki so lahko izjemoma napisani v slovenskem jeziku. Kot dodatek so zaželene recenzije drugih publikacij (knjig, monografij …), nekrologi In Memoriam, predstavitve znanstvenih in strokovnih dogodkov, kratke objave in strokovne replike na članke objavljene v RMZ-M&G v slovenskem ali angleškem jeziku. Prispevki naj bodo kratki in jasni.

Avtorstvo in izvirnost prispevkov. Avtorji so odgovorni za izvirnost podatkov, idej in sklepov v predloženem prispevku oziroma za pravilno citiranje privzetih podatkov. Z objavo v RMZ-M&G se tudi obvežejo, da ne bodo nikjer drugje objavili enakega prispevka.

Vrste prispevkov

Optimalno število strani je 7 do 15, za daljše članke je potrebno soglasje glavnega urednika.
Izvirni znanstveni članki opisujejo še neobjavljene rezultate lastnih raziskav.
Pregledni članki povzemajo že objavljene znanstvene, raziskovalne ali strokovne dosežke na novem znanstvenem nivoju in lahko vsebujejo tudi druge (citirane) vire, ki niso večinsko rezultat dela avtorjev.
Predhodna objava povzema izsledke raziskave, ki je v teku in zahteva hitro objavo.
Strokovni članki vsebujejo rezultate tehnoloških dosežkov, razvojnih projektov in druge informacije iz prakse.
Recenzije publikacij zajemajo ocene novih knjig, monografij, učbenikov, razstav …(do dve strani; zaželena slika naslovnice in kratka navedba osnovnih podatkov - izkaznica).

In memoriam (do dve strani, zaželena slika).
Strokovne pripombe na objavljene članke ne smejo presegati ene strani in opozarjajo izključno na strokovne nedoslednosti objavljenih člankov v prejšnjih številkah RMZ-M&G. Praviloma že v isti številki avtorji prvotnega članka napišejo odgovor na pripombe.
Poljudni članki, ki povzemajo znanstvene in strokovne dogodke (do dve strani).

Recenzije. Vsi prispevki bodo predloženi v recenzijo. Recenzent oceni primernost prispevka za objavo in lahko predlaga kot pogoj za objavo dopolnilo k prispevku. Recenzenta izbere Uredništvo med strokovnjaki, ki so dejavni na sorodnih področjih, kot jih obravnava prispevek. Avtorji lahko sami predlagajo recenzenta, vendar si uredništvo pridržuje pravico, da izbere drugega recenzenta. **Recenzent ostane anonimen**. Prispevki bodo tudi tehnično ocenjeni in avtorji so dolžni popraviti pomanjkljivosti. Končno odločitev za objavo da glavni in odgovorni urednik.

Oblika prispevka

Prispevek predložite v tiskanem oštevilčenem izvodu (po možnosti z vključenimi slikami in tabelami) ter na disketi ali CD, lahko pa ga pošljete tudi prek E-maila. Slike in grafe je možno poslati tudi risane na papirju, fotografije naj bodo originalne.

Razčlenitev prispevka:

Predloga za pisanje članka se nahaja na spletni strani:

http://www.rmz-mg.com/predloga.htm

Seznam literature je lahko urejen na dva načina:
-po abecednem zaporedju prvih avtorjev ali
-po [1]vrstnem zaporedju citiranosti v prispevku.

Oblika je za oba načina enaka:
Članki:

       LE BORGNE, E. (1955): Susceptibilite magnetic anomale du sol superficiel. *Annales de Geophysique*; Vol. 11, pp. 399–419.

Knjige:

> Roberts, J. L. (1989): Geological structures, *MacMillan*, *London*, 250 p.

Tekst izpisanega izvoda je lahko pripravljen v kateremkoli urejevalniku. Na disketi, CD ali v elektronskem prenosu pa mora biti v MS Word ali v ASCII obliki.

Naslovi slik in tabel naj bodo priloženi posebej. Naslove slik, tabel in celotno besedilo, ki se pojavlja na slikah in tabelah, je potrebno navesti v angleškem in slovenskem jeziku.

Slike (ilustracije in fotografije) in tabele morajo biti izvirne in priložene posebej. Njihov položaj v besedilu mora biti jasen iz priloženega kompletnega izvoda. Narejene so lahko na papirju ali pa v računalniški obliki (MS Excel, Corel, Acad).

Format elektronskih slik naj bo v EPS, TIF ali JPG obliki z ločljivostjo okrog 300 dpi. Tekst v grafiki naj bo v Times tipografiji.

Barvne slike. Objavo barvnih slik sofinancirajo avtorji

Označenost poslanega materiala. Izpisan izvod, disketa ali CD morajo biti jasno označeni – vsaj z imenom prvega avtorja, začetkom naslova in datumom izročitve uredništvu RMZ-M&G. Elektronski prenos mora biti pospremljen z jasnim sporočilom in z enakimi podatki kot velja za ostale načine posredovanja.

Informacije o RMZ-M&G: urednik prof. dr. Peter Fajfar, univ. dipl. ing. metal. (tel. ++386 1 4250316) ali tajnica Barbara Bohar Bobnar, univ. dipl. ing. geol. (tel. ++386 1 4704630), Aškerčeva 12, 1000 Ljubljana
ali na E-mail naslovih:
peter.fajfar@ntf.uni-lj.si
barbara.bohar@ntf.uni-lj.si

Pošiljanje prispevkov. Prispevke pošljite priporočeno na naslov **Uredništva:**
- RMZ-Materials and Geoenvironment
    Aškerčeva 12,
    1000 Ljubljana, Slovenija
oziroma jih oddajte v
- **Recepciji** Naravoslovnotehniške fakultete (pritličje) (za RMZ-M&G)
    Aškerčeva 12,
    1000 Ljubljana, Slovenija
- Možna je tudi oddaja pri uredniku oziroma pri tajnici.

Navodila veljajo od avgusta 2009.

TEMPLATE

The title of the manuscript should be written in bold letters (Times New Roman, 14, Center)

Naslov članka (Times New Roman, 14, Center)

Name Surname[1], …. , & Name Surname[x] (Times New Roman, 12, Center)

[x] University of ..., Faculty of ..., Address…, Country ... (Times New Roman, 11, Center)

*Corresponding author. E-mail: ... (Times New Roman, 11, Center)

Abstract (Times New Roman, Normal, 11): The abstract should be concise and should present the aim of the work, essential results and conclusion. It should be typed in font size 11, single-spaced. Except for the first line, the text should be indented from the left margin by 10 mm. The length should not exceed fifteen (15) lines (10 are recommended).

Izvleček (Times New Roman, navadno, 11): Kratek izvleček namena članka ter ključnih rezultatov in ugotovitev. Razen prve vrstice naj bo tekst zamaknjen z levega roba za 10 mm. Dolžina naj ne presega petnajst (15) vrstic (10 je priporočeno).

Key words: a list of up to 5 key words (3 to 5) that will be useful for indexing or searching. Use the same styling as for abstract.

Ključne besede: seznam največ 5 ključnih besed (3–5) za pomoč pri indeksiranju ali iskanju. Uporabite enako obliko kot za izvleček.

Introduction (Times New Roman, Bold, 12)

Two lines below the keywords begin the introduction. Use Times New Roman, font size 12, Justify alignment.

There are two (2) admissible methods of citing references in text:
1. by stating the first author and the year of publication of the reference in the parenthesis at the appropriate place in the text and arranging the reference list in the alphabetic order of first authors; e.g.:
   "Detailed information about geohistorical development of this zone can be found in: Antonijević (1957), Grubić (1962), ..."
   "… the method was described previously (Hoefs, 1996)"
2. by consecutive Arabic numerals in square brackets, superscripted at the appropriate place in the text and arranging the reference list at the end of the text in the like manner; e.g.:
   "... while the portal was made in Zope environment. [3]"

Materials and methods (Times New Roman, Bold, 12)

This section describes the available data and procedure of work and therefore provides enough information to allow the interpretation of the results, obtained by the used methods.

Results and discussion (Times New Roman, Bold, 12)

Tables, figures, pictures, and schemes should be incorporated in the text at the appropriate place and should fit on one page. Break larger schemes and tables into smaller parts to prevent extending over more than one page.

Conclusions (Times New Roman, Bold, 12)

This paragraph summarizes the results and draws conclusions.

Acknowledgements (Times New Roman, Bold, 12, Center - optional)

REFERENCES (TIMES NEW ROMAN, BOLD, 12)

In regard to the method used in the text, the styling, punctuation and capitalization should conform to the following:

FIRST OPTION - in alphabetical order

CASATI, P., JADOUL, F., NICORA, A., MARINELLI, M., FANTINI-SESTINI, N. & FOIS, E. (1981): Geologia della Valle del'Anisici e dei gruppi M. Popera - Tre Cime di Lavaredo (Dolomiti Orientali). *Riv. Ital. Paleont.*; Vol. 87, No. 3, pp. 391–400, Milano.

FOLK, R. L. (1959): Practical petrographic classification of limestones. *Amer. Ass. Petrol. Geol. Bull.;* Vol. 43, No. 1, pp. 1–38, Tulsa.

SECOND OPTION - in numerical order

[1] TRČEK, B. (2001): *Solute transport monitoring in the unsaturated zone of the karst aquifer by natural tracers.* Ph. D. Thesis. Ljubljana: University of Ljubljana 2001; 125 p.

[2] HIGASHITANI, K., ISERI, H., OKUHARA, K., HATADE, S. (1995): Magnetic Effects on Zeta Potential and Diffusivity of Nonmagnetic Particles. *Journal of Colloid and Interface Science, 172*, pp. 383–388.

Citing the Internet site:

CASREACT-Chemical reactions database [online]. Chemical Abstracts Service, 2000, updated 2. 2. 2000 [cited 3. 2. 2000]. Accessible on Internet: http://www.cas.org/CASFILES/casreact.html.

Texts in Slovene (title, abstract and key words) can be written by the author(s) or will be provided by the referee or by the Editorial Board.

PREDLOGA ZA SLOVENSKE ČLANKE

Naslov članka (Times New Roman, 14, Na sredino)

The title of the manuscript should be written in bold letters (Times New Roman, 14, Center)

IME PRIIMEK[1], …, IME PRIIMEK[X] (TIMES NEW ROMAN, 12, NA SREDINO)

[X]Univerza…, Fakulteta…, Naslov…, Država… (Times New Roman, 11, Center)

*Korespondenčni avtor. E-mail: ... (Times New Roman, 11, Center)

Izvleček (Times New Roman, Navadno, 11): Kratek izvleček namena članka ter ključnih rezultatov in ugotovitev. Razen prve j bo tekst zamaknjen z levega roba za 10 mm. Dolžina naj ne presega petnajst (15) vrstic (10 je priporočeno).

Abstract (Times New Roman, Normal, 11): The abstract should be concise and should present the aim of the work, essential results and conclusion. It should be typed in font size 11, single-spaced. Except for the first line, the text should be indented from the left margin by 10 mm. The length should not exceed fifteen (15) lines (10 are recommended).

Ključne besede: seznam največ 5 ključnih besed (3–5) za pomoč pri indeksiranju ali iskanju. Uporabite enako obliko kot za izvleček.
Key words: a list of up to 5 key words (3 to 5) that will be useful for indexing or searching. Use the same styling as for abstract.

UVOD (TIMES NEW ROMAN, KREPKO, 12)

Dve vrstici pod ključnimi besedami se začne Uvod. Uporabite pisavo Times New Roman, velikost črk 12, z obojestransko poravnavo. Naslovi slik in tabel (vključno z besedilom v slikah) morajo biti v slovenskem jeziku.

Slika (Tabela) X. Pripadajoče besedilo k sliki (tabeli)

Obstajata dve sprejemljivi metodi navajanja referenc:

1. z navedbo prvega avtorja in letnice objave reference v oklepaju na ustreznem mestu v tekstu in z ureditvijo seznama referenc po abecednem zaporedju prvih avtorjev; npr.:

   "Detailed information about geohistorical development of this zone can be found in: Antonijević (1957), Grubić (1962), ..."

   "… the method was described previously (Hoefs, 1996)"

ali

2. z zaporednimi arabskimi številkami v oglatih oklepajih na ustreznem mestu v tekstu in z ureditvijo seznama referenc v številčnem zaporedju navajanja; npr.;

   "... while the portal was made in Zope[3] environment."

Materiali in metode (Times New Roman, Krepko, 12)

Ta del opisuje razpoložljive podatke, metode in način dela ter omogoča zadostno količino informacij, da lahko z opisanimi metodami delo ponovimo.

Rezultati in razprava (Times New Roman, Krepko, 12)

Tabele, sheme in slike je treba vnesti (z ukazom Insert, ne Paste) v tekst na ustreznem mestu. Večje sheme in tabele je po treba ločiti na manjše dele, da ne presegajo ene strani.

Sklepi (Times New Roman, Krepko, 12)

Povzetek rezultatov in sklepi.

Zahvale (Times New Roman, Krepko, 12, Na sredino - opcija)

Izvedbo tega dela je omogočilo ………

V<small>IRI</small> (T<small>IMES</small> N<small>EW</small> R<small>OMAN</small>, K<small>REPKO</small>, 12)

Glede na uporabljeno metodo citiranja referenc v tekstu upoštevajte eno od naslednjih oblik:

PRVA MOŽNOST (priporočena) - v abecednem zaporedju
C<small>ASATI</small>, P., J<small>ADOUL</small>, F., N<small>ICORA</small>, A., M<small>ARINELLI</small>, M., F<small>ANTINI</small>-S<small>ESTINI</small>, N. & F<small>OIS</small>, E. (1981): Geologia della Valle del'Anisici e dei gruppi M. Popera – Tre Cime di Lavaredo (Dolomiti Orientali). *Riv. Ital. Paleont.*; Vol. 87, No. 3, pp. 391–400, Milano.
F<small>OLK</small>, R. L. (1959): Practical petrographic classification of limestones. *Amer. Ass. Petrol. Geol. Bull.;* Vol. 43, No. 1, pp. 1–38, Tulsa.

DRUGA MOŽNOST - v numeričnem zaporedju
[1] T<small>RČEK</small>, B. (2001): *Solute transport monitoring in the unsaturated zone of the karst aquifer by natural tracers.* Ph. D. Thesis. Ljubljana: University of Ljubljana 2001; 125 p.
[2] H<small>IGASHITANI</small>, K., I<small>SERI</small>, H., O<small>KUHARA</small>, K., H<small>ATADE</small>, S. (1995): Magnetic Effects on Zeta Potential and Diffusivity of Nonmagnetic Particles. *Journal of Colloid and Interface Science, 172*, pp. 383–388.

Citiranje spletne strani:
CASREACT-Chemical reactions database [online]. Chemical Abstracts Service, 2000, obnovljeno 2. 2. 2000 [citirano 3. 2. 2000]. Dostopno na svetovnem spletu: http://www.cas.org/CASFILES/casreact.html.

Znanstveni, pregledni in strokovni članki ter predhodne objave se objavijo v angleškem jeziku. Izjemoma se strokovni članek objavi v slovenskem jeziku.

IRGO

Inženirska geologija
Hidrogeologija
Geomehanika
Projektiranje
Tehnologije za okolje
Svetovanje in nadzor